TÉCNICO LISBOA

Analysis of LED lighting strategies in vertical urban farming for enhancement of plant productivity and energy consumption

João Miguel Rodelo Pereira

Thesis to obtain the Master of Science Degree in

Energy Engineering and Management

Supervisor: Prof. Maria da Glória de Almeida Gomes

Examination Committee

Chairperson: Prof. Duarte de Mesquita e Sousa

Supervisor: Prof. Maria da Glória de Almeida Gomes

Member of the Committee: Prof. Carlos Augusto Santos Silva

October 2023

Declaration

I declare that this document is an original work of my own authorship and that it fulfils all the requirements of the Code of Conduct and Good Practices of the Universidade de Lisboa.

Acknowledgements

I would like to express my sincere gratitude to all the ones who have supported me throughout the journey of completing this thesis work.

First and foremost, my deep appreciation to my thesis supervisor Prof. Maria da Glória Gomes, for accepting to join me on this challenge with the most enthusiasm and positive attitude. I deeply appreciate her mentorship, patience, and thoughtful insights through this long journey and for directing this research towards this rewarding outcome.

Secondly, I would like to express my gratitude to the company Raiz Vertical Farms for accepting and allowing the realization of this study in their facility, as well as to all the people from the company who embraced me as part of the team from day one. A special thanks goes out to Emiliano Gutierrez who constantly pushed for innovative thinking and always allowed my voice to be heard. My work could not have been developed without the help and advice of Yannick Keyßner and Simmon Szalai who taught me about so many new tools and approaches. Our intellectually stimulating discussions have certainly enriched the depth of this thesis. Thanks to Kitija Konošonoka and Lúcia Salas for the patience and effort to make sure my project was developed successfully and aligned with the farm operation, and for all the provided knowledge on plants and sustainability.

A special thanks to Bruno Vaz for all the hands-on support with the electrical parts and good disposition, to João Ajuda for the big help with 3D printing and to Artem Plotnikov for making my life easier with data handling platforms.

A special thanks to all my friends and family who gave me the energy to keep going and to my girlfriend who put up with me on the most frustrating days.

To all those mentioned and others who played a role in this academic endeavour, I extend my heartfelt thanks. This achievement would not have been possible without your contributions.

Resumo

Este estudo no desenvolvimento e implementação de um sistema de controlo de iluminação composto por sensores de luz (AS7341), LEDs (Hortiblade) e microcontroladores (Raspberry Pi), para controlo automático da luz artificial em função das condições de luz solar numa estufa agrícola vertical. O sistema desenvolvido surge no âmbito da agricultura sustentável em ambiente controlado como uma solução para melhorar a eficiência energética na iluminação, que tende a representar um elevado consumo de energia nestas aplicações. O trabalho foi desenvolvido com a empresa Raiz Vertical Farms, introduzindo um controlo personalizado da intensidade e duração de iluminação para melhorar a produtividade agrícola na sua instalação agrícola em Lisboa. O sistema desenvolvido fornece complementos de luz artificial LED depois do por do sol para atingir com precisão metas pré-definidas de Integral de Luz Diária (DLI) sob vários de padrões diários de luz natural. Além disso, o crescimento de duas variedades de plantas de manjericão (Gustosa e Pluto) foi testado sob diferentes metas de DLI de 12,5, 15 e 17,5 $mol.m^{-2}.d^{-1}$ fornecidos por luz natural e artificial. Os alvos de DLI definidos foram. A campanha experimental durante um ciclo de colheita (4 semanas depois da germinação) revelou rendimentos e consumo de energia variados com base em diferentes regimes de DLI. Para o manjericão Pluto, a produtividade foi de 47.5g de massa comestível, com um regime de DLI de 17.5 $mol.m^{-2}.d^{-1}$, consumindo 13.75 kWh de energia LED total (3.45 g/kWh por planta); o regime de DLI 15 $mol.m^{-2}.d^{-1}$ conduziu a uma produtividade média de 32.5g por planta e 12.43 kWh de consumo (2.61 kWh); e o regime DLI de 12.5 $mol.m^{-2}.d^{-1}$ produziu uma média de 35,3g por planta, consumindo 4.48 kWh (7.81 g/kWh). O sistema implementado foi capaz de reduzir o consumo de energia pelo menos 40%, em comparação com a operação original dos LEDs.

Palavras-chave:

- Agricultura Urbana Vertical
- Desenvolvimento de plantas
- Controlo LED
- Integral de luz diária
- Densidade do fluxo de fotões fotossintéticos
- Testes experimentais

Abstract

This study proposes the assembly and tunning of a lighting control system composed of light sensors (AS7341), LEDs (Hortiblade) and microcontrollers (Raspberry Pi), for automatic control of artificial light in a vertical farm greenhouse depending on sunlight conditions. The developed system appears in the scope of sustainable controlled environment farming as a solution for improving energy efficiency in lighting, which represents high energy consumption in these applications. The work was developed with Raiz Vertical Farms company, introducing tailored control of light intensity and duration to maximize plant yield at their farm facility in Lisbon. The developed system provides artificial light complements after sunset to deliver predefined Daily Light Integrals (DLI) targets under various natural light patterns. Additionally, the growth of two varieties of basil plants (Gustosa and Pluto) was tested under different DLI targets of 12.5, 15 and 17.5 $mol.m^{-2}.d^{-1}$ delivered by a mix of natural and artificial light. The experiment was carried during one harvest cycle (4 weeks after germination) revealing varied yields and energy consumption based on different DLI regimes. For Pluto basil, at DLI of 17.5 $mol.m^{-2}.d^{-1}$, the average yield per plant was 47.5g of edible mass, with 13.75 kWh of LED energy consumption (3.45 g/kWh per plant). The DLI regime of 15 $mol.m^{-2}.d^{-1}$ resulted in an average of 32.5g per plant, using 12.43 kWh (2.61 g/kWh), and DLI of 12.5 $mol.m^{-2}.d^{-1}$ in an average of 35.3g per plant, consuming 4.48 kWh (7.81 g/kWh). The lowest DLI regime was the most energy-efficient, consuming about one-third of the energy compared to the highest DLI regime. The implemented system reduced energy consumption by at least 40%, compared to the original LED operation.

Keywords:

- Vertical Urban Farming
- Plant Development
- LED Control
- Daily Light Integral
- Photosynthetic Photon Flux Density
- Experimental Testing

Symbology

F_{ADC}	Analogue-to-digital converter frequency	[Hz]
Dim_{LED}	Dimming level of the LED	[mol.m^{-2}.d^{-1}]
Dim_{PWM}	Dimming percentage PWM signal	[%]
DLI_m	DLI (solar) measured	[mol.m^{-2}.d^{-1}]
DLI_t	DLI target	[mol.m^{-2}.d^{-1}]
t_{int}	Integration time for one measurement interval	[ms]
I_{LED}	LED Intensity	[%]
P_{LED}	LED Operation Period	[h]
n_{step}	“Night step” value	[µmol.m^{-2}.s^{-1}]
P_{dark}	Period of Darkness	[h]
η_{PPF}	Photon efficiency	[µmol/J]
b_{blue}	PPFD conversion coefficients for the AS7341’s blue channel output	-
b_{clear}	PPFD conversion coefficients for the AS7341’s clear channel output	-
b_{cyan}	PPFD conversion coefficients for the AS7341’s cyan channel output	-
b_{green}	PPFD conversion coefficients for the AS7341’s green channel output	-
b_{indigo}	PPFD conversion coefficients for the AS7341’s indigo channel output	-
b_{orange}	PPFD conversion coefficients for the AS7341’s orange channel output	-
b_{red}	PPFD conversion coefficients for the AS7341’s red channel output	-
b_{violet}	PPFD conversion coefficients for the AS7341’s violet channel output	-
b_{yellow}	PPFD conversion coefficients for the AS7341’s yellow channel output	-
$PPFD_{LED}$	PPFD from LED	[µmol.m^{-2}.s^{-1}]
$PPFD_p$	Predicted PPFD value from linear regression	[µmol.m^{-2}.s^{-1}]
τ_v	Visible transmittance	-

Acronyms

API	Application Programming Interface
CO_{2eq}	Carbon Dioxide Equivalent
CEA	Controlled Environment Agriculture
DLI	Daily Light Integral
EC	Electrical Conductivity
EOP	End-Of-Production
FR	Far Red
GMOs	Genetically Modified Organisms

GHG	Greenhouse Gas
IEC	Indirect Evaporative Cooling
IR	Infrared
LCA	Life Cycle Assessments
LED	Light Emitting Diode
CH_4	Methane
NASA	National Aeronautics and Space Administration
N_2O	Nitrous Oxide
PAR	Photosynthetic Active Radiation
PPF	Photosynthetic Photon Flux
PPFD	Photosynthetic Photon Flux Density
PF	Plant Factory
PSU	Power Supply Unit
PWM	Pulse Width Modulation
RA	Regenerative Agriculture
RTG	Rooftop Garden
SSH	Secure Shell Protocol
SCL	Serial Clock
SDA	Serial Data
UV	Ultraviolet
VF	Vertical Farming

Contents

List of Figures

List of Tables

1. Introduction

1.1 Motivation

Last year, in 2022, the world population reached 8 billion people, only 11 years after reaching 7 billion, in 2011. According to the United Nation's projections, the world population could grow to around 9.7 billion by 2050, reaching a peak of 10.4 billion by 2080 [1]. This means that there are around 2 billion people more to be fed in a period of 30 years. Even more challenging is the fact that the world population is getting richer and improving the quality of life, usually meaning more calorie-intense diets, containing more amounts of meat and dairy [2]. Despite this being positive news and a sign of prosperity, it leaves us with a tough environmental challenge in providing global food security without compromising our climate or saturating the planet's resources. According to National Geographic Magazine, by 2050, even though the world's population will increase by 25%, there is a need to "roughly double the amount of crops we grow" [3]. A real challenge as the costs of energy, labour and fertilizer rise, resources like water and fertile land become scarcer, and extreme weather events more frequent.

The methods used to grow food need to be seriously reassessed and redesigned for us to have a chance against the current climate crisis. This industry capitalizes on boosting natural growth cycles and yields, which often disrupt nature's balance, leading to multiple complex environmental issues. It is an industry that serves the most fundamental global need of the population – food – thus, it is under constant pressure of demand. This pressure in large markets tends to lead producers to adopt mass-production practices that use excessive amounts of resources, (like water, fertilizers, and land), which tend to be wasteful and pollutant. These issues are systematic and deeply rooted in current methods, which challenge the sustainable shift, but at the same time, there is a large room for improvement, which can fuel innovation. The next charts of Figure 1 published by Our World in Data give a clear picture of how much this industry is affecting our planet's environment. The numbers are worrying. From the greenhouse gas footprint, resource exploration, pollution, to overwhelming shares of livestock on global biodiversity, this industry has a huge impact on the environment.

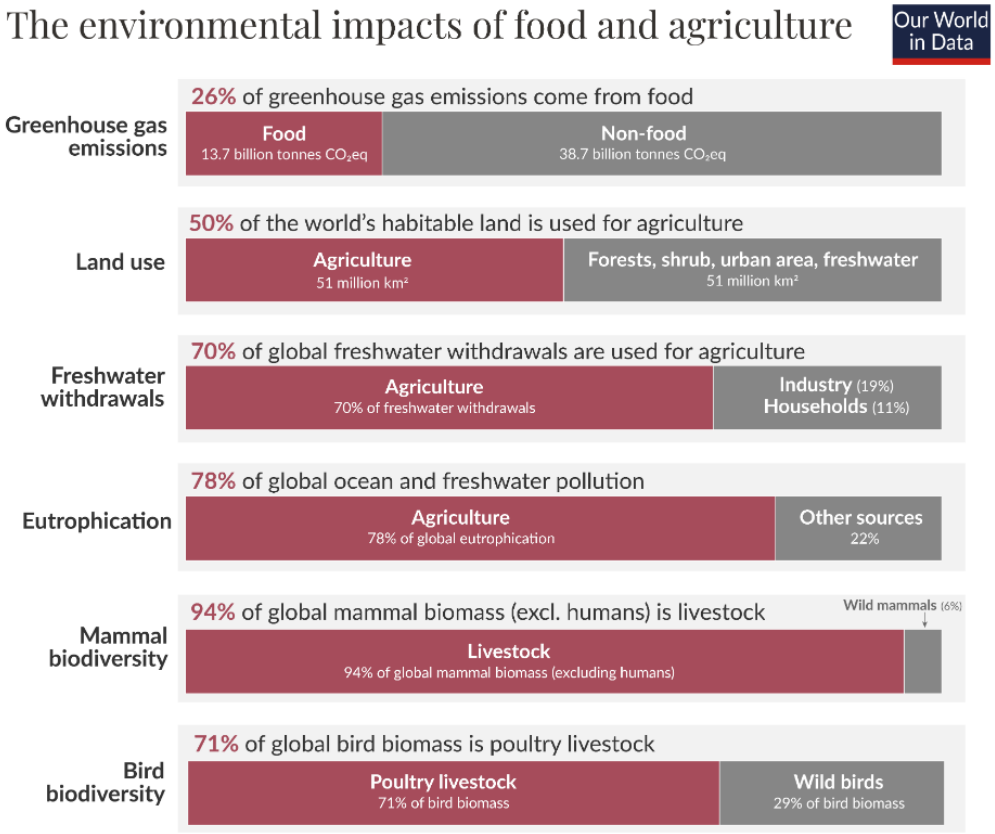

Figure 1- Main environmental Impacts of food and agriculture [4] (2018)

1.1.1 Emissions in Agriculture

The agriculture sector is responsible for around one quarter of total annual global emissions [5]. The main types of greenhouse gases (GHG) emitted in this sector are carbon dioxide (CO_2), methane (CH_4), and nitrous oxide (N_2O). The sources of pollution of current agricultural practices are various and depend on factors such as the use of chemicals/fertilizers, type of waste treatment, deforestation, organic soil drainage, on-farm energy use, and consequent industrial and transportation processes. Biological processes also have a significant contribution to emissions, like the notorious methane release from cow's food digestion (enteric fermentation) and nitrous oxide from manure/organic matter discomposure. Methane and nitrous oxide are a serious threat to global warming since they cause 28- and 265-times higher warming effect than a CO_2 molecule, respectively [6], representing more than half of the total impact in terms of equivalent CO_2 (CO_{2eq}) emissions in agriculture [7]. Emission problems as enteric fermentation seem to be difficult to solve while constantly supplying populations with meat and dairy products. However, there are malpractices with significant global impact that are simply outdated with current better alternatives available.

1.1.2 Waste and Drainage

In organic waste management, there is a massive quantity of uncontrolled and controlled burnings compared to sustainable upcycling treatment methods (for energy generation, soil treatment, etc);

Drainage of organic soils is another significant cause of emissions in agriculture. There are large quantities of carbon retained in the soil in wetland ecosystems with large amounts of organic matter. These soils retain 30% of total soil carbon and therefore have an important role in maintaining Earth's carbon balance. The cultivation of permanent crops (like palm oil in southeast Asia) disrupts the soil structure causing water drainage, oxidation of underground organic matter and eventually release of CO_2 and N_2O into the atmosphere [8].

1.1.3 Fertilizers

Throughout history, fertilizers have commonly been used to improve crop yields. More recently, in the last century, synthetic production of fertilizers was discovered and massified letting farmers produce even more with less land. Despite the advantages of nitrogen (one of fertilizer's main nutrients) for plant growth, it has a large footprint on the environment. The manufacturing of nitrogen starts with the production of ammonia, which is a very heat-intensive process, therefore powered with fossil fuels and difficult to decarbonize. The application of these fertilizers is also reported to be excessive and inefficient, as plants only absorb half of the nitrogen from fertilizers applied to the soil [9]. The runoff nitrogen can contaminate waterways or end up as nitrous oxide gas released to the atmosphere. These contaminations are notorious in this sector, as seen in Figure 1, 78% of global eutrophication is due to agriculture. (Despite the increase of chemical restrictions on the agricultural soils in some developed countries, water pollution is still very hard to trace and give accountability for). Moreover, the presence of synthetic fertilizers in the soil disrupts the soil's natural microbial cycles and tends to cause loss of soil fertility. Synthetic fertilizer accounts for 20% of agricultural emissions and 2.4% of global emissions [10]. Not only there is a need to produce it more sustainably (using renewable energy or making organic fertilizers affordable), but also to improve the effectiveness of application and promote practices and crops that are less dependent on it.

1.1.4 Land Use and Deforestation

Furthermore, there is the problem of deforestation and land degradation. The pressure to feed a larger and richer world population brings the need for more land area for crop/livestock production. The destruction of natural forests and grasslands is a common procedure for this end, especially in the regions of South America and Africa [11]. The previous chart of Figure 1 show that half of the world's habitable land is already used for food production. Recalling National Geographic's prediction that food production needs to roughly double in 30 years, there is simply no space for it if we continue to grow as usual. With deforestation, not only does the forest's ability to capture CO_2 from the atmosphere disappear, but also all the carbon previously captured is often released in burnings. Massive agriculture companies opting for deforestation tend to use practices of mass monoculture production (single species cultivated in large areas for long periods), often more susceptible to disease and aggressive to the soil resulting in loss of fertile land. Crops like coffee, cotton, palm oil with a huge presence in international markets have a natural tendency to fasten the process of soil erosion [12]. Overall, these practices cause severe destruction of ecosystems,

disrupting pre-existing natural balances, losing land structure, and contaminating soil and water courses nearby. To fight unfertile soils and compensate low yields, more fertilizers are used, as well as more deforestation is caused, keeping unsustainable agriculture in a vicious cycle.

1.1.5 Food Transport and Retail

Another issue of the food supply chain is the centralized mass production of multiple crops that enable developed countries to have a high variety of food available all year round, which also requires constant transportation around the globe. Products like fruit and vegetables have a short expiration period which means international transportation must be the fastest, thus by aeroplane, (highly pollutant per mass transported). Transportation of fruit and vegetables has more impact than their production and transport accounts for 19% of total food-system emissions [13]. Moreover, the separation of food consumption and production points is increasing worsening the problem of pollution in food transportation. Even considering national markets, the production and consumption of food tend to be relatively distant. The rural areas are increasingly more dedicated to production and the urban (growing) centres to consumption. On top of that, there are entire industrial sectors dedicated to the processing, packaging, and retailing of food products that come with significant emission impacts. This is aggravated by immoral marketing campaigns, overconsumption, excessive food aesthetic standards and food waste. In cultures of excessive consumption and supply, such as in the United States, 30 to 40% of food is thrown away, letting to rot resulting in high amounts of methane being released [14].

1.1.6 Water Use

It is easy to forget how valuable water is when it is cheap and in abundance. Despite covering most of our planet's surface, only 0.3% is fit for human use/consumption, and even most of that is unattainable underground as soil moisture and aquifers [15]. Thus, it is worrying that food production alone is responsible for 70% of global freshwater consumption and that by 2030, the water supply is expected to fall 40% short of meeting global water needs [16]. Part of the reason for this high consumption of water in this field is the waste and contamination happening in farm and pasture applications. The irrigation methods tend to be inefficient either due to large availability of water and lack of regulation or due to lack of investment (mostly in poor countries often in water-scarce regions). These inefficiencies appear in traditional irrigation techniques, where most water escapes into the ground or evaporates before it gets absorbed by the plants. Proximity of irrigation to plants roots, scheduling, storage, and policies over water withdrawals and drainage are important subjects to be addressed to prevent social-economical water crises. Particularly on a planet with more frequent and severe climate catastrophes (like floods and droughts) [17].

1.1.7 Vertical Farming

One alternative method to produce food promising for its sustainable benefits is Vertical Farming (VF). This is a type of Controlled Environment Agriculture (CEA) where environmental parameters

such as temperature, humidity and light are regulated inside the farm for constant optimal conditions. In VF plants are usually staked vertically sharing water circuits which substantially reduces the amount of land and water used per crop compared to open field practices. This means that these production facilities can be implemented in urban centres closer to demand, eliminating long course transportation and waste. Controlling environmental conditions means seasonal crops to grow all year round and new crops to grow in different regions, all while eliminating the need of pesticides. The next section of Literature Review explains the historical context leading to VF in this industry, its real environmental impact and the causes of it.

1.2 Objectives and Research Questions

This study aims to develop and analyse a Light Emitting Diode (LED) dynamic control system for a vertical farm greenhouse facility in Lisbon. The system will contain light sensors measuring natural light and actuators controlling the artificial light intensity and timing of the LEDs. The system's algorithm will be programmed to identify different natural light conditions and command the LED operation accordingly. This way, certain targets of light can automatically be met regardless of weather conditions. These targets are expressed as the Daily Light Integral (DLI) which represents the quantity of light accumulated at the end of the day. The assembly, installation and tuning of the control system will be carried out in the first phase of this work, and a study on its impact on basil plants ("Gustosa" and "Pluto") under different DLI targets will be performed secondly to identify optimal DLIs for increased yield and minimal LED energy consumption.

The main points to be analysed regarding the lighting control system are:

- The functionality of the installed hardware components, namely light sensors, microcontrollers and LED dimmers.
- The accuracy of calibration of the AS7341 multi-spectral light sensors in providing measurements in DLI units.
- The reliability of the LED light intensity dimming method regarding precision of light intensity and energy performance.
- The performance and feasibility of an automated LED control system and algorithm with dynamic response to variable natural light patterns.

And for the plant growth performance study:

- Compare results of biomass and size growth for plants with different lighting strategies (DLI).
- Compare results of energy consumption between different lighting strategies.
- Identify the most energy-efficient strategy for each basil variety.
- Discuss limitations and possible add-ons to the hardware/algorithm in the scope of scaling up the solution.

Ultimately, the present work aims to answer the following research questions:

1. What's the optimal DLI target for a plant growing in an environment with mixed natural and artificial light exposure?
2. What are the advantages of the different LED lighting strategies on energy consumption?
3. How is the natural and artificial light influencing the development of basil plants in a greenhouse VF?

1.3 Structure of Thesis

This work is composed of seven chapters: "Introduction", "Literature Review", "Case Study – Raiz Vertical Farm", "LED Control System Assembly and Tunning", "Experimental Procedure and Performance Indicators" and "Results and Discussion" and "Conclusion and Future Developments".

The first chapter presents the motivation for the need to increase sustainable agriculture in the coming years, as well as the main goals of this report and the structure of the thesis.

The second chapter includes an extensive literature review starting with the history of sustainable agriculture practice, from regenerative agriculture to the technological advancements leading to Controlled Environment Agriculture (CEA), specifically vertical farms (VFs). The environmental footprint of CEA is assessed, and sources of emissions identified. A list of environmental parameters influencing plant growth are described together with their optimal ranges based on published studies. Special attention is given to the light quality and spectral composition. Equipment of CEA facilities and respective energy consumption is addressed at the end.

The third chapter describes the case study. It starts with the description of the partnering company developing vertical farm solutions – Raiz, their first farm where the experiment will be conducted, its location and describing the problem: Low-level control of the LEDs. Follows a detailed description of the farm materials, the crops cultivated and the energy consumption at the farm.

The fourth chapter explains all the equipment installation and tunning required to build the LED control system before beginning the experimental study. It covers the setup of the microcontroller, light sensor and LED dimming, as well as the final system setup and algorithm logic.

The fifth chapter describes the basil plant species cultivated and the environmental and cultivation conditions of the experiment. It provides a deeper explanation of the light condition at the farm and the different lighting strategies that will be implemented for three testing growing barrels.

The sixth chapter consists of the analysis and discussion of results including the performance of the dynamic LED control system and robustness of the algorithm for representative days, as well as the analysis of the experiment results of energy consumption and plant productivity characterized mainly by plant weight and size at harvest. Anomalies are identified and justified.

The seventh chapter will summarize the main findings of this work and suggest future developments for the scalability of the LED control system.

All the references consulted for this report can be found at the end of the document.

2. Literature Review

2.1 Historical Context - Innovations in Agriculture

The issue of unsustainable agriculture and food security is very complex, and each region has its own specific challenges. This problem cuts across social, economic, and political systems where multiple approaches and policies can be implemented to facilitate the sustainable shift. This study focusses on methodological and technological innovations that can contribute towards this end. Each application has its challenges, and a single solution cannot solve for all. Therefore, is crucial to understand the specifications of each case to identify the most suitable solution. Before discussing technological contributions to clean agriculture, it is important to note that some crop management techniques can bring significant benefits without high-tech investments. Recall one of the main issues previously mentioned soil degradation and harmful practices that lead to vicious cycles of soil infertility and CO_2 emissions. Regenerative Agriculture (RA) has the opposite effect causing a chain of positive events in the ecosystems that can lead to economic and social benefits. Some RA practices include [18]:

- **Crop rotation** - Growing commentary plants each year with different nutritional needs and root fixture can cancel each other's harmful effect on the soil and ecosystem.
- **Soil Amendments** – Organic materials like biochar, manure and compost can be upcycled and applied to the soil, changing its physical properties i.e., improving fertility and carbon sequestration.
- **Conservation Tillage** – Reducing or eliminating tillage practices (mechanically rummage of the soil) has benefits in water retention, microbial/plant relationships and carbon sequestration.
- **Multispecies Coexistence** – Ranching livestock with regenerative crops, growing trees with companion crops, integrating livestock in forests are alternative ways of producing that promote biodiversity, soil fertility and avoid emissions.

Regarding water use, techniques such as drip irrigation (developed in 1959), can increase the efficiency of root water absorption significantly. This method allows plants to absorb 95% of the water applied compared to 50% of traditional sprinkler systems. Despite its advantages, only 5% of global farms use this type of irrigation [19] due to lack of investment and/or water being inexpensive. More recently, hydroponic, aeroponic and aquaponic systems can bring significant reductions in water consumption. These techniques consist of growing plants without soil. Hydroponic systems submerge plant's roots in water with appropriate nutrients and pH levels. The water that is not consumed by the plants can be recirculated and saved for later use. Aquaponics is very similar to hydroponics, but the nutrients originate from the waste produced by farmed fish and other aquatic animals, rather than being synthetically added in the water. Furthermore, the aeroponic process is where a plant's roots are suspended in the air and sprayed with a water mist rich in nutrients. These techniques are claimed to reduce water consumption by 98% compared to open-field agriculture, as well as offering other benefits in efficiency of nutrition,

climate control and pest control [20]. Nutrients like nitrogen can be added directly to the water and be absorbed more efficiently, reducing nitrous oxide emissions to almost zero [21] Collecting evaporated water for reuse is another measure being done in indoor/greenhouse applications to reuse and reduce water consumption [22].

Another field where scientific development can help agriculture is in specific breeding and artificial genetic manipulation. Breeding the most efficient and resistant crops and animals is an ancient practice to improve yields and resistance to diseases. Today, crops produced by large industries are usually the most optimized varieties available. However, it is important to increase their availability in underdeveloped regions that never had access to them and where food production needs to increase the most in the next years. The subject of genetically modified organisms (GMOs) is target of some controversy. On one hand, plant genetics are modified to resist pests and insects meaning less pesticides used, better yields and less land use, on the other, there are still health and safety concerns about molecules that are added [23].

Regarding technological contributions in the cultivation fields, the last century's advancements in machinery have helped expand the scale, speed and productivity of crops leading to more efficient cultivation with less dependence on physical effort. On the other hand, this same machinery is most likely fossil fuel powered, thus adding to the environmental problem of CO_2 emissions. Innovation in this sector is enabling the electrification of machinery, as well as integrating digital technology that improves resource efficiency and rational use. The advancements in satellite technology, like GPS, allowed better mapping and tracking of field performance and better weather examination. Drones and other robots allowed further automation of farm tasks like seeding, spraying, and harvesting in a more precise and intelligent manner. In a sector characterised by intensive and expensive labour, this automation comes with economic advantages by performing difficult tasks around the clock [24]. The more recent advancements in digitalization allow connectivity of farmers with the crops and with other stakeholders in an unprecedented way. In this field of "Smart Farming", technology can monitor crops, analyse multiple variables, and optimize resource utilization. Integrating sensors of temperature, moisture and soil/crop composition, together with data analytic intelligence, allows farmers to make the best decisions on water, fertilizer, and pesticide use [25]. Image recognition technology is another example where artificial intelligence can make early detection of diseases or sub-nutrition allowing timely intervention, avoiding spread and production losses. The amount and variety of data that can be processed is huge, from environmental conditions to market trends, allowing predictive models that have never been so accurate. Additionally, supply chain transactions can also be optimized for food security, quality, and transparency. These new technologies can upgrade decision-making, allowing better risk and variability management, optimizing yields, and improving economics. All this improves productivity while minimizing waste, cost, and environmental impacts [26].

Despite the huge potential of these smart technologies, their application in the agriculture sector is happening slower compared to other industries. Firstly, it requires certain power and

telecommunication infrastructure to allow connectivity. This isn't the case in most developing countries in charge of a large part of global food production. Secondly, this technology had to be sufficiently proven for a wide range of crop species and environmental conditions, which is a timely process. Moreover, its cost-effectiveness can be hard in small-scale applications [27].

2.2 Controlled Environment Agriculture

Following the digitalization trend in agriculture appeared the will to further control environmental conditions such as temperature, humidity, light and CO_2 levels that plants are exposed to. Controlled Environment Agriculture, therefore, appeared as an interesting solution enabling farming in a controlled and contained space, resulting in climate-resilient and season-independent production [28]. This technological push allowed agriculture to shift to new areas, particularly urban, tackling the issue of available (fertile) land, transportation needs and food losses in the entire chain. There are many types of CEA facilities: advanced greenhouses, vertical farms, rooftop gardens (RTG) and plant factories (PF) [29]. These conditioned farms tend to have advanced technological systems for high control and manipulation targeting the needs of specific plants. This ensures higher volumes, better quality, and more predictability of harvests [28]. Inside a single farm there can be different environmental conditions applied for crops in different areas allowing flexibility of cultures in the same building. These spaces are also better protected against pathogen contaminations from surroundings, which rarely happen with correct sanitary practices [30]. Plants are often grown vertically for space optimization, allowing much higher yields per meter squared. In a new generation of indoor vertical farming (VF) developed by NASA in 2021, water consumption was reduced by more than 99% and the area of cultivation by 99.7% [31] compared with traditional methods.

2.2.1 VF Environmental Footprint

Vertical Farms are the most common CEA facilities representing around 70% of the market share [32]. Despite the advantages of VF, this practice can still result in high CO_{2eq} emissions per kilogram of crop produced compared to more traditional systems. Looking at Life Cycle Assessments (LCA) of crops grown in VF, the carbon footprint is minimized for transportation, heavy machinery use, and fertilizer/pesticide use [28]. However, they can have very high electrical energy consumption to achieve optimal conditions indoors regarding temperature, light, humidity, and ventilation. Depending on the sources of electricity, VF can represent much higher emission levels than traditional greenhouses and open-field agriculture. The study [28] shows an LCA of lettuce produced over different methods, and a sensitivity analysis for different shares of renewable energy in the electricity mix. Table 1 shows the average carbon footprint, in $kg_{CO2eq}/kg_{lettuce}$, associated with VF production of lettuce in Scotland according to the national electricity mix situation, taken from [28].

Table 1 - Average emissions in $kg_{CO2eq}/kg_{lettuce}$ of VF in years with different RE penetration based on [28]

Year/Scenario	RE Penetration	Emitted $kg_{CO2eq}/kg_{lettuce}$
2019	90.1%	1.49
2020	98.6%	0.42
Fully Renewable	100%	0.33

It is noticeable the importance of the electricity source in the environmental impact of VF. Providing full power from renewable energy has shown a carbon footprint average of 0.33 $kg_{CO2eq}/kg_{lettuce}$ and minimum of 0.16 $kg_{CO2eq}/kg_{lettuce}$ according to [28] in agreement with [33]. Looking at Table 1, a 10% penetration of non-renewables (like in 2019) can increase the carbon footprint by almost five-fold compared to a fully renewable scenario. This high sensibility means that VF environmental performance can rapidly rise to 6 $kg_{CO2eq}/kg_{lettuce}$ (6000 $kg_{CO2eq}/ton_{lettuce}$) for a mix with low RE penetration [33]. Figure 2 is taken from the study [33] and shows the average emissions in kg of CO_{2eq} per ton of lettuce produced for the different systems.

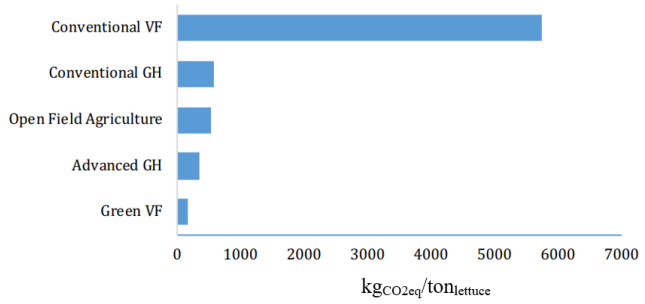

Figure 2 - Average CO2 emissions [kgCO2eq] per ton of lettuce produced for different farming methods (VF – Vertical Farming; GH – Greenhouse) [33]

Conventional VF represented here is based on 2018 average energy consumption in a wide scenario containing a mix of natural gas, coal, or non-renewable energy sources from multiple regions of Asia, northern and southern Europe and the Americas. Exact values of renewable share in the mix are unspecified. Nonetheless, in the global context, it gives a clear idea of the severe impact of VF without clean electricity supply, which can be up to 10 times worse than open-field, as shown in Figure 2. On the other hand, by adopting renewables as the only source of energy ("Green VF"), emissions can drop 97% from 6.424 to 0.158 $kg_{CO2eq}/kg_{lettuce}$. It is important to note that open field production reportedly represents averages of around 0.5 $kg_{CO2eq}/kg_{lettuce}$ [28, 33] and greenhouse production (without heating) can reach 0.25 & 0.35 $kg_{CO2eq}/kg_{lettuce}$ [28 & 33] or 2.94 $CO_{2eq}/kg_{lettuce}$ (with heating) [28].

Depending on the case, VF may or not appear as the best agriculture alternative to reduce emissions. Factors that can reinforce their position as a sustainable agriculture solution are energy efficiency, rational use, and recovery, together with renewable energy penetration. These cover 98% of the emission reduction potential [33]. Incorporating renewable energy in the grid or in a local system is crucial to drop the carbon footprint of controlled environment crops. Not only

are governments pledging to reduce fossil fuel use, but also, businesses are adapting to become more sustainable intrinsically, leading to their own decentralized renewable energy production, (ex: photovoltaics). At the same time, it is important to minimize energy consumption without compromising crop health and yield to fully explore the benefits. Note that around 90% of emissions associated even with the “greenest” vertical farms come from electrical energy consumption and therefore, optimizations here are very significant for overall impact. Passive strategies should be explored for energy conservation, especially when outside conditions, like natural light and temperature, align with the plant’s requirements.

When VFs are implemented sustainably, CO_2 emission reductions can be as high as 70% compared to traditional open field practice [33]. Figure 3 taken from [33] compares maximum and minimum carbon footprint, and its sources, of current methods against green VF, in $t_{CO2eq}/t_{lettuce}$.

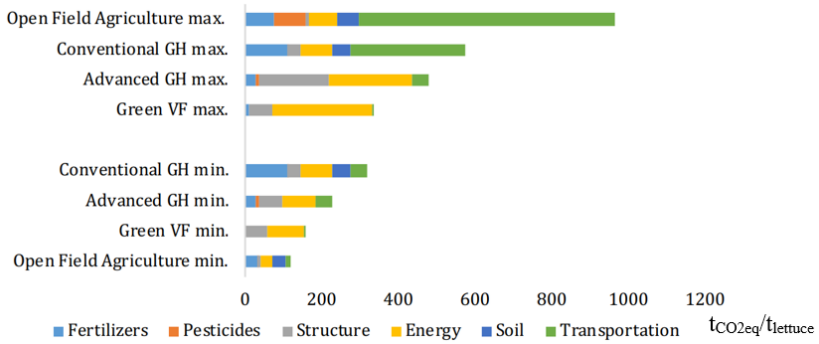

Figure 3 - Distribution of CO_2 emissions per ton of lettuce for Green Vertical Farming, Advanced Greenhouse, Conventional Greenhouse and Open Field Agriculture (32).

There are clear reductions in transportation emissions (80-99% less), in fertilizer, where traditional N_2O and CH_4 emissions from the soil are eliminated (the only potential impact is in their transportation and production) and pesticides are (ideally) eliminated. The impact represented on the graph associated with newly built infrastructure can be highly damped by retrofitting abandoned buildings or other unused spaces in cities. There is also the advantage of reduced waste losses with VF, which traditionally represents around 30% of total food production. These, correspond to on-farm losses, nonmarketable crop, retail and transportation losses. VF can almost eliminate food waste (reducing it to 1-7%) from farm to distribution centres through a uniform, year-round and highly marketable production. This improves efficiency of production, minimizes resource consumption, and consequently reduces the carbon footprint.

There is a large deviation from case to case though. Depending on distance of transport, energy efficiency, pesticide and fertilizer usage, conventional techniques may compete with green vertical farms at emissions levels. However, regarding other environmental aspects like water and land use, there is a unanimous agreement in literature that VFs are much more beneficial in all scenarios, showing reductions of at least 90% in both. From the analysis of [33], water use efficiency can be as low as 4 L/ $kg_{lettuce}$ (vs 60 L/$kg_{lettuce}$ open field) and yield per acre of 2400 $t_{lettuce}$/ha (vs 23 $t_{lettuce}$/ha open field).

2.2.2 Growth Environment Parameters

To understand the high electricity consumption of CEA facilities, it is important to assess exactly what is the energy being used for. Plants are very complex biological systems where environmental factors influence biochemical processes through multi-variable, non-linear correlations that are specific to each species [34]. Follows an investigation of the main environmental parameters that influence plant growth, specifically basil plants which are the most relevant for this report's analysis. Temperature and humidity are investigated to a basic level and light to a deeper level to understand their role and how much control these require. Other environmental factors also affecting plant growth include CO_2 concentration in the air, air-current speed, nutrient solution, water pH, and root-zone conditions [35] that will not be reviewed in this work.

2.2.2.1 Temperature

In general, plants have a minimum (or base), maximum, and optimal temperature of growth [36]. Temperatures outside of this range can stop plant development or even harm the plant and compromise productivity when critical levels are passed. Moreover, studies often report a saturation temperature, representing a limit temperature for optimizing a certain performance indicator (ex: plant fresh mass). Surpassing it does not necessarily mean unhealthy plant development. Temperature has important functions in chemical processes like rate of cell division, photosynthesis and transpiration, consequently affecting plant maturation, flowering, fruiting and seeding for most species [36; 29]. The rate of these processes tends to be proportional to temperature until optimal (saturation) levels are reached, meaning that higher temperatures (within the limits) favour them [36]. Furthermore, temperature has different effects on plants depending on the phase of maturity and period of the day (day or night). Many studies like [37, 38, 39] opt to subject plants to different temperatures for day and night. This parameter is referred to as DIF in [39] and represents the day minus the night temperature. It is claimed to be beneficial compared to constant temperatures due to facilitating plant respiration during cooler night periods [40]. Optimal temperature levels despite being species-dependent, are also dependent on other conditions like light intensity and wavelength, humidity, CO_2 concentration, etc [41]. This multi-variable dependency can be challenging, however for most experiments in literature other parameters are kept at a standard level to find optimal temperatures. Similar is done with humidity and light analysis. For basil plants, the optimal ranges of temperature targeted according to literature differ for day and night. During the day it is recommended to keep indoor temperature between 18 and 30 ºC to avoid unhealthy development [42] [43]. However, to boost basil plant's growth is recommended to keep temperatures on the higher end of this range, usually around 25 ºC [44] [45]. During the night, the temperatures are recommended to be lower around 13 to 25 ºC, which corresponds to a DIF around 5 ºC.

2.2.2.2 Humidity

The humidity level is another determinant variable of plant's development. Similarly to temperature, there are also minimum, maximum and optimal levels of humidity for each plant species. It has roles in the multi-variable chains of chemical events that define plant's physiology at different maturity stages. Relative humidity is the preferred method of measuring this variable in the literature, combined with temperature and vapour pressure influence crucial molecular reactions in the plant's organism [46]. Humidity affects the transpiration rate where dry environments promote the release of water vapour through the leaves and humid ones promote water retention [34]. Healthy root development also depends on adequate humidity levels, where low humidity can cause water stress, damaging the root and overall plant. Flowering and fruit deployment are also known to be triggered by specific humidity levels. Moreover, high humidity levels are beneficial for fungal pathogens to develop and potentially infect plants with diseases like mould and mildew [47]. The recommended levels for optimal basil growth are reported between 50 and 75% [34] [48].

2.2.2.3 Light

Light is the primary driving force for all photosynthetic plants. Light fuels multiple processes of plant growth, development and physiology, like root growth, flower production and vegetative growth. A principal reason for this is that light enables photosynthesis supplies the energy needed to fix carbon and build biomass, as well as plays an important role in health metabolisms [49].

Regarding the evaluation of the effects of light in plant development, there are two main directions of study, hereby addressed as the light quantity and light quality. Light quantity is related to the number of light units reaching the plant and light quality to its spectral composition. In the botanical context, light quantity is measured in units of flux of photons impacting per area and time frame. The quantity of light received by a plant is directly related to the light intensity, direction and duration of light shed [49]. The latter is referred in literature as the photoperiod, which consists of the period of light hours during one complete day. Regarding the intensity of light, botanical studies mostly analyse the effects of the Photosynthetic Photon Flux Density (PPFD) in $\mu mol.m^{-2}.s^{-1}$. It represents the amount of light photons in the Photosynthetic Active Radiation (PAR) radiating per area and second. The PAR is the only band of light radiation that plant organisms can use in the process of photosynthesis and it has spectral wavelengths between 400-700nm (similar to the visible spectrum) [50]. The light quantity can be referred to merely as Photosynthetic Photon Flux (PPF), in $\mu mol.s^{-1}$. This approach disregards spatial considerations and is more often a property defining the source of light emission. This report will address light quantity as PPFD. The other important aspect, the light quality, is the spectral composition of the light radiation, which corresponds to the frequency/wavelength of the light wave. This report will focus on light mostly in the visible part of the spectrum (PAR) but ultraviolet (UV) and infrared (IR) radiation will also be accounted for. In botanical studies, light quality is usually measured in ratios of specific wavelength bands (colours, UV or IR) relative to others (ex: Red:Blue – 3:1), represented by different graphical "light curves" in the spectrum.

2.2.2.3.1 Light Quality

It is documented that plants subjected to different colours show different developments and exposure to radiation outside the visible spectrum can also influence plant behaviour [51]. Different classes of photoreceptors perceive radiation wavelengths corresponding to blue (B, 445–500 nm), green (G, 500–580 nm), red (R, 620–700 nm), far-red (FR, 700–775 nm) and ultraviolet (UV, 300-400 nm) [52]. Since the last century it has been demonstrated that, for most plant species, the most useful wavelength for photosynthesis is in the blue and red regions, as these trigger the key genetic signals in the plant's physiological and metabolic systems [53]. Plenty exposure to red light generally enhances plant's leaf size, main branch development, flowering, and seedling. Light with this composition (characteristic of spring and summer seasons) promotes the absorption of chlorophyll which consequently increases the rate of photosynthesis [54]. Light of blue composition is characteristic of autumn and winter and has important roles in phototropism (movement towards the light) [55]. It is claimed to trigger the development of side stems making plants shorter, wider and bushier. Moreover, it influences the opening of stomas resulting in the acceleration of the metabolism and overall development [51]. The importance of the presence of these two light colours in plant health and productivity seems unanimous in literature for most species, but the recommended blue and red ratios vary. Table 2 sums up several article studies about the effects of blue and red light on different plant species (common in indoor farming) and the main findings.

In the extensive studies on blue (B) and red (R) light influence, the addition of a smaller percentage of B to the R light is claimed beneficial in multiple cases. It is also noticeable in the literature that the same B/R ratio shows different results for different total light intensities, calling attention to the absolute quantities in addition to the ratios. The B/R ratio should be chosen in function of the species grown, intensity of light in the application and even phase of maturity.

Table 2– Articles studies and their main findings on the effect of blue and red light on different crops.

Reference	Crop	Findings
[54]	Lettuce	Monochromatic red light shows better growth of lettuce than monochromatic blue light, both worse than with a certain combination of red and blue.
[56]	Spinach	The addition of a smaller percentage of B to the R light improves transpiratory control in spinach.
[57]	Strawberry	The addition of a smaller percentage of B to the R light gives bigger strawberry fruits with higher sugar content.
[58]	Tomato	Shown that the plants behaviour is more related to the absolute blue light intensity rather than the B/R ratio.
[59]	Lettuce, spinach, kale, basil, and Sweet Pepper	Hypothesized that B requirements vary with the age of the plant according to the phases of growth.

Exposures to the far-red part of the spectrum have also been documented for their benefits in increasing fruit weight and plant size [60]. It was also claimed that the FR presence in tomato cultivation affects the leaf orientation and stem architecture [61]. This exposure resulted in less

leaf self-shading, and consequently better light penetration and more efficient use of light. Ultra-violet radiation from sunlight that reaches Earth's surface can be divided into UVA and UVB, corresponding to 320-400nm and 280-320nm wavelengths, respectively. UVA does not have any harmful effect on DNA, as opposed to UVB which rarely reaches Earth's surface. Single UVB radiation was reported to cause reductions in photosynthesis and biomass [62], although UVA has been reported to have positive effects on plant development. UV light supplements have been shown to enhance resins and oils concentrations, as well as prevent stress and biotrophic diseases [63]. Green light has been documented to bring certain advantages to plant development, but to a much lesser extent, as uncertainties in the biochemical processes are still frequent. Statements of increased shade avoidance and regulation of secondary metabolisms through G light exposure were documented in [64]. There is an indication that plants lack receptors for this colour, as plants grown with monochromatic green light are extremely weak [51]. Another aspect analysed is the effect of light in final maturation phases known as End-Of-Production (EOP), claimed important in vertical farming [65]. In this article is shown that subjecting basil plants to far-red EOP enhanced the fraction of dry mass in the leaves, as opposed to prolonged explosion, which promoted stem growth.

2.2.2.3.2 Light Quantity

As mentioned, regarding the light quantity that reaches plant's leaves, the photoperiod and light intensity are identified to be the key properties in regulating plant growth. There is extensive research on their influence noting that productivity tends to increase with the amount of light, although with limitations and specific to each plant species.

Regarding the photoperiod and light intensity, minimal variations can trigger significant shifts in physiological responses such as flowering, stem growth and bud development [66]. According to the flowering process, which can be a significant indicator of plant's productivity, there are basically three types of plants: long-day; short-day; and day-neutral. Long-day plants require more than 12h of light to flower, these are often seen blooming during spring/summer season. Short-day plants start flowering when exposed to less than 12h of light per day and day-neutral ones are independent of the day length to flower [67]. This definition assumes similar light intensities between them. In the literature, analyses on light quantity treat photoperiod and PPFD (intensity) as interdependent. Generally, what matters for the studies is a parameter containing information from both photoperiod and PPFD, called Daily Light Integral (DLI). That defines the total amount of PAR photons inserted per area, accumulated throughout the entire day [$mol.m^{-2}.d^{-1}$]. The DLI, therefore, depends on the photoperiod (duration) and PPFD (intensity) of light. Figure 4 represents the usual correlation between DLI and plant growth. As with other environmental parameters, insufficient DLI results in untapped plant growth potential while excessive levels mean wasted energy and potential plant damage. The optimal or saturated DLI level is the point of best plant performance to which increments show no significant improvements.

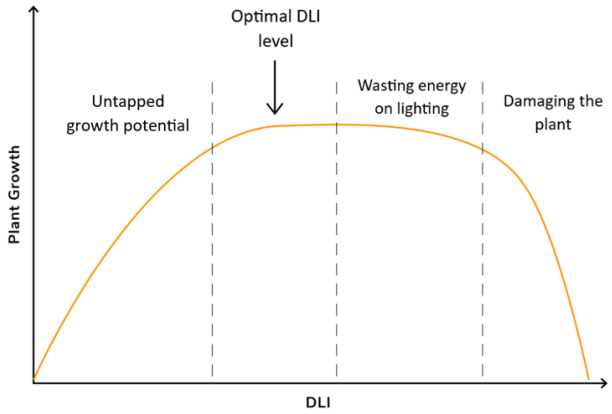

Figure 4 - Relation between plant growth and DLI [68]

Table 3 shows a list of several article studies about the effects of photoperiod and PPFD (and resulting DLI) on different plant species and the main findings.

Table 3 - Articles studies and their main findings on the effect light PPFD and DLI on different crops.

Ref.	Plant	Findings
[69]	Lettuce	Considers four light intensities and two photoperiods, suggesting ideal growth for a 16h photoperiod with a PPFD of 250 µmol.m^{-2}.s^{-1}, (DLI = 14.4 mol.m^{-2}.d^{-1}).
[70]	Basil	Compared three photoperiods (13h, 14h and 16h) at constant intensity (not stated), showing best results for 16h photoperiod in leaf area, height, shoot weight. 14h photoperiod is the most energy efficient (similar results with less energy).
[71], [72]	Lettuce	Both reported that the preferred photoperiod range is between 16- to 20-hour light.
[73]	Rosemary and Spearmint	Claimed results were similar with PPFD from 200 to 800 µmol.m^{-2}.s^{-1}, when there was no water stress on plants.
[74]	Basil	Three species of basil grew with a 16h photoperiod with irradiances of 300, 400, 500, and 600 µmol.m^{-2}.s^{-1} from cool-white incandescent lamps. Edible biomass peaked at 500 µmol.m^{-2}.s^{-1} (DLI = 28.8 mol.m^{-2}.d^{-1})
[38]	Basil and Lettuce	Basil and Lettuce grew at photoperiod of 16h and five PPFD regimes 100, 150, 200, 250 and 300 µmol.m^{-2}.s^{-1}. Peak of biomass production for both lettuce and basil at PPFD of 250 µmol.m^{-2}.s^{-1}(DLI = 14.4 mol.m^{-2}.d^{-1}). Most energy efficient results for 200 (lettuce) and 250 µmol.m^{-2}.s^{-1} (basil)
[75]	Basil	Develops a photosynthetic model of sweet basil cultivated under 20 ºC and 18h photoperiod based on CO2 assimilation rate. LEDs with blue:red ratio of 3:7. Light saturation point for photosynthesis was 545.2 µmol.m^{-2}.s^{-1} (DLI = 35.3 mol.m^{-2}.d^{-1})
[39]	Basil	Analyses the impact of four light intensities through different shading states for sweet basil. Concludes that the peak benefits in fresh weight are for a DLI of 13.5 mol.m^{-2}.d^{-1}.

These findings are the most important for the scope of the present work. Recall the importance of addressing overall environmental conditions since the results of plant development are always linked to multiple factors and dependent on their combinations. As for the temperature of the air in the growing chambers of the previous experiments for basil (most relevant plant for this work), the most common values were around 25 ºC, always in the range of 20-29 ºC for daytime. The DIF parameter (day minus night temperature) is kept around +5 ºC, ranging from +4 to +7 ºC.

Regarding relative humidity for basil studies, it is usually kept around 65%, ranging between 55-75%. The CO_2 concentration in the grow chambers is another parameter that hasn't been reviewed but is also influential for plant development. In Table 3 cited studies, basil was kept at an environment CO_2 concentration around 450 ppm, ranging from 350-650 ppm.

The optimal values of light intensity (Table 3) are taken for plant/leaf fresh mass or edible biomass mass maximization. These performance indicators are considered the most relevant in the context of commercial vertical farming. The lighting growth conditions tend to consist of LEDs with a spectral composition of red and blue light (and sometimes others) with red:blue ratios between 2 and 3. From the main findings of Table 3 on basil, it can be concluded that the optimal light intensity is a photoperiod of 16h (and 8h of darkness) together with a PPFD between 234 to 545 $\mu mol.m^{-2}.s^{-1}$ (DLI = 13.5 to 31.4 $mol.m^{-2}.d^{-1}$). Most studies report productivity peaks suggesting an ideal PPFD of between 200 and 300 $\mu mol.m^{-2}.s^{-1}$ for multiple varieties of basil, meaning a DLI between 11.5 and 17.3 $mol.m^{-2}.d^{-1}$ is more likely to be in the optimal range.

One parameter used in literature is the biomass growth efficiency per received light which measures how efficiently plants utilize light photons to produce biomass, in units of plant biomass per amount of light (DLI) received, ($g.DLI^{-1}$). This is a parameter to maximize for yield improvement, as well as energy consumption reduction of artificial lighting. The study [76] investigated the growth of basil plants under nine lighting regimes with a mix of natural and artificial light, observing biomass efficiencies with an average through the year from 1.89 to 4.37 $g.DLI^{-1}$ per plant for different amounts of artificial light complements, with higher efficiencies shown for higher percentage of natural light relative to the total light received.

2.2.2.3.3 Other Light Aspects

There are other sub-aspects of quantity of light that have been manipulated in the literature for plant development optimization, such as the light period (duration of a complete light cycle, with 24h default) [77] and the dark period [40].

- Day Period

The manipulation of the day period corresponds to the modification of the diurnal period duration, meaning the light/darkness cycle will restart after a particular number of hours instead of the usual 24 hours. The shorted or elongated periods are named non-circa days and influence plant's behaviour. It has been reported in [78] pine seedlings growing better in a natural 24h period (ex: 12L:12D light/dark) compared to non-circa days of equal L:D ratios with different timings (ex: 10L:10D or 14L:14D). The study in [79] addressed the effects of different light periods on lettuce growth. Unlike the previous, this analysis shows the effects of the same number of light hours per circa day (photoperiod) but divided in two 9L:3D or three 6L:2D cycles. The 9L:3D cycle showed highest fresh shoot weight while the 6L:2D cycle showed greatest leaf width. Similar manipulation of period and L:D ratio, the [80] investigation on lettuce crops analysed light period variations from

18 to 24 hours, with a constant 16h photoperiod. The results showed shorter periods had the best growth although higher energy consumption.

- Dark Period

While the period of light is stablished important for critical processes like photosynthesis, so is the period of darkness for plant respiratory and metabolic functions. The optimal period of darkness is, again, specific to species and dependent on other factors. Generally, short-day plants will not develop properly with less than 14-16 hours of darkness, and long-day plants require 8-10 hours [40]. The study [74] reports that having basil under a constant 24-hour irradiance resulted in stunting, chlorosis and leaf deficiencies, justifying that for normal growth these plants need a period of darkness. Having excessive darkness is equivalent to insufficient light which, as previously seen, is undesirable. The search of the optimal dark period for 24h days is implicit in previous findings of the optimal photoperiod, as it will be the remaining time of the 24 hours. It has also been stated in [55] that the flowering of certain species can be manipulated by artificially controlling the dark periods into short/long days for a certain result. More interestingly, this manipulation can simply consist of flashing light in the middle of the night for some seconds, avoiding shifting the entire light cycle.

2.2.3 Energy Consumption

As previously mentioned, energy consumption in VF is responsible for most of its carbon footprint. Follows a review of energy equipment used at these facilities and the tendency of energy needs and consumption. The study cases in literature provide a view of the state of energy efficiency per growth area and plant yield, the main limitations, and points of improvement in this industry.

Energy Equipment

Usually, in a controlled environment agriculture facility, there are mechanical, electrical, and thermal control systems responsible for lifting/rotating platforms, lighting, heating/cooling, ventilation, dehumidification, air/water fertigation, irrigation, and osmotic systems (to purify water). These are composed of equipment such as LEDs, vents, air conditioners, heaters, dehumidifiers, pumps, lifts, CO_2 and nutrient injectors and water filters, amongst others. The hardware is often linked with sensors, actuators and controllers that enable an automated precise operation, maintaining the indoor environment at optimal conditions for plant growth [81] [31].

LEDs are the lighting technology dominating this sector due to their high energy efficiency, longevity, and declining cost. These lighting systems can last for 5-10 years with 55% electricity-to-photon efficiency (compared to 5% in incandescent light bulbs) still with theoretical potential improvements of an additional 25% [82]. Moreover, LEDs are highly programmable in terms of light intensity (dimmable), colour spectrum and timings for automated precise operation. The spectral composition can be targeted from 250 nm (ultraviolet) to 1000 nm (infrared) allowing any distributions. LEDs of different colours can be combined to obtain a tailored light spectrum at the desired intensity and duration to modulate the different plant functions, providing a useful tool to

control plant growth and photomorphogenesis [83]. These are powerful advantages for indoor farming operations, eradicating traditional fluorescent and incandescent lighting. Their use in indoor farms is highly dependent on whether the structure allows natural light penetration, such as greenhouse facilities. Alternatively, plant factories meet their lighting needs exclusively using artificial lighting. Some studies explore the advantages in energy savings of having pulsed LED lighting as opposed to continuous illumination. This is a dimming method called pulse width modulation (PWM) and is characterized by turning on and off the LED at very high frequencies (kHz). Each ON/OFF cycle is called a duty cycle with a defined portion of ON and OFF state indicating the dimming level. In the study [19], the amount of energy (PPFD) supplied to the plants was equivalent between two modes, pulsed and continuous, but the electricity consumption was less for the first. The plant's production was not affected (since the PPFD received by the plant was the same) and the energy consumption [kWh] was reduced by at least 12% in 8/10 cases.

Regarding thermal control, to satisfy cooling needs, air conditioning and refrigeration systems are the dominant solutions for greenhouse VF cultivation. Indirect Evaporative Cooling (IEC) technologies are claimed more energy efficient by eliminating the need for a compressor [31]. Technologies such as evaporative pads and fogging systems can be considered, although with some impact reported on the uniformity of indoor temperature and relative humidity. Forced-air heaters and aerial pipe systems may be used in greenhouses to prevent unwanted low nighttime temperatures [31] or even during the day for more severe climates [84]. The heat generation source may vary from efficient heat pumps, district heating to gas boilers depending on economic and climacteric constraints.

Regarding ventilation, it has important roles in cooling and dehumidifying the growing space and its effectiveness is dependent on outdoor conditions. It also enables air circulation and negative pressure inside preventing accumulation of unsafe chemicals and pathogens. Exhaust fans are the commonly used active methods and their size depends on the crop species. Dehumidifiers and dryers can also be present to control humidity levels.

Energy Consumption

A study [81] published by the company iFarm, deconstructs the energy consumption at their farms. According to iFarm, generally for farms using exclusively artificial light from LEDs, lighting represents around 55% of the total consumption, air conditioners 30%, dehumidifiers 10% and the remaining devices use less than 5%. The reported total annual consumption per growing area to grow Romaine Lettuce is 918.6 kWh/m^2/year and for strawberry cultivation is 1497.8 kWh/m^2/year [81]. According to [82], an operation using exclusively artificial light of LEDs, expects lighting to account for 50-65% of the electricity costs, depending on factors like equipment efficiency and crop lighting needs, which can more than double from one crop to another.

The study [84] analyses six study cases of CEA applications with glass facades and proposes optimal designs for potential net zero energy applications in seven locations in the USA. The analyses of these potential farms considered dimensions of 710 m^2 of ground area by 4.5m height

of cultivation space, and general environmental requirements for lettuce, herbs, and micro-green crops. The total energy consumption of these facilities was estimated between 859317 to 1820267 kWh/year, depending on the climate conditions of the region (corresponding to 1210 to 2564 kWh/m^2/year). Climate factors are shown to have a significant influence on the energy consumption due to wide variations in energy spent on thermal regulation. In places like Austin and Sacramento, the heating energy needs are relatively small and less than cooling ones. For these locations, both represent around half of the total energy consumption. In colder regions of Minneapolis and Rochester, the heating needs alone represent 2/3^{rds} and cooling only around 1/18th of total energy consumption. Lighting energy needs remain approximately constant for all cases, varying from 13 to 30%. Regarding the consumption of ventilation systems, it also remains constant for every case, representing between 10 and 20% of total. The remaining equipment is responsible for only 2 to 5% of the total consumption. Noticeably, these greenhouse facilities (with transparent glass envelope) require higher energy in thermal control and less in artificial lighting. The total energy consumption per growing area also appears higher than other case studies.

Another study [31] developed on a plant factory (no natural light penetration) reported an annual energy consumption of 17382.4 kWh for 783.8kg of annual production. Lighting accounted for 69.9% while HVAC contributed to 27.9% of the annual energy consumption. The study [85] investigates a lettuce VF facility and potential energy cost optimization strategies. This facility has a growing space of 150m^2 (10 800 kg/year) and its energy consumption was indicated to reach approximately 130 000 kWh/year (or 867 kWh/m^2/year). Lighting appeared as the main source of energy consumption, especially in warm months, reaching 75% maximum. The [86] analysis of the operational costs of CEA facilities can be an approximate indicator of the energy consumption trend. The study found that electricity is one of the greatest cost drivers (slightly above labour) representing 28% of total operational costs of this facility. Lighting accounted for most of the electricity costs (about 70-80%). Table 4 shows a list of the environmental factors that affect plant growth which require the most significant energy spendings, the most common equipment necessary to control these parameters and range energy shares of each, based on the values observed from the previous studies.

Table 4 – Environmental factors affecting plant development, equipment and energy consumption share.

Factor	**Equipment**	**Energy Share** [%]	
		Plant Factory	Greenhouse
Light	LEDs	50-80	15-30
Temperature (Heating)	Boilers, Furnaces, Heat Pumps, District Heating,	0-30	12-66
Temperature (Cooling)	ACs, Evaporative Cooling, Foggers	0-18	5-26
Relative Humidity	Dehumidifiers, Dryers and Humidifiers	10-20	
Air Flow	Ventilation	5-20	

Note that the energy consumption and shares values differ significantly according to type of facility (Greenhouse or Plant Factory), type of crop, equipment efficiency and the climate conditions, especially depending on the heating needs. Additionally, it becomes difficult to compare the absolute energy consumption values between different facilities per growing areas of the farm facilities as each has a different utilization of space and the actual (vertically stacked) growing areas are unclear.

The energetic consumption per mass of plant produced is more useful for making energy performance comparisons between farm facilities. The study [76] reported the energy consumption of the LED lighting systems in a greenhouse application growing basil plants under a yearly average natural light DLI of 9.90 $mol.m^{-2}.d^{-1}$ and different artificial light DLI supplements of 1.08, 2.16, 3.24, 4.32, 6.48, 8.64 $mol.m^{-2}.d^{-1}$. The average energy consumption per growth cycle was 20.25, 40.50, 60.75, 81.00, 121.5 and 162.00 kWh, respectively. Considering their reported average plant fresh mass final yield results, the observed biomass growth per LED energy consumption during a harvest cycle was from 0.30 to 1.83 g/kWh. This measure of energy efficiency in biomass growth in greenhouse applications tends to decrease for lighting regimes with higher use of artificial light since natural light (alone) is usually responsible for most biomass growth. Nonetheless, for scenarios with similar natural light conditions, this parameter can provide an indication of the efficiency of the LED light complements in plant yield. This is the case for the current work which analyses basil growth in a greenhouse farm facility with a similar average amount of solar DLI insertion for the experimental period and similar LED rated power per cultivation area, however, comparisons of this type are also dependent on the natural light condition, the total DLI regime applied, the disposition of the plants relative to the LEDs and characteristics of the equipment.

Energy Optimization

Optimizing energy consumption brings environmental benefits by reducing emissions, lowering operational costs of the most significant expenditure and may include production benefits if more efficient and precise technology is adopted. Adopting energy-efficient equipment, such as LEDs and heat pumps, is crucial to optimize consumption, together with rational use and operation to minimize energy waste. Energy reduction strategies for vertical farming include electricity-price response, which generally means shifting operations to off-peak demand night period when electricity is cheaper and greener. Passive strategies taking advantage of outdoor atmospheric conditions can bring significant energy reductions without the need for additional technology. These consist in coordinating the system needs with the outdoor environment factors, for example, using transparent walls and natural ventilation is a minimalistic way to take advantage of natural light seen in previous studies with potential to drop the lighting share from around 70 to 20%. Outdoor temperature/humidity should be explored when favourable, although daily and seasonal variations should be assessed for each application. Using free cooling can drop energy consumption in air cooling by around 25% with low external temperatures during the night [81].

2.3 Gap in Research

There is extensive research on optimal DLI levels for plant growth in controlled environment exclusively with artificial lighting as the source. These experiments are often carried out for a specific composition of LED light that remains equal throughout the study. On the other hand, studies on greenhouse VFs appear addressing energy consumption and other factors but lack specification on DLI targets (and precision in meeting them) when natural light is involved. The present work aims to perform a study on how DLI influences basil plant growth in a real-case greenhouse CEA facility with natural light penetration. The performance of the plants will be analysed for a light routine of fixed DLI targets met using natural light and complementary artificial light from LEDs.

A parallel goal of this study will be to assemble, install and tune the equipment necessary to develop a dynamic light control system with sensors and LED dimmers. The entire process of the system setup will be documented and analysed prior to the DLI study. The main aim is to prove the automated functionality of such system for a greenhouse application using inexpensive materials and fine-tuning methods for improved precision, energy efficiency and plant productivity in vertical urban farming.

3. Case Study - Raiz Vertical Farms®

Raiz Vertical Farms® is a start-up company of vertical farming with its first concept farm placed in Beato, Lisbon (Figure 5). It is one of the first companies developing smart farming solutions in Portugal and their first “flagship” farm is a proof of concept that food can be grown inside urban centres with a small fraction of the water and land resources. The establishment serves the local needs of multiple restaurants and markets since it was founded in 2021. The project is developing towards a more automated and intelligent farming solution, with the goal of reaching communities and organizations internationally. This concept farm serves as a learning tool for the community and for the company to improve the solution. Various challenges in horticulture, technology and scalability are still to overcome. Questions on the feasibility of growing different crops, the automatic control of the environment and the adaptability of the growing systems for different spaces are currently main concerns. The present study aims to contribute to the development of a dynamic light control system and further assessment of LED energy consumption and the impact of light on crop productivity.

Figure 5 - Raiz Vertical Farms® concept farm

The farm is composed of two containers, the lower contains the seed germination station, water reservoir and material storage, and the upper one is where plants grow in a controlled environment. This way, conditions such as temperature, humidity and light are maintained optimal for the crops to thrive, allowing seed-to-harvest cycles of about 45 days (for herbal plants like basil) throughout the whole year, regardless of the seasons. The translucent polycarbonate glazing walls of the growing container are also a distinguished feature of this vertical farm allowing natural light to reach the plants reducing the LED energy consumption.

3.1 Location and Climate

Table 5 shows the location of the farm in Lisbon, Portugal and some of the main climatic conditions of the region during winter and summer.

Figure 6 - Location of Raiz's concept farm in Arroz Estúdios.

Table 5 - Daily average, max and min values of temperature, shortwave (visible and UV) solar power and relative humidity conditions for the region during winter and summer [96].

Average Condition	Day duration [hrs]	Max. Temperature [^{o}C]	Min. Temperature [^{o}C]	Shortwave Solar Power (noon) [kW/m^2]	Relative Humidity (%)
Winter	10h 20m	16.8	10.2	0.38	78.6
Summer	12h 50m	25.5	16.5	0.95	72.0

The climate conditions in Lisbon are very beneficial for agriculture, characterised by high sunlight presence due to a large number of days with predominant clear sky condition (around 300 per year), long days and mild temperature/humidity throughout the year which promotes plant development.

3.2 Farm Facility

Figure 7 shows a schematic representation of the top view of the upper container where plants are grown in a controlled environment.

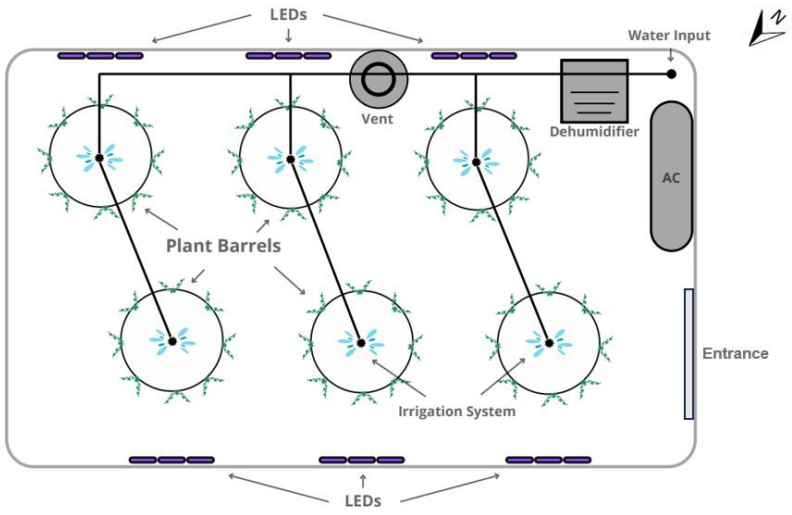

Figure 7 - Schematic representation of the growing container of Raiz's concept farm (top view).

The farm has a floor area of 14.4 m^2 (2.4x6.0m) and the crops grow vertically on the walls of cylindrical plastic barrels (2.0m high and 0.6m diameter) with hydroponic systems (i.e. without using soil). There are six barrels in the upper container and each one has 131 growing slots where one plant can be placed, giving a total of 786 potential plants. The total barrel growth area i.e., the lateral surface of the barrels is 22.6 m^2 resulting in a plant growth density of 34.8 plants/m^2 of barrel area. More importantly, the growth density considering the flat area of the farm is 55.7 plants/m^2, which indicates the efficiency of growth per urban space used. The next Figure 8 shows a growing barrel outside and inside view, used at Raiz's concept farm.

Figure 8 - Hydroponic plant barrel used at the farm. Outside view of barrel with herbal plants (left) and inside bottom view of barrel with vegetable plants (right).

This hydroponic system operates with water containing the required nutrients and PH being inserted on the top of the barrels through tubes and then dripping through the inside of its walls through the roots. The excess that is not absorbed by the plants is gathered at the bottom of the barrel and channelled to the water reservoir in the lower container. Afterwards, it is pumped back

up (to the water input of Figure 7), always circulating in a closed loop. In the water circuit there is also a particle and carbon filter that keep the water clean and a UV light purificator that prevents pathogenic microorganism appearance.

The growing container walls are made of polycarbonate translucent material to allow passing the natural light for plant photosynthesis. As seen in Figure 9, this material has a vertically striped composition and disperses the solar light rays entering the container, allowing a more uniform light distribution with reduced shadows inside of the container. These walls have a thickness of 18mm and visible transmittance, τ_v, of 0.66, allowing most of the sunlight to pass while blocking the UV radiation band potentially harmful to the plant's tissues almost entirely. The enclosure of the space with this material brings other advantages typical of greenhouses, such as warmer temperatures inside and protection against meteorologic harms and (some) contaminations.

Figure 9 Polycarbonate wall of Raiz's growing container.

3.3 Plant Crops

Regarding the plants cultivated at the farm, the focus is on the leafy greens, particularly different types of basil, as these are easily grown in hydroponic systems and have constant demand in the region. Additionally, there are larger vegetables like cucumber, tomato, okra, chilli pepper, aubergine and bell peppers growing and being successfully harvested. These must be placed in a separate barrel with an independent water circuit separated from the main one since they require different nutrients and water pH than the rest of the herbal plants. There are four types of basil growing in the herbs barrel and six vegetables in the veggie barrel. Other species like mustard, rosemary, spearmint, dill, jambu, red amaranth and pack choi are examples of plants that have been successfully cultivated at the farm before. Figuere10 a) to f) show examples of the vegetables currently in the vegetable barrel of the farm.

a) **Cucumber** (*Cucumis sativus*)

b) **Tomato** (*Solanum lycopersicum*)

c) **Aubergine** (*Solanum melongena*)

d) **Sweet Pepper** (*Capsicum annuum*)

e) **Chili Pepper** (*Capsicum solanaceae*)

f) **Okra** (*Abelmoschus esculentus*)

Figure 10 a) to f) – Vegetables cultivated at the farm.

These vegetables, despite being successfully grown and harvested, are not in the short-term cultivation plans due to small scale of the operation and lack of consistent demand, among other factors. On the other hand, basil will be consistently grown in the foreseeable future due to the constant demand and cost-effectiveness of the crop. The varieties of basil cultivated are “Sweet” Gustosa basil, Pluto basil, Red Basil and Gigante Napolitano. The first two are guaranteed to be available for cultivation at the time of this experiment and, therefore, the ones being investigated in this study analysis. Figure 11 and 12 show images of these species of basil.

Figure 11 - Gustosa Basil (Ocimum basilicum L.)

Figure 12 - Pluto Basil (Oscilicum basilicum “Pluto”)

3.4 Environmental Control Equipment and Energy Consumption

This section will describe the main characteristics of the equipment used at the farm to measure and control environmental conditions with particular focus on the light, followed by their energy consumption.

Regarding the lighting control on the growing container, there are sensors measuring light, microcontrollers processing data and LEDs complementing plant lighting needs with artificial lighting. There are 6 modules of LED strips placed vertically on the container walls in front of each barrel (see Figure 7). The LEDs used are the Horti-Blade Linear model from Vertically Urban® (Figure 14). Each LED blade has a length of 2340mm, power rated capacity of 72W and input current of 1700mA. The optical characteristics include a photosynthetic photon flux, PPF of 180 [$\pm$18] μmol/s and photon efficiency η_{PPF} of 2.5 μmol/J. The LED light spectrum model is the HB04 (previously named LMR) which, apart from the usual high intensity in the red zone of the spectrum, offers elevated blue and green content and white light appearance for general growth promotion. The blue:red light ratio is 1:3.7. Figure 13 shows the details of the spectrum photon distribution of these LEDs.

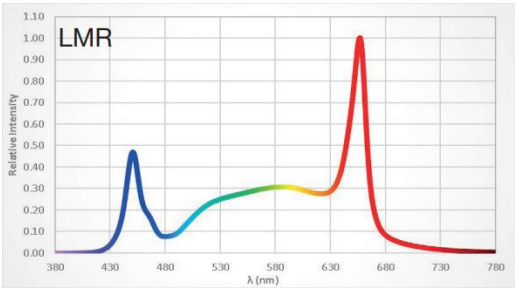

Figure 13 - LED spectral photon distribution. Blue (17%), Green (36%), Red (45%), Far Red (2%) (Vertically Urban, 2021)

The LEDs are connected in series in sets of three strips to a Power Supply Unit (PSU) which is the driver EUM 240S150LG seen in Figure 15, making a total of 6 drivers and 18 LED strips. The drivers are dimmable, which means that the current feeding the LEDs can be regulated and consequently their light intensity. This requires the installation of additional hardware equipment in the scope of the current work as it will be described in section 4.

Figure 14 - Horti-Blade ® LEDs (Vertically Urban®)

Figure 15 - EUM 240S150LG Driver (Inventronics®)

The light sensors used at the farm are the Adafruit 11-Channel Multi-Spectral Digital Sensors AS7341 seen in Figure 16, which is a low-cost sensor (14.36 € per unit). In the present study, a total of 9 units were used. The sensor channels have a footprint of 3 mm by 2 mm and are located in the centre of a 20mm by 30mm board with a low current consumption of only 210 μA at 1.8V during a measurement. The spectral response is defined by individual channels covering approximately 350nm to 1000nm wavelength. It contains 8 channels in the visible spectrum, plus one near-infrared and a clear channel capturing unfiltered light. The counts displayed for each channel are numerical representations of the voltage output from the photodiode that detects incoming light photons from a specific wavelength range. To interpret the light physical aspect of PPFD, a sensor unit conversion will be performed (see section 4.3.2.1). Figures 17 and 18 represent the sensor's optical channel summary and normalized spectral responsivity, respectively.

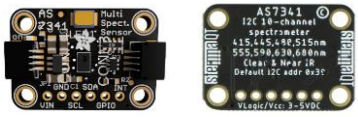

Figure 16 - Adafruit Multi-Spectral Sensor AS7341 front (left) and back (right).

Channel	Center Wavelength [nm] typical	Full Width Half Max [nm] typical
F1	415	26
F2	445	30
F3	480	36
F4	515	39
F5	555	39
F6	590	40
F7	630	50
F8	680	52
NIR (Near IR)	910	n/a
Clear	Si response/non filtered	n/a
FD (Flicker Detection)	Si response/non filtered	n/a

Figure 17 - Optical channel summary of AS7341 [87].

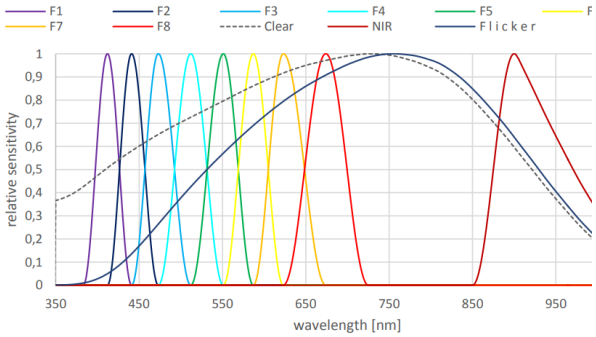

Figure 18 - Normalized Spectral Responsivity of AS7341 [87].

Data processing boards (microcontrollers) are required to be connected to the sensors (and other hardware) to read and control them. The microcontroller used was the single board Raspberry Pi Zero 2W (18,95 € per unit) of Figure 19. It has dimensions of 65mm x 30mm, powered via a micro-USB, incorporates a quad-core 64-bit Arm Cortex-A53 CPU, clocked at 1GHz, and has 512MB LPDDR2 of memory [88]. This device operating system is Linux and was programmed with Python coding language.

Figure 19- Raspberry Pi Zero 2W

Besides the lighting system, the farm contains devices to control other environmental parameters in the growing container and additional equipment for daily operations at the lower container. The cultivation greenhouse contains equipment for air temperature and humidity regulation, and ventilation, and the lower one, devices for irrigation, water purification and germination of seeds. The temperature regulation consists in a cooling and heating through an air condition (AC) unit (targeting a 24Cº temperature) to lower the high indoor temperatures reached during the day and increase them at night. The dehumidifier controls the indoor relative humidity targeting a level of 65%, preventing excessively high humidities favourable for fungi proliferation. Regarding irrigation, there is a main pump in the reservoir in the lower container, pumping water to 5 barrels with a flow rate of 25.75 L/h and a secondary pump watering the vegetable barrel independently due to different fertigation needs. After the main pump, the water passes through a carbon and sediment (passive) filter, as well as an electric UV light water purificator. The germination station (2x2x1m cabinet) is another crucial component of the operation which provides optimal light, air flow and water to seedlings developing in the first two weeks before transposition into the greenhouse. The fertigation and pH regulation processes are currently done by manually, as well as planting and harvesting of plants. Additional lights are also illuminating the lower container.

The total energy consumption of the Raiz farm will result from the operation of all the equipment described. The thermal control operation of the AC is significantly more energy intense than all

others, partially due to the presence of natural light penetration which reduces artificial lighting needs and increases heat gains indoors. Nevertheless, the LED operation represents a significant share of the overall energy consumption, such as ventilation, dehumidification, and water pumping. Table 6 lists all the equipment described, their power capacity, average operation time and daily energy consumption for the period of September. The energy consumption was taken from the electrical metering device Shelly Plus 1PM which was connected to the LEDs, AC, dehumidifier, ventilation fan and pumps. The remaining equipment's energy consumption was roughly estimated based on an average rated power and operation time.

Table 6– Equipment used at the farm, power capacity, operation times and energy consumption of each.

Equipment	Units [#]	Unit Capacity [W]	Total Capacity [W]	Operation Time [hrs/day]	Energy Consumption [kWh/day]	Energy Consumption Share [%]
LEDs	18	72	1296	4	5.18	16.5
AC	1	7000	7000	24	10.00	31.9
Dehumidifier	1	400	400	9	3.60	11.5
Ventilation Fan	1	100	100	24	2.40	7.7
Pumps	3	50/100/405	555	3,43	1.90	6.1
UV Water Purificator	1	50	50	24	1.20	3.8
Germination Station	1	250	250	24	6.00	19.2
Sensors	3	10	30	24	0.72	2.3
Storage Lights	1	500	500	0,5	0.25	1.0
Total			10181		31.25	

The LED lighting energy consumption is responsible for the third highest energy consumption share of 16.5% of total spendings and aligned with the trends seen in literature. The LED energy consumption is based on an agreed number of hours of LED operation depending on the season providing satisfying yields. This level is to be improved with the development of the current work.

3.5 Current Lighting System Limitations

Currently, a lot of operations at the farm still require time-consuming manual work. This is an obstacle for a streamed-lined efficient farming allowing human errors and difficult problem detection. This can be a large burden for a startup with limited personnel resources, requiring large amounts of time and effort spent on everyday tasks to maintain the healthy growth of the plants. Some of these activities, namely control actions, can be easily automated without major costs to reduce the stress and work time of staff, and simultaneously improve the efficiency and reliability of the operations.

This work focuses on the automation and optimization of the LED lighting system operation. Initially, some of the equipment in the farm (LEDs, AC, vent, water pumps and dehumidifier) can be remotely controlled through the application programming interface (API) of the Shelly 1PM device. This is an electrical relay switch and current metering device which can remotely regulate the equipment operation to a simple degree and monitor the electrical power consumption. The issue for the artificial lighting operation is that this control simply consists of the on/off scheduling of the LEDs at full/null intensity. This means that there are initially two issues to tackle:

1. The lack of control of light intensity level.
2. The lack of adaptability of artificial light operation to external natural light conditions.

The first problem happens because the components for LED dimming are currently not installed, possibly resulting in excessive light (and energy) usage and unpleasant visual effects on the surroundings. The second problem creates the need to adjust the scheduling of the LEDs in the app depending on the time of the year, weather conditions and type of crops. This controlling method requires a lot of attention and is subjected to human misperceptions, causing inefficient light consumption and/or plant productivity. By implementing an adjustable lighting control system capable of measuring the natural light exposure and commanding the LEDs, the entire operation can be done automatically. Each plant's lighting needs can be tailored and delivered with precision, independently of the outdoor environmental conditions. These data-driven systems also allow the monitoring and documentation of performance results of different lighting strategies for different species, as well as detection of problems otherwise unnoticed. The energy consumption can eventually be reduced with possible advantages in plant development through light dimming of the LEDs and controlled response to natural light condition. The current LED operation at the farm is simply based on the natural photoperiod and recommended period of light supplementation to optimize general herbal plant development. This results in another problem:

3. Uncertainty on optimal DLI levels considering a mix of natural and artificial light exposure for plant growth.

By testing different lighting strategies according to the DLI exposure, the actual optimal lighting requirements can be determined for this facility and correlated with the energy consumption. Moreover, an application with a mix of natural and artificial light exposure may suggest different methods for lighting optimization and LED operation, which will be analysed in the results section.

As seen in the literature, other environmental variables, such as temperature and humidity, are important factors in plant's health and productivity, and it is important to have them controlled and kept between crucial limits. Similarly to lighting, the control of these conditions is still at a basic level, done by defining an operation schedule for the equipment previously mentioned. Although, this is a limited way of controlling these parameters, the temperature and humidity effects on plant productivity are not in the scope of this report, as opposed to the effects of light. Without disregarding the data, as long as these conditions remain approximately equal for all test barrels in the farm space, the analysis of the effects of different lighting strategies should be sound.

4. LED Control System Assembly and Tunning

To address the previous issues of the limited lighting system regarding control, adaptability and DLI optimal delivery, a new LED dynamic control system will be presented in this section. The solution hereby presented aims to deliver a wide range of artificial light complements in an automated manner according to the weather conditions experienced daily. The improvement of the LED's control level will allow the system to operate in function of a customizable DLI target guaranteeing optimal conditions every day while optimizing energy efficiency. Further exploration of optimal DLI level will be performed utilizing the new LED control systems installed in three of the barrels and setting different targets according to the optimal levels found in literature (12.5, 15 and 17.5 $mol.m^{-2}.d^{-1}$).

4.1 System Setup

For each barrel there will be a control system composed of 3 light sensors AS7341 and three Horti-Blade LED strips, both connected and controlled by the microcontroller Raspberry Pi Zero 2W. This system is able to capture and measure the intensity of the natural light reaching the plants and consequently command the light intensity level and duration of the LEDs. The entire system is represented in the scheme of Figure 20 and picture of Figure 21, including components such as light sensors, multiplexer, microcontroller (Raspberry Pi), PWM-to-Voltage signal converter, LED driver, Shelly digital switch and the LED loads. The LED driver/power supply unit powers the entire system and the shelly device is connected beforehand and is capable of digitally switching on and off the flow of electrical current, as well as measuring it. The driver's dimming cables are connected to the voltage converter output (VOUT), receiving variations depending on the dimming percentage signal initially sent by the microcontroller. The regulated voltage is supplied to the LED's load and translated to the corresponding intensity level of artificial light. The initial dimming command from the microcontroller is determined by the sensor's sunlight measurements throughout the day, which must pass the multiplexer (Inter-Integrated Circuit) I2C-address conflict-solver. The detailed description and setup procedure of each of the system's components can be found in the next section.

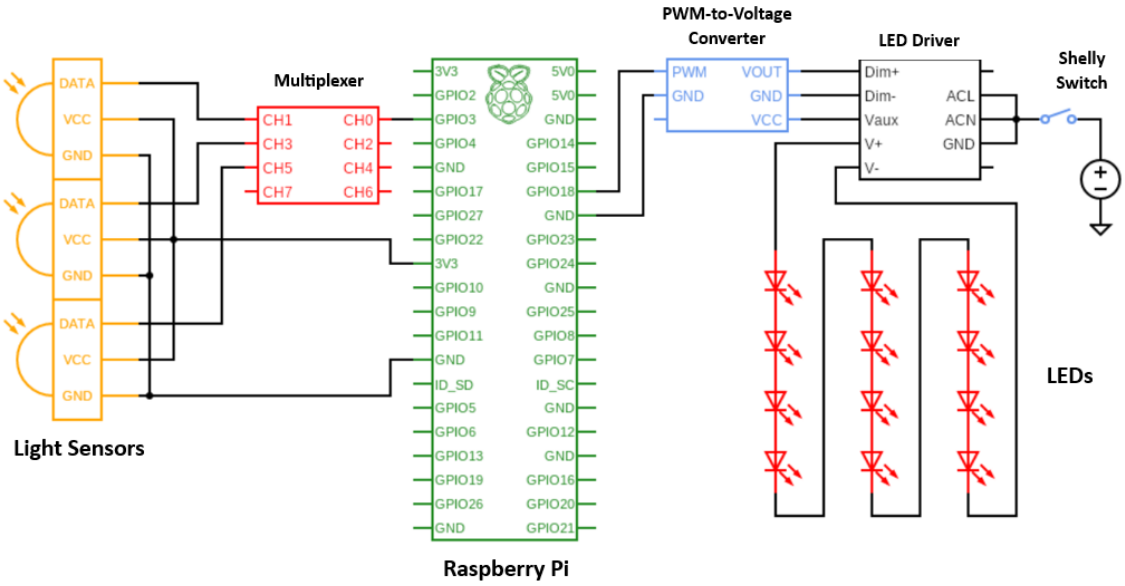

Figure 20 – Electrical Diagram of the entire LED control system including main components light sensors (yellow), Raspberry Pi (green), LED load (red) and driver (black), and secondary components multiplexer (red), PWM-to-Voltage Converter (blue) and Shelly Plus 1PM (blue). The positioning and distances are not accurate.

Figure 21 – Image of the LED control system installed at the farm

4.2 System Operation

From the literature review, it was seen that the optimal range of DLI for basil plants is around 15 $mol.m^{-2}.d^{-1}$. As it will be seen in next sections, the DLI from the sunlight will usually not reach this amount, especially outside of the summer season. During September at the farm, the sunlight DLI was registered between 6 and 13 $mol.m^{-2}.d^{-1}$ (for the middle barrel), depending on the weather conditions during the day. This means that to reach the plant's optimal light requirements for plant growth the LEDs must supply additional artificial light.

The LEDs will activate after sunset with a certain constant light intensity dependent on the solar DLI measured for the day and for a certain operation period. The LED operation period will be constrained by the time of sunset and a predefined period of darkness (7h) that plants must experience. This period of darkness is from the moment the LEDs turn off until sunrise and has an important role in plant development (as seen in LT). The operation time of the LEDs will always be the maximum that guarantees 7 hours of darkness, thus dependent on the sunset and sunrise times. These will vary gradually throughout the period of the experiment (September and October) resulting in shorter days and, therefore, longer LED operation periods. The LED light intensity will be the main variable adjusting each day to fit DLI targets. Figure 22 shows a schematic of the LED control system operation for an example day.

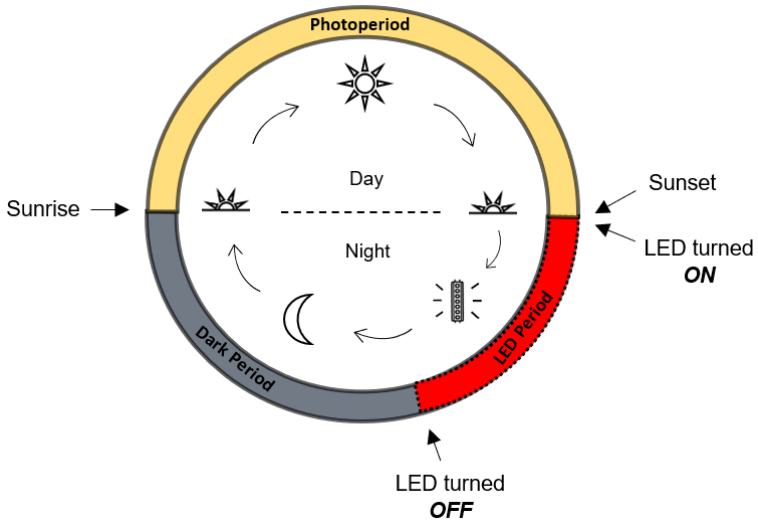

Figure 22 – Schematic of the LED control system operation for an example day

The example day of the scheme has a photoperiod of 12h from 7:00h to 19:00h (approximate for September) for which the LED's operation period would be 5 hours, from 19:00 to 00:00, with a certain constant intensity level. Note that the solar DLI is collected during the photoperiod, the artificial light DLI during the LED period and the total DLI (targeted) will be the sum of the two, thus collected from sunrise until the LED is turned off. The term total DLI (Daily Light Integral) is not hereby referring to light accumulated in a circadian day of 24h (00:00 – $00:00^{+1}$) but in the total period of (any) light exposure, which may pass midnight depending on the sunrise time. This method was agreed more adequate than diurnal artificial light complement since it simplifies the

control without compromising plant development (assuring enough dark period). Regarding the range of artificial DLI complements, this LED setup can deliver a maximum of 2.7 $mol.m^{-2}.d^{-1}$ per hour, which means the most demanding DLI regime (17.5 $mol.m^{-2}.d^{-1}$) can be fulfilled exclusively with artificial light in 6.5 hours of LED operation. This allows a secure margin for delivering most intense complements (during winter, when the night period is around 14h) while guaranteeing the 7-hour dark period. Additionally, the algorithm is set to activate the LEDs when the natural light PPFD is below 20 $\mu mol.m^{-2}.s^{-1}$ (and up to 2 hours before sunset), rather than a fixed hour of the day. This allows an earlier start of the operation in days with heavy overcast condition, providing a longer timespan to deliver the larger LED complements required these days.

4.3 Equipment Setup and Tunning

Some of the LED control system's materials were already present and functional at the farm (previously described in the Case Study section), others required additional installation and/or configuration, (light sensors, microcontrollers, LED dimmers). In this section follows a more detailed description of the preparation and installation of all the subcomponents required for the lighting control system.

4.3.1 Raspberry Pi

The Raspberry Pi Zero 2W® (Figure 23) microcontrollers (Pi for short) are programmed to run the sensors, compute their readings, and eventually send action commands to the LEDs regarding the timing and intensity of the artificial light. In total, there were three Raspberry Pi's installed at the farm to measure light and control the LEDs of three plant barrels (full detail in Cultivation Setup section). The microcontroller was accessed through a "headless" wireless Wi-Fi connection via SSH (secure shell protocol) to enable access from a personal computer. First, a microSD card was formatted (flashed) on a computer with the Raspberry Pi Operating System [89]. After formatting the SD card with the local Wi-Fi details, it was inserted into the Raspberry Pi and connected to a power source. After some minutes, the Pi was able to be accessed through the computer Windows PowerShell using SSH by calling its defined hostname/IP address. Now the Pi can be operated with a personal computer through Linux OS (Figure 24)

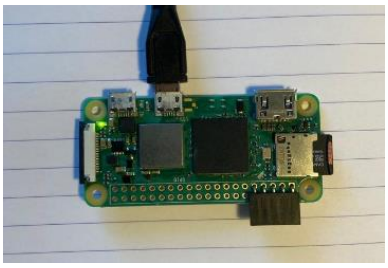

Figure 23 – Raspberry Pi Zero 2W

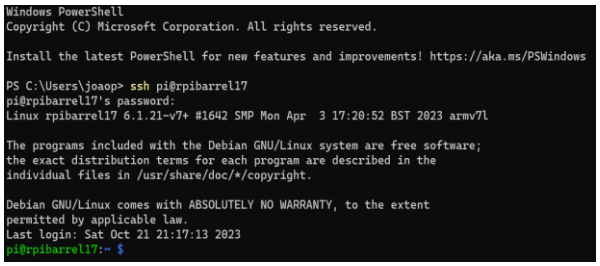

Figure 24 – Raspberry Pi being accessed through SSH.

Some initial upgrades and updates were made to the Raspberry Pi and the Python programming language was installed. All installations and their commands can be found in Appendix 1. These include Circuit Python packages to enable the light sensor readings, time stamping and Google Cloud Platform connection, namely the Big Query package. The latter allows data from sensor measurements and LED operation to be constantly sent from the Pi to the cloud platform and be accessed remotely. Big Query is this work's method of organizing the data in customizable tables where it can be logged in real-time. Deepnote, a free online data science notebook, was the tool ultimately handling the data by importing it from Google Cloud and enabling easier management and visualization. This tool is easy to program and offers built-in graphical outputs which facilitate data analysis that will be seen in section 6.

4.3.2 Light Sensor

The light sensor is one of the most important tools for this study since it measures the intensity (and wavelength) of light reaching the plants inside of the farm. This is the crucial variable for the programming of the LED operation. The previously presented Adafruit multi-channel light sensors were connected to the Raspberry Pi in modules of three sensors for each Pi. This was the test configuration chosen for each barrel to have three sensors collecting an average of light exposure. The signalling is transmitted with I2C protocol, meaning serial communication bus had to be enabled in the Pi's system. The wires connecting the sensors were the "STEMMA QT" 4-pin I2C cables (3V, SDA - Serial Data, SCL - Serial Clock, and ground) with JST SH connectors. These sensors have a fixed (non-editable) I2C address (0x39) through which the microcontroller calls and receives their data. For this reason, when connecting multiple AS7341 sensors to the same Pi there will be a conflict of I2C addresses preventing access to their readings. An I2C multiplexer device can constantly switch between target devices at extremely high frequencies allowing only one active output at any given time [90]. Thus, it must be connected to the Pi between the light sensors to avoid I2C address conflicts. In this case, a PCA9548AP M5Stack board with a multiplexer TCA9548A at heart seen in the next Figure 25 was used for each Pi with a cost of 11,95€ per unit. Since the multiplexer cable entrances are the larger JST PH, an additional STEMMA cable converter (JST PH to JST SH) had to be purchased for each sensor (1€ per unit).

Figure 25 – Multiplexer PCA9548AP

Figure 26 - LTC4311 Active Terminator

Devices that use the I2C protocol have limitations in the length of cables transmitting the data due to their added capacitance and resistance which can be problematic [91]. To tackle this issue an LTC4311 Active Terminator from Adafruit seen in Figure 26 was connected in series with the sensors which is claimed to allow clean signals to propagate over cables 30m long, therefore feasible for this experiment setup. The next Figure 27 shows an image of the setup connection of the AS7341 light sensors to the Raspberry Pi and the additional components PCA9448AP multiplexer and LTC4311 terminator.

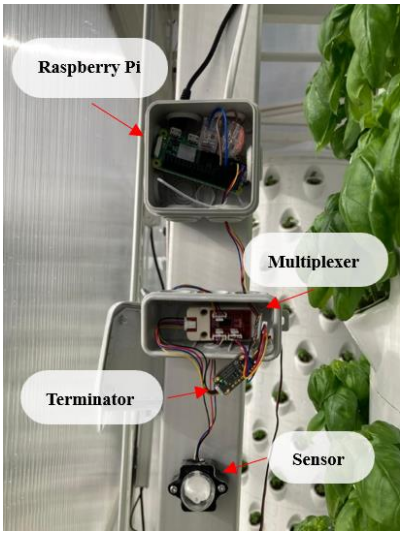

Figure 27 – Assembled setup of light sensor, multiplexer, terminator, and Raspberry Pi.

Regarding the sensor placement, three light sensors are positioned on the top part of the barrels where the tested plants will be placed, facing the wall where the LEDs are attached. They were positioned to capture enough possible light variations through the testing surface height, and close to the plant's base without risking getting covered by the leaves. The light exposure in the testing surface will be assumed uniformly distributed with an intensity equal to the average of the three sensors. The placement of the three sensors was not completely uniform due to shortages of cables and other components, however, this did not compromise a reliable placement range. They are aligned in a vertical disposition with approximately 7cm spacing between the top and middle one and 20cm between the middle and the bottom one. The top sensor is placed 4cm from the barrel's surface and 31cm from the wall while the others are 15cm from the barrel and 20cm from the wall. Figure 28 shows the disposition of the sensors for each control system at each barrel of study.

Figure 28 – Light sensor positioning on a testing barrel.

4.3.2.1 Sensor Casing and Unit Conversion

To perform the analysis of the effects of light on plant productivity, it is important to work with the light units Photosynthetic Photon Flux Density (recall, it is the amount of photons with wavelength between 400 and 700nm, per square meter and second in $\mu mol.m^{-2}.s^{-1}$). Measuring the PPFD of light in delicate applications is usually done with expensive quantum PAR sensors. The work [92] studied the relationship between total quanta (photons) and total energy proposing linear conversion metrics to roughly estimate PPFD based on the solar radiation in [W/m^2]. The issue is that the energy carried by light photons depends on their wavelength and therefore it is not straightforward to convert irradiance to quantum units. In the present work, the PPFD will be calculated based on the readings of the multi-spectral channels in the AS7341 light sensors, replicating the novel approach presented in [93] that converts the sensor's channel readings into PPFD. For this reason, the AS7341 light sensors need to be adapted to convert its original count readings of the nine channels to a single value of PPFD with similar methodology as in [93]. For each channel a numerical light photon count is registered during one measurement depending on the integration time for one measurement interval, t_{int}, multiplied by the analogue-to-digital converter frequency, F_{ADC}, as seen in Eq. (1):

$$counts = F_{ADC} * t_{int} \qquad \text{Eq. (1)}$$

The integration time (t_{int}) is user-modifiable (maximum of 700ms) which determines the sensor's maximum count value and the frequency (F_{ADC}) controls the sensibility of the sensor (i.e. the minimum portion of the light signal that can be observed). The latter can be subjected to a certain gain (1x; 3.7x; 16x or 64x) that increases sensibility and enables smaller variations to be detected. The original setting of the sensor is an integration time of 327.7ms, a gain of 1x (or no gain) and an ADC frequency of 2MHz, meaning that the number of photon counts of each channel is from 0 to 65535.

In the initial tests of the sensor, it was noted that the maximum count number was easily reached with low amounts of natural light. In fact, the readings of the channels would easily reach the

maximum of 65535 counts without being directly under sunlight, namely the sensor's unfiltered channel ("clear") and others measuring higher wavelength (such as "red/680nm" and "orange/630nm"). The lower-wavelength channels would max their counts with higher luminosities, however, all channels would already be saturated when exposed to weak sunlight. This happens due to the sensor being very sensible and meant for delicate applications of colour identification. This issue was compromising the study since the difference between weak and strong sunlight could not be distinguished by the saturated sensor. To solve this, an acrylic white filter was built using a 3D printer (Ultimaker S5) and placed in front of the sensor's channels in the centre of the chip. A housing box made of black plastic was also 3D printed to fit the filter chip and protect the sensor from water and physical damage. The housing box illustrated in the CAD scheme and image of Figure 29 and is made of two parts that can be screwed together, with an opening for the STEMMA cables to plug in, eventually covered with black duct tape for extra protection and light blockage. A transparent plastic dome was fitted on top of the filter circumference to disperse the light reaching the filter and avoid dirt accumulation. Each sensor and its housing have small dimensions of 23 x 30 x 18 mm and a weight of 13g. This model was inspired by the work in [93].

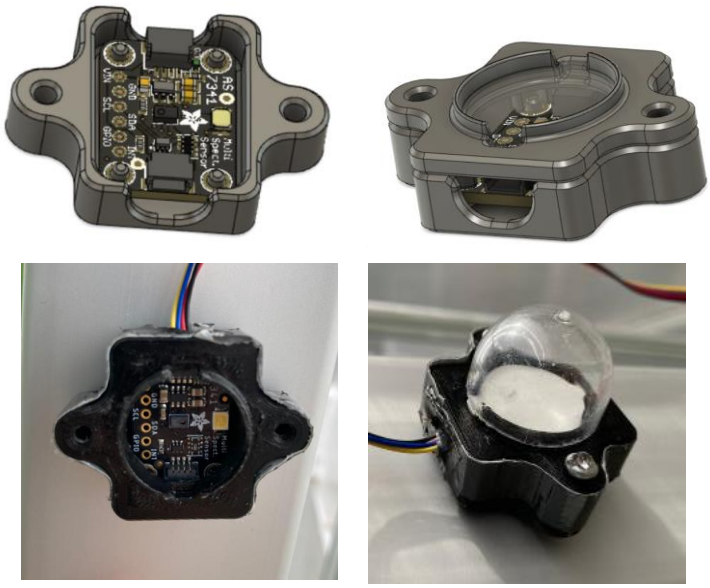

Figure 29 - CAD Scheme of the sensor casing (upper left and right) and image of sensor casing with (lower right) and without (lower left) light damping filter and plastic dome.

The filter has the purpose of blocking a fraction of the light, serving as an intensity divisor which decreases the sensor's sensibility that was originally too high for sunlight measuring applications. Different thicknesses and material compositions were tested to find a dimension that damps light an adequate amount. This means allowing the strongest sunlight to be measured without saturation and still having enough sensibility to capture subtle sunlight changes. Eventually, a suitable filter was built that filtered 90% of the light corresponding to a gain of 0.10 which was obtained by dividing the corresponding average daily filtered readings by the unfiltered (non-saturated) ones.

Once the readings of the sensor had a suitable gain for high intensities of light, the multiple reading outputs needed to be converted to a single PPFD value. The NIR channel measures light in the near-infrared region of the spectrum, corresponding to wavelengths larger than 850nm, thus it will not influence the PPFD. The 11th channel detects light flickering which is information unrelated to spectral composition. Therefore, the remaining 9 channel readings are the ones addressing PAR between 415 and 680nm (recall Figure 18 of section 3). These 9 outputs were converted to a single value of PPFD using a multiple input linear regression (MLR), following the methodology of [93]. The inputs were the measurements from the eight channels of colours plus the clear channel, and the outputs were the PPFD measured from a reference smartphone application called "Photone" [94] which uses the phone's camera as the light sensor. It provides light measurements in PPFD [$\mu mol.m^{-2}.s^{-1}$] and other parameters like illuminance in [lux], light colour temperature in [Kelvin] and DLI (approximates) in [$mol.m^{-2}.d^{-1}$]. It can measure the PPFD according to different types of light (blue and red LEDs, sunlight, luminescent lamps, among others). The app is claimed to have an accuracy around $\pm 5\%$ compared to research-grade laboratory equipment (like quantum PAR sensors) [94], which was considered sufficient for the present application and, therefore, it will be used as the reference sensor for the AS7341 calibration and conversion of the channel counts to PPFD. The regression was done by recording 198 sample measurements of sunlight from the AS7341 sensor and phone app at the same moment inside the farm walls. For this procedure, the phone and sensors were attached to a rigid plastic transparent surface (moveable) and placed side by side on the same plane, thus, same light angle of incidence. The 9 outputs from the AS7341 sensor readings (counts) and one from the phone (PPFD) were recorded using the average of three (random) sensors. The measurements were taken for a wide range of light intensities with PPFD from 0 to 1505 $\mu mol.m^{-2}.s^{-1}$. The lower limit corresponds to light measured during nighttime at 22:00 (September) and the higher limit corresponds to measurements taken under the sunlight normal to the light angle of incidence at 13:00 (September). Note that the maximum PPFD that the Earth receives from sunlight is 2500 $\mu mol.m^{-2}.s^{-1}$ at noon in the equator [95], so inside the farm polycarbonate walls it is reasonable to assume that the maximum PPFD experienced will not significantly surpass 1505 $\mu mol.m^{-2}.s^{-1}$ during this time of the year. Upon performing the linear regression with the samples taken, a linear conversion function of eq.2 was obtained using Matlab.

$$PPFD_p = \sum_{i=1}^{n} (b_i * x_i) + e \qquad \text{Eq.2}$$

Where x_i are the count output of each sensor channel and b_i are the conversion coefficients determined by the MLR given the reference PPFD samples from the Photone app. Eventually, a predicted PPFD, ($PPFD_p$), can be obtained with a given error, e. Table 7 presents the nine obtained "count-to-PPFD" conversion coefficients:

Table 7 - Resulting PPFD conversion coefficients of the multiple linear regression for the AS7341's channel F1–F8 outputs.

b_{violet}	b_{indigo}	b_{blue}	b_{cyan}	b_{green}	b_{yellow}	b_{orange}	b_{red}	b_{clear}
-0.2598	0.5194	-0.3257	-0.1469	0.1904	0.2034	-0.1507	0.0114	-0.0016

The obtained coefficient of determination was $R^2 = 0.982$ and the root mean square error, RMSE = 56.58. These are positive values that indicate a reliable MLR conversion algorithm. Figure 30 show graphical representations of the MLR-predicted results of PPFD (left) and residuals (right) to better understand its behaviour.

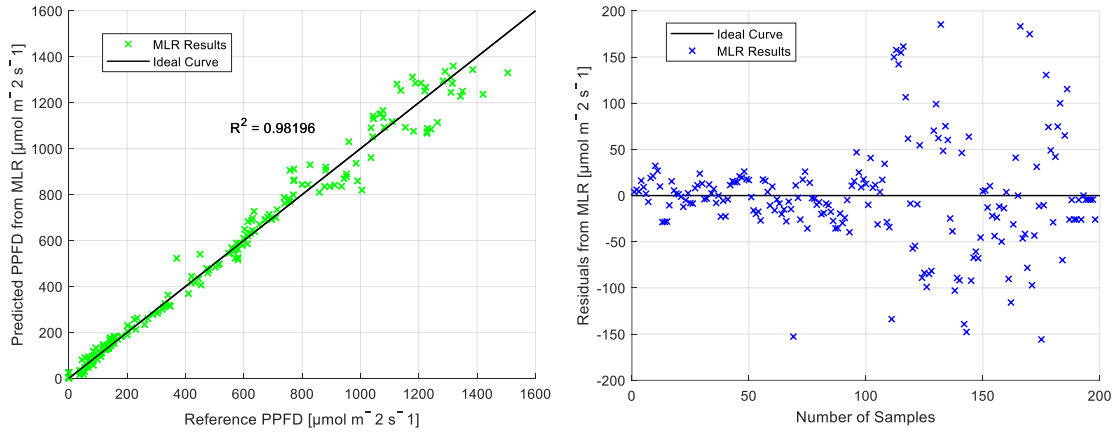

Figure 30 – MLR distribution of predicted PPFD results based on a reference PPFD (left) and PPFD residual values obtained for each sample (right).

The graphs of Figure 30 easily depict how the MLR model has different accuracies predicting higher and lower PPFDs. For PPFD < 750 µmol.m^{-2}.s^{-1}, the error is much lower than for PPFD > 750 µmol.m^{-2}.s^{-1}. This was because higher light intensities were only obtained under direct sunlight (inside farm walls) and lower samples were taken for indirect light insertion. The problem was that the plastic dome covering the sensors was not 100% transparent and has a small, rugged dot at the top (note that these domes were cut off from another plastic component that was cheap and abundant). This rugged dot came from manufacturing and, depending on the light angle, could cause a small shade on the sensor filter resulting in faulty measurements, which justify the larger errors for that case. This issue was considered with negligible effect on the model's robustness since: all plastic domes had the same defect; the errors mostly between +/- 100 µmol.m^{-2}.s^{-1}, meaning an error of 13% maximum (compared to 750 µmol.m^{-2}.s^{-1}); the incidents of direct sunlight hitting the sensors are less frequent than ones of indirect light.

It is important to note that this conversion function is exclusive to the lighting environment conditions it was calibrated on, i.e. natural light inside Raiz's farm. Despite the wide range of light intensities tested, the spectral composition of light varies throughout the day/year and farm space, factors not accounted for the previous calibration. Moreover, this process was done using the average readings of three sensors and nine were used in total, three for each LED control system.

Each of the nine sensors is subjected to its own imperfections causing errors. These may be related to the sensor cleaning state, case/filter composition and finish, plastic dome imperfections, etc. These are some possible sources of error, as well as any human or instrument errors occurring while taking samples. For this reason, a test of viability was performed for each sensor by comparing readings after the model conversion to PPFD again with the reference PPFD from the Photone app. This process was not as meticulous as the previous calibration, it was a simple check of results in the case of bright intensity (around 500 μmol.m^{-2}.s^{-1}) and lower intensities (<150 μmol.m^{-2}.s^{-1}) depending on the time of the day without direct sunlight. Table 8 shows the deviation of all nine sensors set up (three per barrel) in the three tested barrels (labelled Barrel 2, 4 and 6) and the sum deviation of each barrel.

Table 8 – PPFD deviations in μmol.m^{-2}.s^{-1} of each light sensor placed on each testing barrel compared to the Photone app after the initial calibration

Barrel		2	4	6
PPFD ≈ 500				
Sensor	Top	0	-60	-20
	Middle	+30	0	0
	Bottom	0	-15	0
	Sum	+30	-75	-20
PPFD ≈ 50				
Sensor	Top	+30	-35	-15
	Middle	+35	+20	-30
	Bottom	-45	+20	+30
	Sum	+20	+5	-15

Measurements in μmol.m^{-2}.s^{-1}

The sum of each sensor's errors is what matters the most for the setup since the system is working with the averages of three sensors in the same barrel. The main discrepancies occurred in sensors not used during the calibration process as expected. On the other hand, sensors used for calibration showed close to no error. The measurements for higher light intensities show smaller relative errors than for lower intensities. For higher intensities, the larger error found considering the sensor sum at each barrel was -75 μmol.m^{-2}.s^{-1}, which is equivalent to 15%. The main issue was the deviations for lower intensities, which not only represented higher relative errors (up to 40%) but also may compromise the system's awareness of end/start of the day. For this reason, the PPFD read by the sensor sum of each barrel was taken at night (22:00) where the reference is 0. This "night step" value was the new constant (n_{step}) introduced to the upgraded conversion function of eq.2.

$$PPFD_p = \sum_{i=1}^{n} (b_i * x_i) - n_{step_B} \qquad \text{Eq.2}$$

The night step constant, n_{step_B}, was specific to each barrel sensor set as follows: Barrel 2 with a night step of +14 μmol.m^{-2}.s^{-1}), Barrel 4 with +4 μmol.m^{-2}.s^{-1} and Barrel 6 with -9 μmol.m^{-2}.s^{-1}. These values align with the discrepancies of Table 8 for low light conditions, meaning the addition of this constant reduces these errors significantly. For high intensity it also reduces the errors although to a lesser extent (especially in Barrel 4).

4.3.2.2 Light Measuring Algorithm

The light sensors are set to take measurements of PPFD every 3 seconds and the reading itself takes a certain time to complete (around 5 seconds). After 4 cycles (≈32s), an average PPFD for each measurement is taken and assumed constant for the duration of the 4 cycles. The PPFD [μmol.m^{-2}.s^{-1}] is multiplied by the duration of the 4 cycles (in seconds) giving the accumulated PPFD for that period μmol.m^{-2}. (4 cycles)s^{-1}]. The process repeats infinitely and the average PPFD is accumulated in a running sum every 4 cycles. The total time the PPFD takes accumulating together with time stamps of that accumulation are registered. At the end of the day the PPFD accumulated, converted in [mol.m^{-2}.d^{-1}], will be the solar DLI and the time accumulated will be the photoperiod [h]. The timestamps are taken for data organization and cross-checking of timings. The next Figure 31 explains this logic.

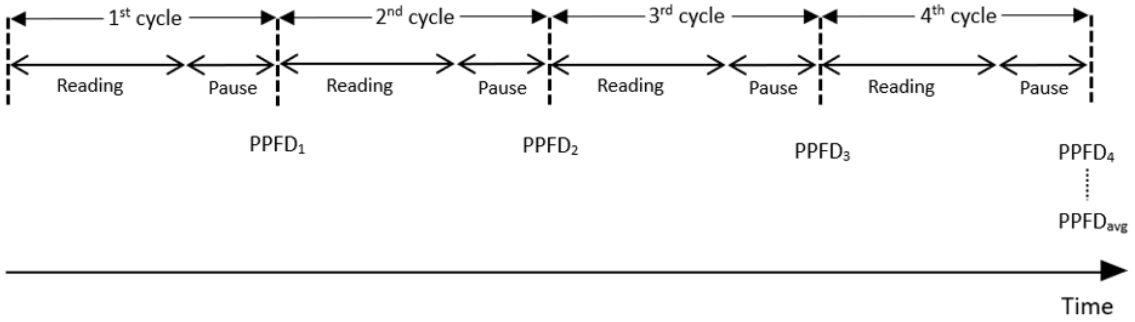

Figure 31 – Schematic of light sensor measuring logic.

During the final stages of maturity of basil plants, these can get quite large potentially cover the sensors. In addition to monitoring this situation, there is a condition in the sensor reading algorithm to disregard these types of faulty measurements if one sensor gets covered. The condition is if the lowest measurement of the three is lower than 30% of the average of the remaining two, it is disregarded, and the average of the barrel counts only with the average of the other. If this condition checks, that means that only one is measuring much lower lighting than the rest, which is likely due to an unrealistic shadow. A scenario where expected shading caused by the LEDs strips or the greenhouse structure beams may also occur during the day, but it is unlikely to strike solely one sensor since they are quite close, and these shadows tend to be more dispersed. In this case, it is very unlikely that the shadow is only hitting one of the sensors in such a disproportional way (recall the farm walls disperse solar radiation indoors) thus the shade-avoiding condition will not activate. After all, this type of shading is affecting the plants in a way that should be accounted for. The code for the sensor operation was written with Python and can

be found in Appendix 2. This includes sensor calling, measuring loop including timing the duration of sensor readings and disregard of unrealistic shading.

4.3.3 LEDs

4.3.3.1 Light Dimming

The other main part of the system are the LEDs and its ability to adjust the intensity of their light. As mentioned, initially the LEDs were solely capable of turning on to the maximum intensity (100%) or off (0%). The process of dimming the artificial light was also carried out for this study. The LED's driver unit is dimmable from origin, meaning that it allows a voltage regulator to be connected to the circuit to regulate the output voltage reaching the LEDs and therefore control the light intensity between 0 and 100%. The actuator responsible for sending a control signal regarding the dimming level and timing is the microcontroller (Raspberry Pi) which calculates that based on data collected from the sensors. The easiest way to provide the dimming command from the pi is through a PWM signal. This method consists of sending a pulsed signal of a fully ON/OFF (duty) cycle with a certain percentage of it being ON and the remaining OFF. For example, dimming the output voltage by 75% would mean a cycle with a maximum current 75% of the time and zero current 25% of the time. Figure 32 shows some examples of duty cycles representing different voltage outputs.

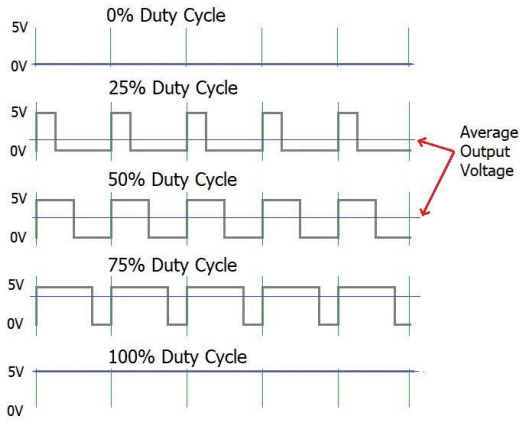

Figure 32 – Examples of duty cycle percentages in PWM signals and corresponding average output voltage.

The voltage output level for an LED load will represent its dimming level and, consequently, the light intensity. The period of these cycles is usually very fast [ms] (duty cycle frequency around 2000Hz) in a way that the human eye cannot detect, simply resulting in less intense light. For the Raspberry Pi Zero 2W microcontroller the voltage amplitude of these signals varies between 3.3 and 0 volts. The LED driver accepts PWM dimming, but not only does it require the Pi's default voltage output to be increased, but also an additional Inventronics programming component to enable this dimming method. The predefined dimming method of these LED drivers is analogue dimming 0-10Vwhich require relatively cheap circuit board converters of PWM signal to analogue VDC signal, which were already present at the farm. Therefore, the PWM dimming signal from

the microcontroller was converted to an analogue 0-10V signal which the LED driver incorporates and ultimately controls the intensity of the LED artificial light, with no additional costs or circuits.

According to the LED driver specifications, the dimming output range is between a maximum current of 1.5A and a minimum of 10% of that current (0.15A). This means that the output status is not guaranteed for dimming signals less than 1V. Even with dimming input voltage regulation between 0-10V, the output current feeding the LEDs will vary approximately between 1 and 10V (10 to 100%). Turning the LEDs fully OFF requires an additional switch to cut power at the driver. This was possible with the Shelly 1PM switch devices previously installed at the farm. These were connected to most of the hardware equipment enabling basic control (ON/OFF, scheduling, etc) via the Shelly smartphone application. Therefore, the LED light intensity control was done with the microcontroller (PWM signals converted to 1-10V) for regulation between 10 and 100%, together with a power switch for shutting off the LEDs. The regulation between 0 and 10% of intensity is unattainable with the current setup but with no significant importance.

4.3.3.1 Dimming Linearity

Once the dimming circuit was installed and the controller was regulating the LED's light intensity, the linearity of dimming was investigated to ensure the voltage regulation indeed translated to light intensity regulation in a linear manner. For this, the artificial light from the LEDs was measured for different dimming levels. These were defined by primary PWM signals from the pi at a duty frequency of 500Hz and ratios from 0 to 100% with 10% increments. The luminosity was measured in PPFD from the Photone phone app set for Red/Blue LED light measurements, which mostly coincide with the light composition of LEDs used at the farm. The DC voltage feeding the LED driver after the PWM signal conversion was also measured with a voltmeter for each dimming level. Additionally, the electrical power withdrawal from the PSU is measured by the Shelly meter was also recorded to verify if it matched with the other variables. The data samples can be found in Table 9 and the linearity was tested with single input Linear Regressions considering the duty cycle percentages as the inputs and the different measured variables as the outputs.

Table 9 – Linearity test of the LED light PPFD level compared to the dimming signal (PWM and Vout) and electrical power required from the PSU.

PWM Duty Cycle [%]	**100**	**90**	**80**	**70**	**60**	**50**	**40**	**30**	**20**	**10**	**0**
LED PPFD [µmol.m^{-2}.s^{-1}]	533	481	440	395	343	302	253	202	150	97	52
Voltage Output, Vout [V]	9.57	8.38	7.57	6.73	5.88	5.02	4.15	3.25	2.35	1.42	0.64
Electrical Power [W]	221	207	190	164	140	118	98	76	54	32.5	21.8

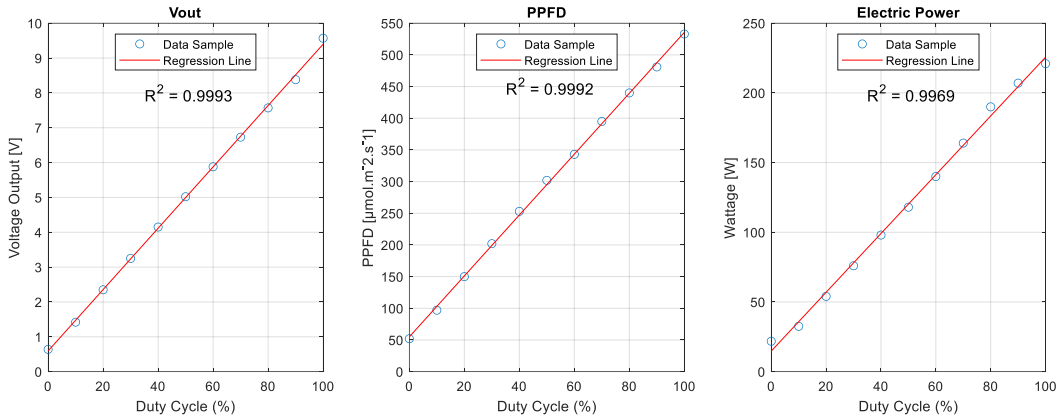

Figure 33 – LR of the correlations between the duty cycle percentage of the PWM signal with the Voltage Output of the PWM-to-voltage converter, LED light PPFD and Electric Power required.

As can be seen in the previous graphs, the voltage output and consequent PPFD and electrical power presented a highly linear behaviour with the variation of the initial PWM signal dimming percentage. There were some minor deviations, particularly on the electrical power values presented on the Shelle app, that were considered negligible for further LED control and energy analysis. Another observation is the minimum dimming voltage limit (and dependent PPFD and power) was found to be around 10% after conversion of PWM to voltage signal, as previously mentioned due to the limitation of the hardware. This meant that the percentage level set for the PWM duty cycle from 0-100% was not going to be proportionally reflected in the LEDs light intensity, which varied from 10-100%. To make sure the dimming command actions were made regarding the final voltage dimming range, a simple conversion was applied to the PWM knowing their correlation. The correlation was found based on the previous regression line function of Eq. 3, where Dim_{LED} is the intended level of LED dimmed light intensity and Dim_{PWM} is the initial PWM signal dimming level.

$$Dim_{LED} = 0.90\ (\mathrm{Dim}_{PWM}) + 10.31 \Leftrightarrow \mathrm{Dim}_{PWM} = (Dim_{LED} - 10.31)/0.90 \quad [0 - 100\%] \qquad \text{Eq. 3}$$

The duty frequency also showed an influence on the outcome of these variables and provided different PWM-voltage relations. Higher frequencies (>1000Hz) were recommended, although these values showed the minimum dimming level even higher (Vout range = 18-100% for 1kHz and 26-100% for 2kHz) which limited the LED control further. The highest frequency level which did not result in loss of dimming control of Vout more than 10% was 500Hz (as seen before).

5. Experimental Procedure and Performance Indicators

5.1 Experimental Setup

In this section, the experimental setup including the environmental conditions and cultivation methods will be described, as well as the predefined DLI regimes of each testing barrel and plant growth key performance indicators.

In the present work, the two species of basil plants Gustosa “Sweet” Basil (*Ocimum basilicum L.*) and Pluto Basil (*Ocimum basilicum “Pluto”*) will be investigated. These are cultivated in three different barrels simultaneously, each with its own lighting regime. It is important to note that each barrel contains its own LED control system working independently. The three barrels of interest will be the ones closest to the greenhouse wall facing southeast (see Figure 7 of section 3). The plants studied will be placed at the 5 higher rings of the barrels and in three columns facing the wall, giving a total of 15 plants per barrel. Nine plants of the Gustosa variety and six of Pluto will be placed in equal relative positions in all three barrels and results will be compared between the same species. The next scheme and image show the position of the plants to be studied (highlighted) and some parts of the LED control system.

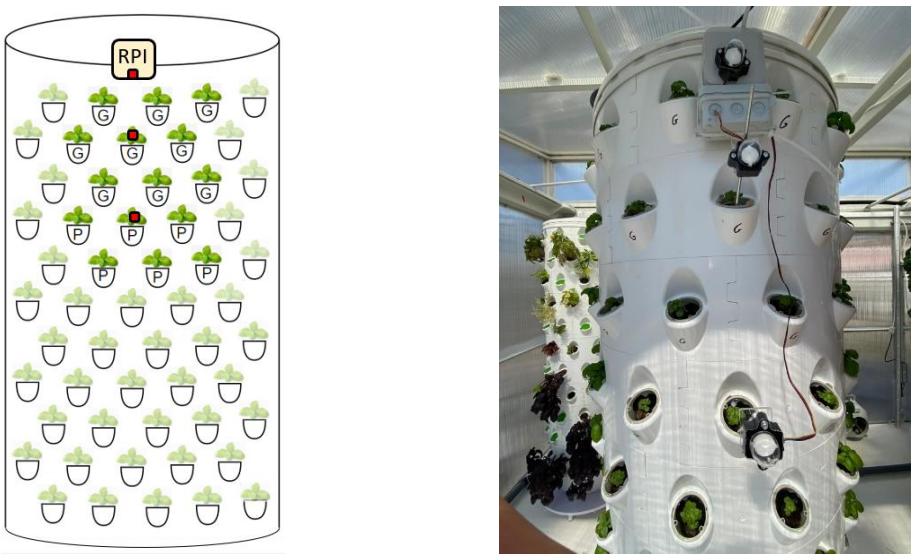

Figure 34 – Scheme (left) and picture (right) of a testing barrel with 9 Gustosa and 6 Pluto plants, 15 in total (G – Gustosa; P – Pluto). Microcontroller on top (RPI) and light sensors (red) distributed vertically through the barrel.

5.2 Environmental and Cultivation Conditions

5.2.1 Temperature and Relative Humidity

Regarding other environmental conditions apart from light, the temperature and humidity are also controlled at the farm with an AC, dehumidifier, and fan ventilation, as previously mentioned. Additional sensors are placed on the farm measuring temperature and relative humidity in

different positions. The AC is constantly working with a target temperature of 24Cº and the average temperature registered during the experiment was 25Cº, with day and night temperatures varying between 35Cº and 16Cº, respectively. The average relative humidity was 61% with day-night variations of 30-90%. The average levels of these variables are aligned with recommended levels seen in the literature, although the variation of relative humidity reaches concerning levels at some periods of the day. Since these conditions were settled for usual farm operation prior to the study, it is understood that plant growth is not compromised, and the experiment will be carried out in this way.

There is a gradient of different temperature levels throughout the greenhouse height which causes plants at higher positions to experience higher temperature (and possibly humidity) than the lower ones. The lighting condition is also more favourable at the top space of the farm as opposed to the bottom (more obstruction to light). The influence of the different conditions across the vertical space was previously noted when comparing the same species of plants harvested from the top and the bottom of the barrel. From the top to the middle of the barrel plants have significantly larger sizes than plants on the bottom. This is the reason why only the top of the barrels will be utilized for this study. Moreover, same-specie plants will be placed in the same two horizontal levels with a 20cm spacing between them. This avoids analysing plants at very different heights where the temperature/humidity/light conditions can differ significantly. Any vertical (or other) gradient of these variables is therefore disregarded for the following analysis by assuming equal temperature/humidity/light between all same species of basil plants.

5.2.2 Irrigation

The water flow for each testing barrel was also measured and equalised before the experiment. This procedure was achieved by attaching an empty water bottle to the irrigation supply hose of each barrel and adjusting the water flow through the taps until the filling time of the bottles approximately matched. The next Figure 35 shows a picture of the procedure.

Figure 35 – Bottles filling for equalization of the water flow for the three testing barrels.

The filling time of the bottles was noted (2m30s), and the water flow was calculated, knowing the volume of the bottles (1.5L). The adjusted water flow coming out of each barrel tube is 0.01L/s. The irrigation frequency defined by the agronomists consists of activating the pump for 3 minutes and 20 seconds and deactivating it for 20 minutes, meaning it operates 14.3% of the time. This results in an actual water flow of 5.15 L/h per barrel. Assuming a completely even distribution of

water inside the barrel walls through the roots for a total of 131 plants the water flow per plant is 0.039 L/h.

5.2.3 Nutrition and pH

Regarding the water nutrients the EC (electrical conductivity) is the indicator of the quantity of available nutrients in the water solution and pH indicates the water acidity. At the time of the experiment, the EC is kept around 1.20 with variations reported from 0.90 to 1.53, and the pH around 6, varying from 4.80 to 7.20.

5.2.4 Sowing, Germination and Harvest

All plant seeds were sowed on August 28th in jiffy pallets (Figure 36) made of peak moss (organic-rich substrate). Three to four seeds are inserted per wet jiffy and placed in the germination station for two weeks while the initial sprouts appear, and the first leaves start to develop. Here the seedlings are subjected to specific amounts of light and other conditions which will not be investigated in this report. The plants were transplanted on September 11th to the hydroponic barrels in the upper greenhouse container giving the start to the experiment. The mass of the jiffies was registered initially for future reference in growth results analysis. The jiffies (alone) had an average mass of 3 grams dry and 20 grams (+/- 2g) wet.

Figure 36 – Jiffy pallets dry (left) and wet (right)

During harvest, the plants are cut at the base of the stem and separated from the roots and remaining of the jiffy material. The basil sold by Raiz is always delivered fresh, shortly after harvested and the price is charged per mass of plant. The plant mass considered for sale only accounts with the plant's stems and leaves (edible part). Other clients require whole basil plants (with roots) to keep them in water/soil to maintain freshness longer. In those cases, the weight considered for sales consists of the weight of the whole plant subtracted by the weight of the jiffy/roots (around 20 to 25g).

5.3 Light Conditions

The light regimes of each barrel of study will differ in the total amount of light subjected to the plants per day, also known as the DLI, measured in mol.m^{-2}.d^{-1}. The only factors that influence this parameter inside the farm are the sunlight and the LED light. It is important to understand the initial lighting conditions in detail of each barrel's position before the analysis of results. Moreover, it is important to register how the natural light and artificial light are illuminating the barrel surfaces

and detect possible differences that the plants are facing from the start. The next sections define the delimitations of the natural and artificial light conditions of the setup.

5.3.1 Natural Light Condition

As mentioned, the three barrels used were the ones facing the farm wall almost exactly aligned at southeast (-2°). The two barrels positioned on the corners are the only ones directly exposed to northeast and southwest walls and all three are equally distant to the wall facing southeast and ceiling. Figure 37 represents the farm top view and the three testing barrels (2, 4 and 6).

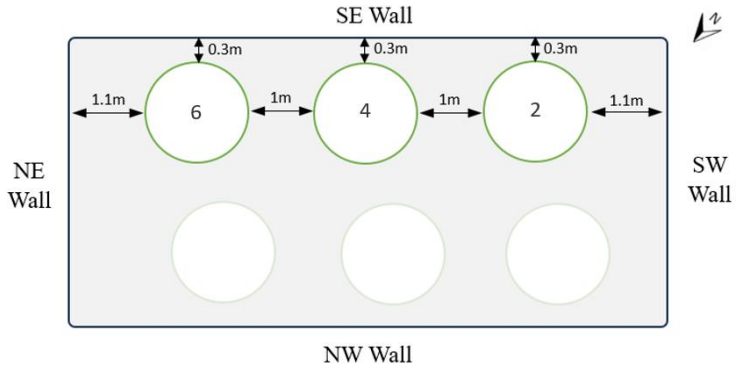

Figure 37 – Schematic of the three testing barrels and orientation of the farm walls

The sunlight intensity of the 25th of September was measured in PPFD (with the Photone app) from each of the four façades of the barrels parallel to the farm walls to understand the differences between the barrels in the penetration of sunlight at different times of the day. The results are presented in the next Table 10

Table 10 – PPFD measurements of each barrel from the façades parrel to each wall of the farm.

Time	**Barrel**	**Farm Wall**				**Ceiling**
		SE	SW	NW	NE	
9:30h	**2**	704	173	117	311	121
	4	659	189	101	278	122
	6	673	197	107	335	116
13:30h	**2**	355	443	158	267	424
	4	304	297	163	233	382
	6	368	287	149	248	382
17:30h	**2**	166	254	148	137	220
	4	156	162	138	128	223
	6	200	166	170	113	224

Units in PPFD [$\mu mol.m^{-2}.s^{-1}$]

In the morning, at 9:30h, the light mainly enters from the southeast wall and, unlike for the other barrel façades, it directly radiates in the barrels testing surface (facing the southeast wall) giving significantly higher levels of PPFD registered. Despite the farm wall's diffusion of light, direct light

exposure has significantly higher intensity compared to the indirect diffused light inside the farm. This is the main reason for the testing surface being restricted to three columns facing the southeast wall, avoiding the lateral areas more susceptible to shading. At 13:30h the sunlight is mostly inserted in the southeast façade and ceiling. Southwest sunlight incidence is high for Barrel 2, however, it is significantly damped for barrels 4 and 6 due to the shading from neighbouring barrels. During the late afternoon, at 17:30h, the overall light penetration decreases significantly, mostly occurring through the ceiling. Barrel 2 receives a significantly higher amount of light compared to the other shaded barrels at this time. These natural light conditions suggest that the peak of solar insertion in the barrels testing surfaces (facing southeast) will be in the morning, significantly decreasing in the afternoon when the sunlight no longer directly penetrates the southeast wall. Further detail is seen in section 6.

5.3.2 Artificial Light Condition

The three LED strips are placed vertically 22cm in front of each barrel directly facing the three plant slot columns of the test. At the distance of the barrel surface (from the LED) is where the leaves of basil stay in the first week of growth and where the stem base remains after that. As the basil grows, its leaves can reach much closer to the LED light source in a region where the PPFD is higher than where the plant started. Figure 38 show some Gustosa basil plants previously planted at the farm in different maturity stages and their distances to the LEDs.

Figure 38 - 1-week-old basil 22cm from the LEDs (left); 3-week-old basil 12cm from the LEDs (middle); 5-week-old basil 3cm from the LEDs (right)

From the figures, clearly, the growth of the plants positions them closer to the LEDs, growing more than half of the total initial distance. This relative approximation to the source results in an exponential exposure of leaf area to light photons (unlike with sunlight). This means that the number of artificial light photons per area (units of PPFD) reaching the leaves alters significantly throughout the plant's life. To account for this variation, the artificial light PPFD was measured for three different distances directly in front of the LEDs at maximum intensity to determine a mean intensity exposure for overall growth cycle (Table 11).

Table 11 – PPFD measurement of LED light at full intensity from different distances from the light source.

Development Stage	**Week 1**	**Week 3**	**Week 5**
Minimum distance from the LEDs [cm]	20	12	3
PPFD [$\mu mol.m^{-2}.s^{-1}$]	533	924	>3000

It is also important to note that not all leaves of the plant reach the same proximity to the light source, part directly exposed to light and part shadowed. Analysis of such details is out of the scope of this study, however, it is important not to assume the intensity of light reaching the closest leaf for the generality of the plant. An estimation of 750 μmol.m^{-2}.s^{-1} was attributed to maximum PPFD intensity from the LEDs reaching a mean position through the 4-week experiment.

5.4 DLI Targets and LED Control Algorithm

Each barrel will have a different target of total DLI (Solar plus LED) to reach every day. The targets set will increase gradually between each barrel with DLIs of 12.5, 15 and 17.5 mol.m^{-2}.d^{-1}. These targets will be mostly above the reach of sunlight alone and met with the LED light complements for the same barrel to receive the same amount of accumulated light every day. There might be exceptions during days of very intense sunlight, where the solar DLI may pass the smaller target of 12.5. This will be discussed in section 6. The period of darkness is the period from the moment the LEDs turn off until sunrise and has an important role in plant development (as seen in LT). From literature the dark period defined for most experiments was between 6 and 8 hours and for this report will be set as 7 hours. The dark period will be fixed throughout the experiment to avoid this factor influencing the results. Consequently, the total period of both natural (photoperiod) and artificial (LED period) light exposure will be 17 hours (24 – 7 = 17h). The operation time of the LEDs will always be the maximum that guarantees 7 hours of darkness and is dependent on the sunset and sunrise times. The main variables defined for the system and the formulas for the LED dynamic parameters are listed in the next Table 12. The full LED control system algorithm can be found in Appendix 3.

Table 12 – Main variables used for the LED operation.

Variable	**Barrel**		
	1	2	3
DLI target, DLI_t [mol.m^{-2}.d^{-1}]	**12.5**	**15**	**17.5**
DLI (solar) measured, DLI_m [mol.m^{-2}.d^{-1}]	[Sensor Output]	[Sensor Output]	[Sensor Output]
PPFD from LED, $PPFD_{LED}$ [μmol.m^{-2}.s^{-1}]	750	750	750
Period of Darkness, P_{dark} [h]	7	7	7
LED Operation Period, P_{LED} [h]	[Night Period Duration] - P_{dark}		
LED Intensity, I_{LED} [%]	$\frac{(\mathrm{DLI_t} - \mathrm{DLI_m}) * 10^6}{PPFD_{LED} * P_{LED} * 3600} * 100$		

5.5 Key Performance Indicators

The results of the experiment will address the development of the two varieties of basil plants and the energy consumption of the LEDs during that period. Regarding plant development, there are multiple aspects investigated in literature including fresh/dry mass, size, number of leaves/branches, concentration of chemicals, etc. In the Raiz vertical farm's commercial

operation, the basil plants are sold according to their edible weight. Therefore, the plant's fresh mass is the most useful parameter for this context, and it will be the main growth performance indicator of the report. It is important to note the distinction between the edible plant's mass, which consists of the leaves (and stems), and the entire plant's mass, which includes the plant's roots and remaining jiffy material. The plant size will also be analysed for additional reliability of results. The plant's size is hereby addressed as the "green profile area" and was only measured in the final week. It is described in the present work as the height from the top of the plant to the bottom of stems, multiplied by width of the plant in the largest region and profile orientation.

The total mass of the plant will be registered weekly, including the roots and wet jiffy. The weekly weightings were made by removing the plants from the hydroponic barrels and taking the weight of each plant individually in a scale with -+1g precision. It was assured that the jiffies were approximately equally wet by taking the plants 5 minutes after irrigation stopped for all barrels. Pictures were also taken of all the plants weekly. This procedure was repeated for four weeks from September 11th to October 9th, 2023, until the Gustosa basil plants were considered mature enough for harvest by the Raiz's team of agronomists. The Pluto basil plants were not completely maturated but the weight and size results at this stage were considered as final due to plant repositioning required for normal farm operation. Therefore, all final results investigated in the next section are obtained 42 days after sowing and 28 days after germination. The physiognomy/appearance of the different parts of the plants will be taken into consideration in the discussion of the results. The goal of this part of the analysis is to detect potential defective development and provide additional remarks which may not be noticed in plant's fresh mass and size results.

The other main parameter to investigate is the energy consumption [kWh] of the LEDs in the dynamic control system under different DLI targets. There will be an assessment of the energy required in artificial lighting for each target and how much of those targets can be met passively by sunlight in a greenhouse application. The theoretical energy consumption of the LEDs can be calculated using the rated power of the LED sets, the period of operation and the level of intensity. The actual energy consumption is going to be slightly different due to hardware inefficiencies, residual voltages, etc. The Shelly meter tool allows the actual energy consumption to be measured for each barrel and compared with theoretical values. The physical energy losses are an indicator of the performance of the installed LED control system and the energy efficiency of the current equipment used.

Regarding the LED operation, there was an attempt to measure the artificial light DLI from the LEDs with the AS7341 light sensors, however, these were calibrated for sunlight spectral composition resulting in unrealistic PPFD values measured from the LEDs. The system was later updated to shift the sensor channel counts-to-PPFD conversion when the LEDs are activated, allowing a more accurate representation of the artificial light in PPFD units. This provided additional information which was useful in confirming the proper LED operation (with some uncertainty). For the integrity of the analysis of the LED's DLI, the details of the artificial light will

be consulted through records of the microcontroller action commands (LED dimming level and operation period) and cross-checked with the registered energy consumption of the LEDs (Shelly). As previously mentioned, the Shelly meters connected to each set of LEDs measured the electricity consumption during the whole experiment. By analysing the consumption history, the actual amount of artificial light (DLI) can be obtained based on the linear correlation of LED's PPFD and electrical consumption, seen in section 4.3.3. The consumption levels will be further verified with the sensor measurements, simply to ensure the electricity consumption indeed represented LED illumination.

Finally, the plant yield of each barrel will be compared against the LED energy consumption for analysis of the yield energy efficiency. This parameter will be addressed in g_{basil}/kWh and is the key energy performance indicator to maximize. Furthermore, a plant growth relation to the DLI regime targets is formulated, addressed in g_{basil}/DLI, considering the experimental limitations observed, eventually suggesting the best-performing DLI regimes.

6. Results and Discussion

The initial part of this section will analyse the reliability of the lighting system measuring the PPFD of natural and artificial light, calculating the corresponding DLI and controlling the LEDs accordingly, for representative days. The analysis of the experimental DLI conditions, plant productivity and energy consumption of the LEDs will be carried out afterwards. All the results were experimentally obtained using data captured by the light sensors and shelly device and stored in the Raspberry Pi and Google Cloud Platform.

6.1 Representative Days

6.1.1 Natural Light Incidence on Testing Surfaces

To understand the natural light patterns experienced in the testing surfaces of the three barrels, follows an inspection of the daily PPFD distributions for representative days of September and October. By analysing each barrel's daily measurements, it is possible to identify common patterns for the entire container and some distinguishing features between the barrels. These light patterns reflect the influence of factors such as the barrel positioning inside the container, the orientation of the farm and the shadows experienced. Figure 39 presents the distribution of PPFD throughout the day for each barrel, for a few days between 20 and 28 of September (darker colour) and days between 7 and 11 of October (lighter colour). These days were chosen due to the low cloud coverage condition, which is useful for identifying sunlight patterns. The distinction between the two months can help characterise how the light patterns evolved during the experiment period.

The PPFD data curves can be very "shaky" throughout the day and may present inconsistent large drops related to temporary cloud coverage. Since the weather condition was mostly clear during this period, the records of the different days should complement each other, compensating for periods of cloud coverage. To understand the trends in solar incidence, it is important to focus on the converging patterns of overall PPFD distribution at the highest points of each hour (for days in the same month). The inaccurate linear PPFD rises seen at the end of the day for Barrel 2 are misrepresentations due to lack of sample points for that period for certain days and, therefore, should be ignored.

The first trend to note from Figure 39 is the differences in PPFD intensity between the morning period (from 8:30h to 11:30h), and the afternoon period (after 13:00h) for all barrels for both months. While the morning period registered levels mostly above 400 $\mu mol.m^{-2}.s^{-1}$, the afternoon one did not capture PPFDs higher than 400 $\mu mol.m^{-2}.s^{-1}$. Furthermore, after 15:00h, the levels dropped below 200 $\mu mol.m^{-2}.s^{-1}$ during all days considered for the 3 barrels. This is related to the barrels testing surface orientation, which is facing Southeast (132º), and not South. The peak intensity period is always in the morning, often between 9:30 and 11h (Barrels 2 and 6) or slightly after 12h (Barrel 4). Furthermore, the light distribution is not symmetrical since during the

mornings, the sunlight seems to increase with a natural pace from sunrise (around 7:45h) until 10:00 for all cases. In the afternoon, before 13:00h, the PPFD suffers a brusque reduction from levels around 600 to 400 $\mu mol.m^{-2}.s^{-1}$ (or 300 $\mu mol.m^{-2}.s^{-1}$ for Barrel 4), and after 13:00h the decline occurs at a much slower pace for all barrels. The regularity of this sequence implies that the PPFD decreases around 13h are caused by the angle of sunlight no longer directly inserting in the farm's southeast wall (in front of the testing surface). The PPFD levels registered after that represent diffused/shaded solar radiation which naturally decreases throughout the afternoon. The farm orientation is the main spatial constraint preventing homogeneous sunlight exposure between the testing barrels.

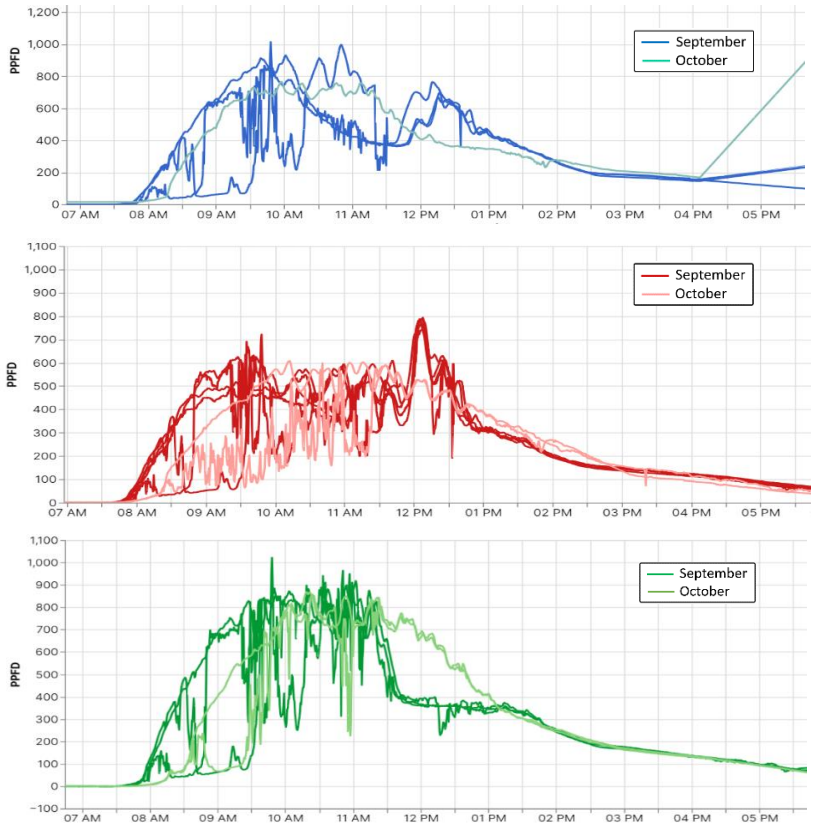

Figure 39 – PPFD daily distribution of Barrel 2 (upper), Barrel 4 (middle) and Barrel 6 (lower) for some days of September and October characterized by clear sky conditions.

Another tendency that can be observed is the different light intensities experienced between the corner and middle barrel at the same time of the day which occurs primarily due to the barrel's position inside the farm. The corner barrels 2 and 6 experienced significantly higher average PPFD levels between 600 and 900 $\mu mol.m^{-2}.s^{-1}$ compared to Barrel 4 registered levels between 400 and 600 $\mu mol.m^{-2}.s^{-1}$. Moreover barrels 4 and 2 appear to experience further shadowing events as their levels appear lower during the morning frontal solar incidence. Barrel 4 had a distinguished peak experienced slightly after 12:00 in September, significantly higher than the morning high levels and probably represents a local interruption of structural shadows, which did not occur for the corner barrels. Barrel 6 appeared to experience a steep PPFD drop at 11:30 for the days of September which did not happen for the inspected days of October. Barrel 2 had a

distinguished low section between 10:00 and 12:00 for some days in September and showed broader rise in the afternoon than the rest of the barrels reaching 600 $\mu mol.m^{-2}.s^{-1}$ until a bit before 13:00, then it followed the general decline trends as the rest. Both these irregularities in the morning period of September are most likely linked to the structure's shadows since in October, when the sunlight angle of incidence is lower, they shifted. The orientation of Barrel 2 next to southwest and southeast walls, would expect higher natural light incidence, but the close positioning and orientation of the testing surface to the southeast wall attenuates this.

All the individual sub-patterns observed for each barrel indicate the influence of temporary shadowing events caused by the LED strips and greenhouse structure beams since they are more regular and coincidental for different days than the "shaky" variations caused by cloud coverage. Moreover, the slightly different position of sensors for each barrel influences their periodical exposure to direct and diffuse sunlight, which significantly alters the amount of light captured by each barrel.

6.1.2 LED Control System Testing

It is important to explore the limitations of the system by understanding the possible range of weather conditions for the region, specifically the sunlight penetration inside the farm. The correct manner to verify this would be by assessing PPFD and DLI results for the three testing barrels throughout the entire year, which was not carried for this report. Nonetheless, during the testing and experiment period a significantly wide range of climate conditions were observed influencing the sunlight penetration at the farm. An example of quite distinct natural light patterns happened between the 8th and the 17th of October, which were days characterized by low and severe cloud coverage, respectively. Figure 40 represent the PPFD (left) and DLI (right) from the sunlight exposed in Barrel 6 for the clear sky (blue) and overcast (grey) days.

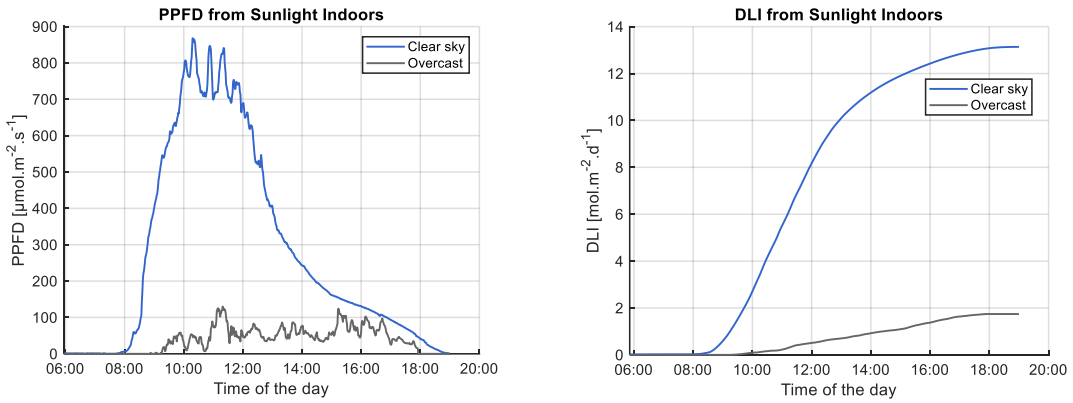

Figure 40– Solar PPFD (left) and DLI (right) recorded indoors (Barrel 6) for a day with clear sky, October 8th, (blue) and overcast, October 17th, (grey) conditions.

The most important results are summarized in Table 13 including the times of sunlight appearance and disappearance and the timespan between them. These are sunrise, sunset and photoperiod values according to the system records, which may differ from the actual geographical sunlight statistics. The table also presents essential information on the PPFD between 9:30 and 17.30

timespan which covers the main solar activity of both days. The DLI registered is only associated with natural light exposure, the artificial light is not represented.

Table 13 – Main characteristics of the natural light exposure recorded indoors (Barrel 6) for the representative days October 8th and 17th.

Day	**Weather Condition**	**Sunrise /Sunset**	**Photoperiod** [h]	**PPFD [µmol.m^{-2}.s^{-1}]** (09:00 – 17:30)			**DLI** [mol.m^{-2}.d^{-1}]
				Min.	Avg.	Max.	
08/10/23	Clear Sky	07:44h/18:57h	11.22	71	405	868	13.14
17/10/23	Overcast	08:52h/17:56h	9.07	7	56	130	1.74

October 8th was a day of rare cloud coverage during the entire day, resulting in a high average PPFD of 405 µmol.m^{-2}.s^{-1} between 09:30 and 17:30. On the other hand, October 17th, can be considered a typical day with overcast sky conditions, resulting in an average PPFD of 56 µmol.m^{-2}.s^{-1} (less than 1/7th of the sunny day). For October 8th the PPFD peaked at 868 µmol.m^{-2}.s^{-1} at 10:18h, compared to a maximum of 130 µmol.m^{-2}.s^{-1} for the 17th, at 11:19h. The sunny day had higher values during the morning (until 12:00h) compared to the afternoon.

Figure 40 shows the DLI is the accumulation of the PPFD throughout the day. For the clear sky day (October 8th), the DLI nearly reached 13.14 mol.m^{-2}.d^{-1}, mostly accumulated during the morning as seen by the steep slope of this period compared to a flatter one in the afternoon. The cloudy day (October 17th) had a much smaller DLI of 1.74 mol.m^{-2}.d^{-1}, around 13% of the sunny day, similar to the ratio between the average PPFD. This makes sense as the sum of all PPFD samples of a day is the same as the average of PPFD multiplied by the total amount of samples, both equivalent to the DLI. It is also noticeable in the cloudy day how PPFD appears in a smaller timespan (photoperiod) resulting in a shorter time of accumulation of DLI, further contributing to smaller values relative to sunny (longer) days.

Even the 7th of October considered a sunny day had a solar DLI inferior to the optimal range of 15 mol.m^{-2}.d^{-1}. This is the case most of the days during this time of the year. For the optimal DLI level to be reached at the farm, additional DLI must be supplied by the artificial light of the LEDs. Figure 41 represents the total PPFD and DLI captured by the sensors of Barrel 4 on the 25th of September, here counting with the LED's light contribution as well.

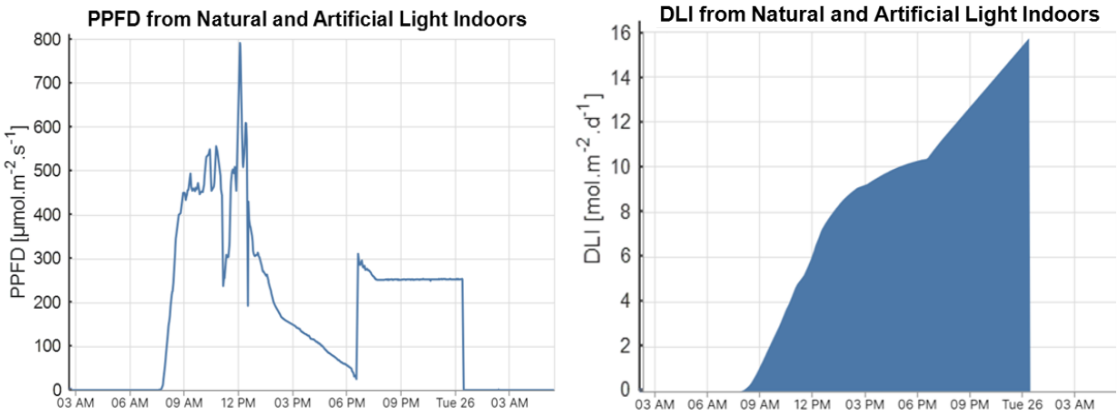

Figure 41 – Natural and artificial light PPFD (left) and DLI (right) for a day with mostly clear sky conditions, September 25th (Barrel 4).

During this day, the PPFD incidence from the sun was felt from 07:45 to 18:35h (photoperiod = 10.8h), ranging from 58 to 790 µmol.m^{-2}.s^{-1} and averaging 294 µmol.m^{-2}.s^{-1}. The farm wall orientation is noticed again through the high PPFD levels during the morning (between 400 and 600 µmol.m^{-2}.s^{-1}) and low ones in the afternoon (below 300 µmol.m^{-2}.s^{-1}). The light of the LEDs is clearly noted at the end of the day by the block-shaped step in the PPFD level. The LED operation started at 18:35h and remained with constant intensity of 251 µmol.m^{-2}.s^{-1} until 00:25h of the next day, resulting in 5.8h of operation period. The LEDs are programmed to start slightly before the solar PPFD completely reaches zero, activating when PPFD < 20 µmol.m^{-2}.s^{-1} to avoid failure turning on in case of sensor miscalibration. Due to this, there is a short initial phase of the LED operation when the PPFD recorded appears slightly above the programmed PPFD for the LED light, which gradually disappears. This represents the remaining sunlight that radiated between the start of the LEDs and the actual sunset. The main indicators of the lighting conditions can be found in the following Table 14.

Table 14 - Main characteristics of the natural and artificial light exposure recorded indoors (Barrel 4) for the representative day (September 25th).

Weather Condition	**Photoperiod** [h]	**LED Period** [h]	**PPFD** [µmol.m^{-2}.s^{-1}]		**DLI** [mol.m^{-2}.d^{-1}]		
			Average Sunlight (09:00 – 18:00)	LED	Sun	LED	Total
Partly Cloudy	10.8 (07:45 - 18:35)	5.8 (18:35 - 00:25^{+1})	294	251	10.33	5.37	15.70

From Figure 41 it can be seen that the sunlight alone had resulted in a DLI of 10.33 mol.m^{-2}.d^{-1} and the artificial light complement an additional 5.37 resulting in a total DLI of 15.70 mol.m^{-2}.d^{-1}. The LED operation is here clearly noted by the linear increase of the DLI at starting at 18:35h after the characteristic curve of solar DLI. The slope of the LED DLI is directly related to the LED dimming level, i.e., the regulated light intensity between 10-100%, which ultimately controls the LED PPFD amount. The recommended DLI target of 15 mol.m^{-2}.d^{-1} was eventually met (with

some error margin) at 00:25h of the next day, around 2/3rds by natural light and the rest by using artificial light complements. At this moment the LEDs are turned off and the system's count of accumulated PPFD (i.e. the DLI) is reset. The accuracy of the system meeting the targets of total DLI will be discussed later in this section for the period of the experiment.

6.2 Experimental Days

Before analysing the results of plant growth and energy consumption corresponding to each DLI regime, the light exposure for each barrel and each day will be inspected to understand the solar and artificial light patterns experienced by the plants. It is important to distinguish between the theoretical light (DLI) targets set initially and the actual DLIs that the plants experienced during the 29 days of the experiment. Part of that distinction was measured by hardware installed at the farm and can be identified by consulting stored data of the light sensor readings and the LED operation. Other factors contributed to the differences between proposed and actual light conditions, and it is important to identify these sources of error for future improvement of the system. This section will have three main parts: First, there will be an assessment of the experimental light conditions based on existing data stored from light sensors and energy meters and compared to the actual conditions and intended light targets. Secondly, the results of plant growth will be analysed for plant fresh mass and size, as well as the energy consumption of each light regime. Lastly, a conclusion on the performance of each DLI regime will be taken for optimal fresh mass and energy consumption. Additional discussion will include potential sources of error in the measuring/actuating light system that may justify the unexpected growth of some plants.

6.2.1 Disclosure – Experimental Setbacks

During the period of the experiment, certain unfortunate events occurred that affected the intended plan of operation of the LED control system, as well as part of the plant samples. It is important to identify and deconstruct these setbacks to understand the actual conditions of the experiment and the system limitations. Nonetheless, upon investigating the actual circumstances, feasible results and conclusions can still be obtained from the experiment.

Recall the DLI targets of 12.5,15 and 17.5 $mol.m^{-2}.d^{-1}$ set for the three barrels of study. An issue occurred when the sunlight (alone) surpassed the lowest DLI target of 12.5 $mol.m^{-2}.d^{-1}$ for days of intense solar radiation. This was not expected based on the initial tests, particularly not during the months of September/October when days get shorter, and the weather tends to become cloudier. In practice this happened for some days of the experiment, making the regime of Barrel 6 exceed the DLI target of 12.5 $mol.m^{-2}.d^{-1}$ and becoming inconsistent throughout the study period. The solar DLI did not surpass the 15 $mol.m^{-2}.d^{-1}$ target at any day during the experiment, and, therefore, did not compromise the other light regimes tested. However, for Barrel 6 the plant growth can no longer be associated with a light regime with DLI of 12.5 $mol.m^{-2}.d^{-1}$. The sunlight measurements will be analysed and a modified (registered) light regime of Barrel 6 will be taken for further discussion instead of the defined initially.

Another experimental setback was caused by a malfunction of the dimming component (PWM-to-Voltage converter) in the LED control system of Barrel 6, on the 17th of September, and it was not possible to replace it during the experiment period. This meant that the regulation of the LED's light intensity was not able to be done by the installed control system. With the broken hardware connected to the LED's driver dimming wires, it was noticed that the LEDs were passively dimmed to 38W constant power, which corresponds to 17% of total power. The control was, therefore, limited to this level and consisted solely of the schedule regulation of the LED period daily on the Shelly app (when possible). This meant that if the LED required to be turned on for more than 17%, it was not going to be possible without disrespecting the maximum period of operation allowed. If the required intensity was below 17%, there was a reduction of the LED operation period via the Shelly app to approximate the DLI complement to the daily lighting target needs.

Regarding the tested plants, an accident occurred at the farm at the end of experiment week 3 which compromised part of the study for the Gustosa basil variety. The harvesting procedure happens every Monday and consists of collecting part of the plants (considered mature enough) at the farm to sell and transplanting new germinated ones to the free barrel slots. The staff responsible for this task accidentally harvested 8 plants out of 9 of the Gustosa variety (despite the warning of the experiment). The plants prematurely harvested were all in the Barrel 2 and therefore there are no results for these for weeks 3 and 4. The remaining Gustosa plant of Barrel 2 will also not be considered for analysis since this sample was one with minimal growth, not representative of the whole set.

6.2.2 Solar DLI

After understanding the PPFD patterns of each barrel and the experimental setbacks, follows the analysis of the key determinant factor of the report – DLI. Figure 42 shows the average DLI in $mol.m^{-2}.d^{-1}$ units registered for the three barrels around sunset time, before the LEDs were turned on, for the 28 days of the experiment (from September 11th to October 8th).

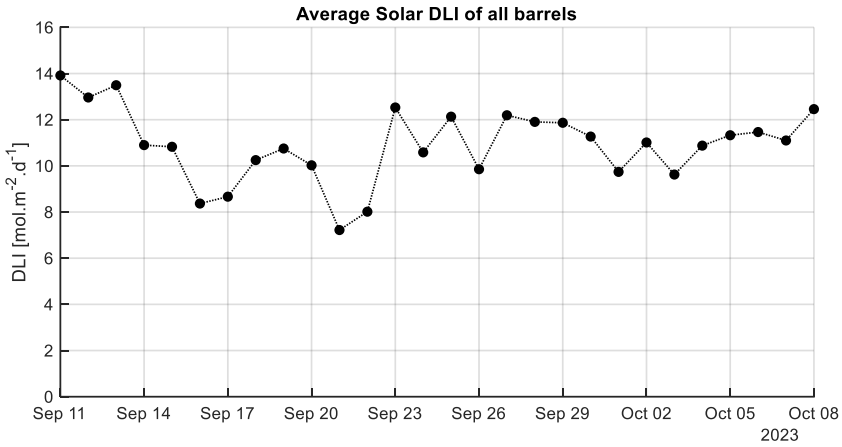

Figure 42 – Solar DLI average levels of all barrels registered during the experiment.

During the period of the experiment, the average solar DLI captured from all barrels had a mean value of 10.92 $mol.m^{-2}.d^{-1}$. These are high average levels of solar DLI compared to the optimal DLI target recommended in literature of 15 $mol.m^{-2}.d^{-1}$. This means that during the months of September and October, the sunlight could, on average, cover more than 2/3rds of the indicated optimal DLI.

The maximum average DLI registered was 13.92 $mol.m^{-2}.d^{-1}$ on September 11th and the minimum was 7.22 $mol.m^{-2}.d^{-1}$ on September 21st. The DLI had moderate variations throughout the experiment period resulting in a standard deviation of 2.49 $mol.m^{-2}.d^{-1}$ (13.7%). The main factor differentiating the DLI each day was the amount of light reaching the outside façade of the farm container (as the indoor conditions were constant for each day), highly correlated to the global solar radiation reaching the surface of the Earth (at specific orientation). This parameter was highly dependent on the cloud coverage conditions since DLI variations with the time of the year were not significantly noticed during the experimental period of approximately one month. Prolongated periods of dense cloud coverage will significantly affect the DLI, while short ones may not be noted. From Figure 42, the DLI registered during the 16th, 17th, 21st and 22nd of September can be seen much lower than surrounding days, with DLIs below 9 $mol.m^{-2}.d^{-1}$. On the other hand, the days of 11th, 12th, 13th, 23rd, 25th, 27th, of September and 8th of October were probably days of mostly clear sky condition with DLIs above 12 $mol.m^{-2}.d^{-1}$. The difference between the highest (September 11th) and the lowest (September 21st) DLIs registered was 6.70 $mol.m^{-2}.d^{-1}$, meaning the influence of cloud coverage conditions had a range somewhere around this level. It can be concluded that there were no days of intense overcast weather conditions since the lowest DLI value registered was only half of the highest, and, as seen in section 6.1.2, extreme overcast can drop the DLI to 1/7th compared to clear sky conditions during this time of the year.

It is also important to analyse the differences recorded in DLI between each barrel. Figure 43 illustrates the DLI values measured by each barrel for each day of the experiment.

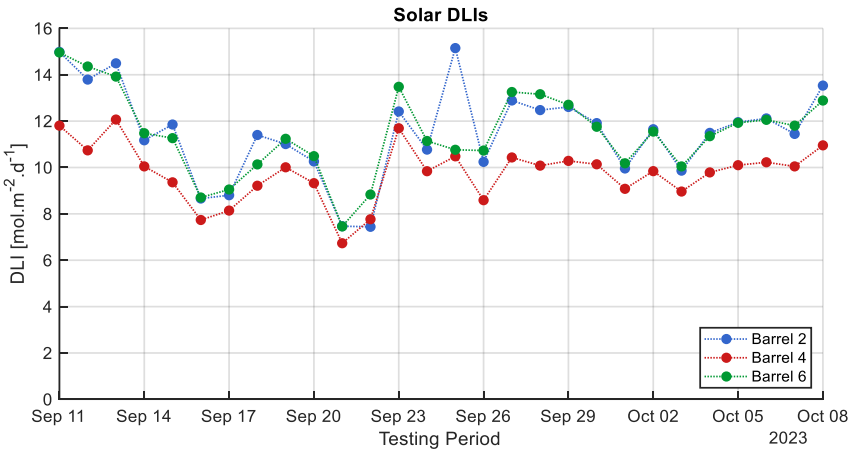

Figure 43 - DLI values measured of each barrel recorded during the experiment.

The DLI curves of the three barrels appear with approximately aligned patterns, suggesting the fluctuations to be related to outdoor factors such as weather conditions. The trend observed in Figure 39 in section 6.1.1 of higher sunlight exposure in corner barrels (2 and 6) than the middle barrel (4) is here demonstrated by the significantly lower DLI curve of Barrel 4 throughout the experiment period. Barrels 2 and 6 averaged a similar solar DLI of 11.57 and 11.42 $mol.m^{-2}.d^{-1}$ while Barrel 4 averaged 9.81 $mol.m^{-2}.d^{-1}$ (about 15% lower). The gap between barrels shows some proportional behaviour to the DLI level. This likely happened since days with lower DLI correspond to the days with higher cloud coverage, thus, less direct sunlight penetration consequently attenuating the impact of shadows in the middle barrel.

The corner barrels have very similar values alternating the records of highest DLI irregularly. This is likely related to differences in solar radiation between the morning and afternoon periods, as Barrel 6 (Northeast) receives higher slightly sunlight intensities in the morning and Barrel 2 (Southwest) receives higher sunlight intensities in the afternoon. An unusual event can also be noted on the 25th of September Barrel 6 had to be cleaned after the harvest (of plants not part of the experiment). This required the removal of the sensors during the morning and temporary placement in a less illuminated place. As a result, the typical increase from the 24th to the 25th was not observed for Barrel 6 (it was even marked by a small decrease).

6.2.3 LED DLI Target Performance

6.2.3.1 Barrel 2

After the evaluation of the DLI levels provided by the natural light at the farm follows the analysis of the supplementary DLI provided by the artificial light of the LEDs. The LED dynamic control system delivered tailored amounts of artificial light for each barrel according to the solar DLI measured during the day and the regime defined for each barrel. By adding the DLI from the sunlight to the DLI from the LED light, the total DLI is obtained for each barrel and each day. It can then be compared to the intended DLI targets (12.5, 15 and 17.5 $mol.m^{-2}.d^{-1}$) to analyse the accuracy of the dynamic LED control system in delivering specific DLIs, as well as understand the actual light regimes that the plants were subjected experimentally. Figures 44 to 46 will present the total DLI for each day of the experiment according to its source and a dashed black line marking the intended target of the total DLI of each barrel.

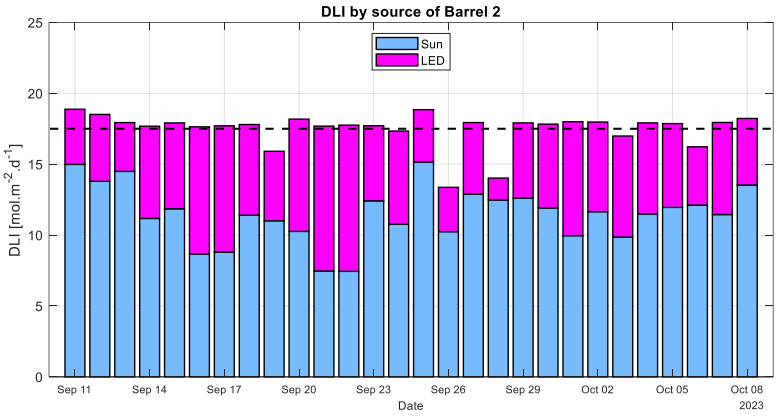

Figure 44 – DLI level registered by light source in Barrel 2 during the experiment period.

Testing Barrel 2 had the most demanding light regime of all with a DLI target of 17.5 mol.m^{-2}.d^{-1}. The DLI from the sunlight remained under the target for all days and the missing DLI gap was complemented by the LED artificial light with a variable margin of error. It can be observed that the control system was behaving dynamically based on the variety of artificial light DLI provided according to the sunlight condition for each day. The accuracy of the LED operation in reaching the target line was not ideal. It had occasions of excessive and deficient illumination, but, for most days, approximately on target. This will be observed for all barrels. The reasons for the inaccurate amount of DLI delivered were highly related to the electrical-to-PPFD inaccuracies and non-linearities, as well as some abnormal events for specific days that prevented normal LED operation. The latter include social nocturnal events that required the LED to be turned off earlier (September 19th and 26th) and the malfunction of certain hardware of the control system (September 28th), which prevented the full targeted DLI from being provided.

It is noticeable that on days with low solar radiation, such as September 21st and 22nd, the DLI collected from the sun was around 7.50 mol.m^{-2}.d^{-1} which corresponds to less than half of the total target. The LEDs were able to provide an additional 10.22 and 10.31 mol.m^{-2}.d^{-1} (around 60%), respectively for each day, by activating at an intensity of around 65% (corresponding to a PPFD of 485 µmol.m^{-2}.s^{-1}) for 5 hours and 50 minutes. This was the most demanding circumstance for the LED operation during the experiment considering all barrel operations. On the other hand, on sunny days like September 11th and 13th the solar DLI reached almost 15 mol.m^{-2}.d^{-1}, highly diminishing the artificial light needs registered to around 3.5 mol.m^{-2}.d^{-1} for both days, corresponding to 20% of total needs. This illumination corresponds to a 1/3rd of the LED light used compared to the previous cloudy days. The overall average LED light DLI for each day considering the inaccuracies of operation in meeting the target was 5.97 mol.m^{-2}.d^{-1}. Added to the average solar DLI seen previously, results in a total average DLI of 17.55 mol.m^{-2}.d^{-1} throughout the experiment meaning that there was a high accuracy meeting the desired DLI target. Moreover, the DLI target of Barrel 2 was met 66% by natural light and 36% by artificial light on average, which represents a relatively low stress for the LED load even though this Barrel had the most demanding DLI regime of 17.5 mol.m^{-2}.d^{-1}.The few days of significantly deficient operation were

compensated by the system's tendency to slightly overshoot (most likely due to a proportional error between dimming command action and LED light illumination).

6.2.3.2 Barrel 4

Figure 45 depicts the total DLI according to the light source experienced by Barrel 4 and a dashed black line marked at its intended DLI target of 15 mol.m^{-2}.d^{-1}. Recall that this regime is recommended by literature for optimal basil development.

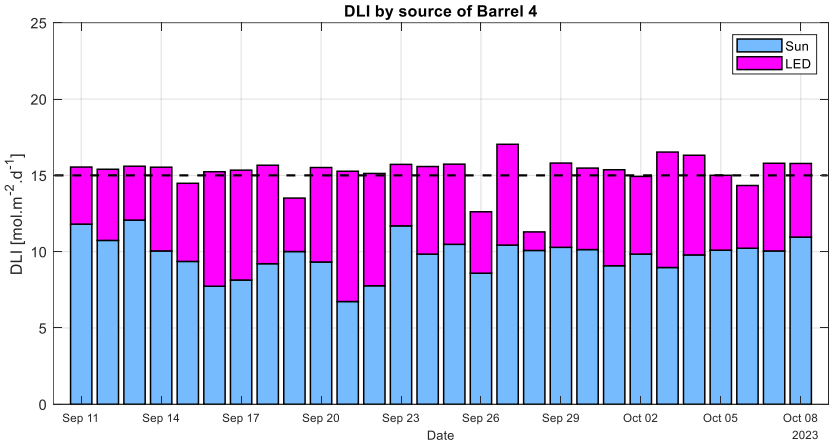

Figure 45 - DLI level registered by light source in Barrel 4 during the experiment period.

The control system installed for this barrel also seems to be functioning dynamically according to the sunlight radiation condition. In general, days with low solar DLI show higher LED light compensations and days with higher solar DLI are the opposite. The LED light requirements were lower than in Barrel 2, as expected, although not in a proportional way since Barrel 4 was characterised by receiving lower amounts of sunlight. To meet the DLI target, an additional 5.41 mol.m^{-2}.d^{-1} was provided by the LED lights on average considering inaccuracies, and added to the solar DLI, resulting in a total of 15.22 mol.m^{-2}.d^{-1}. The intended DLI target of 15 mol.m^{-2}.d^{-1} was met accurately once again, however, the daily inaccuracies were still observed for similar reasons as in Barrel 2. The DLI regime target of Barrel 4 was met 65% by natural light and 35% by artificial light on average, showing how a less demanding regime requires approximately the same LED complements as the previous with 17% higher DLI demand. This stresses the influence of farm orientation and barrel positioning in greenhouse applications in natural light exposure and consequent need for LED operation. Moreover, this type of control system can address shadowing issues, which inevitably occur in these applications, by identifying these regions and boosting operation locally, as seen for Barrel 4.

In terms of the maximum stress of the LED system, it occurred on the (cloudy) day of September 21st when the LEDs provided 8.54 mol.m^{-2}.d^{-1} (57% of target) corresponding to an LED dimming level of 59% and 5 hours and 19 minutes of operation. The minimum LED complement required (relatively on target) was recorded for the 13th of September corresponding to 3.53 mol.m^{-2}.d^{-1}, representing only 17% of the total needs.

6.2.3.3 Barrel 6

Lastly, the DLI information for Barrel 6 with a 12.5 mol.m^{-2}.d^{-1} target is presented in Figure 46.

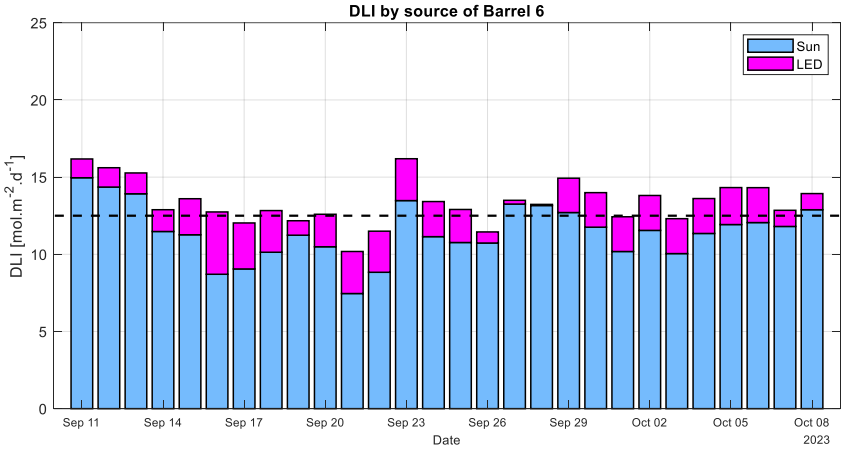

Figure 46 - DLI level registered by light source in Barrel 6 during the experiment period.

The previously explained problems of excessive sunlight DLI and dimming malfunction, are clearly noted in Figure 46. The solar DLI significantly surpassed the 12.5 mol.m^{-2}.d^{-1} target (above 10%) for the three first days, and slightly passed it for 5 other days. The dimming malfunction is noted for days after the 17th of September when the LED's DLI is seen fixed around 2.26 mol.m^{-2}.d^{-1} (17% of LED light dimming) for most days. On the days registered with fewer artificial light DLI (after the malfunction), the control of the LEDs was done through the shelly app when possible.

Nonetheless, Figure 46 provides the actual scenario of total DLI exposure for Barrel 6, from which the following LED energy consumption and plant growth analysis can be made. The average DLI provided by the LEDs for the whole experiment was 1.95 mol.m^{-2}.d^{-1}, (including experimental irregularities), and the maximum DLI required was 4.04 mol.m^{-2}.d^{-1} (32%). Added to the recorded solar DLI of 11.42 mol.m^{-2}.d^{-1}, Barrel 6 experienced an average total registered DLI of 13.37 mol.m^{-2}.d^{-1}, 7% above the intended target of 12.50 mol.m^{-2}.d^{-1}. Despite the dimming hardware malfunction, the target DLI was still approximately met due to the ability to passively fix the dimming level at 17% joined by the usual low needs for LED complements. The Barrel 6 target regime was met 91% by natural light and 9% by artificial light, showing how little the LED requirements are for this DLI target in a greenhouse application.

6.2.4 LED Energy Consumption

The electrical energy consumption of the LEDs is represented in Figure 47 for the experiment period where LED 2, 4 and 6, correspond to the LED sets for each of the testing barrels 2, 4 and 6, respectively. These are the energy consumptions required to radiate the LED's artificial light DLI amounts for each barrel seen previously.

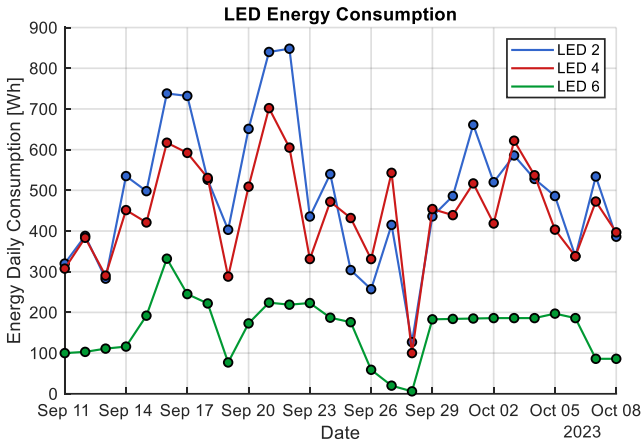

Figure 47 – Energy consumption of each barrel's LED set during the experimental period.

The consumption of electricity registered for each barrel's set of LEDs during the experiment varies according to the DLI requirement set for each, as expected. LED 2, serving a DLI regime of 17.5 mol.m^{-2}.d^{-1}, had the highest average daily consumption for almost all days, averaging 491 Wh per day. LED 4, serving a DLI regime of 15 mol.m^{-2}.d^{-1}, presented an average daily energy spending of 444 Wh, 10% lower than the previous. Lastly, LED 6 which serves a DLI regime of 12.5 mol.m^{-2}.d^{-1}, (and actual average DLI experienced of 13.37 mol.m^{-2}.d^{-1}), presented much lower energy consumption levels than the rest, having an average daily consumption of 160 Wh, corresponding to 33% and 36% of LED 2 and LED 4 consumption levels, respectively. Recalling the original LED consumption prior to the installation of the dynamic control system (Section 3.4), three LED strips used for each barrel have a daily energy consumption of 864 Wh. This means that the control systems installed to deliver DLI targets of 12.5, 15 and 17.5 mol.m^{-2}.d^{-1} were able to reduce consumption levels by 81%, 49% and 43%, respectively, compared to the initial operation during this time of the year, with no significant difference noted in plant in plant aspect at harvest (although no biomass investigation was carried for this case)

LED 4 was subjected to higher stress due to the shaded condition of Barrel 4, as previously seen, which significantly increased its energy needs relative to the DLI regime targeted. The DLI regime of 12.5 mol.m^{-2}.d^{-1} had very little artificial lighting needs in the (corner) Barrel 6 since this target was often mostly met by sunlight requiring little LED energy consumption. For the most demanding DLI target, the daily energy consumption peaked at 848 Wh for the day with the cloud coverage condition and only required 127 Wh for the day with clearest sky condition. This meant the energy needs showed variations of almost sevenfold between weather extremes experienced during the testing period of a month (September to October). This reinforces the high dependency of the system operation, and consequently, energy consumption on the weather conditions in this type of application.

The total energy consumption registered during the experiment (28 days) for Barrels 2, 4 and 6 were 13.75, 12.43 and 4.48 kWh, respectively, which can be approximated as monthly consumptions for this time of the year.

6.2.5 Plant Growth

6.2.5.1 Pluto Basil Growth

This section will assess the plant growth results of the two varieties of basil (Gustosa and Pluto) for the three barrels under the lighting conditions seen before. Recall that each barrel had 6 testing samples of Pluto and 9 of Gustosa. The results of growth will consider the key performance indicators, plant fresh mass and plant green profile area. The first indicator is the most important for the farm's context of production, the profile area serves as added evidence to make conclusions. The mass of each entire plant was measured each week, starting on the first day of the experiment after transplanted from the germination stage on the 11th of September (week 0) until harvest on October 9th (week 4). As previously mentioned, the Pluto basil plants were not harvested in the fourth week, which indicated that they were not yet developed to their full potential according to the agronomists, however, the testing period was determined as finished for operational reasons. Nonetheless, the growth results for four weeks will be assumed as indicators of the full cycle of development of this plant.

Figure 48 shows a statistical representation of the growth progress of all Pluto plant samples of each barrel throughout this period. The coloured boxes represent the weight samples within the upper and lower quartile (25th and 75th percentiles) of each barrel plant set and the line inside the box represents the sample median. The outlier samples are represented in circles and are defined as values that are 1.5 times the interquartile range (box height) away from the top or bottom of the box. The black lines extended above and below each box represents the maximum and minimum value of non-outliers. The dashed and dotted lines represent the evolution of the plant's growth and are connected to plus signs which mark the average value of the samples for each barrel and each week. The progress was also recorded by photographing the plants of each barrel each week (Figures 49 to 53).

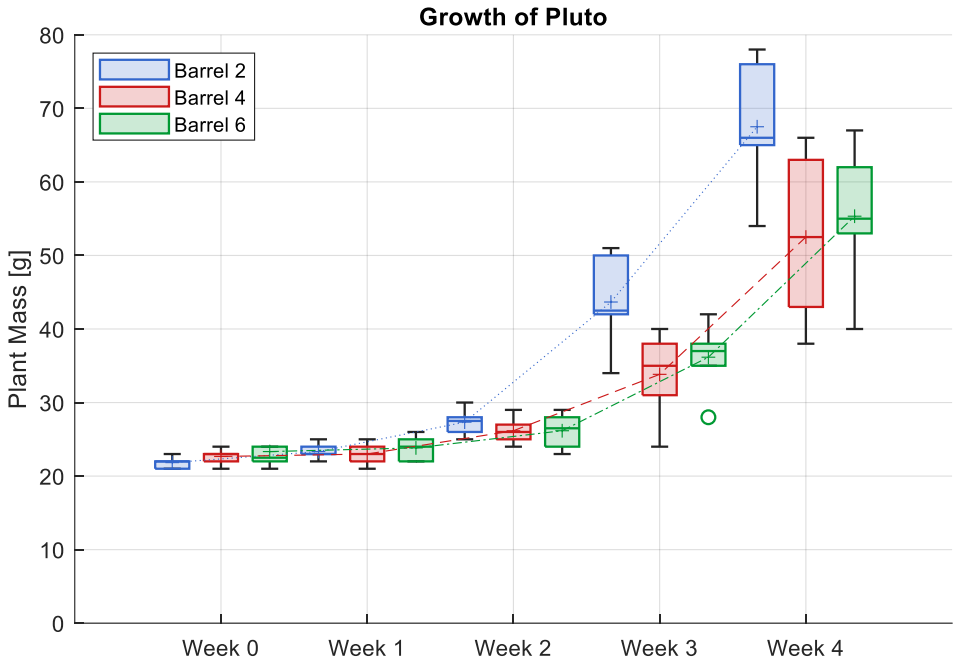

Figure 48 – Fresh mass of Pluto basil (entire) plants on each barrel for each week of the experiment.

The Pluto plants started the testing period coming from the germination stage with very similar mass ranging from 21 to 24g over all samples, mostly representing the mass of the jiffies. The initial average plant mass was slightly lower for Barrel 2 and larger for Barrel 6, with Barrel 4 in between. Figure 49 shows the similar physiological aspects of each set of plants at the starting period.

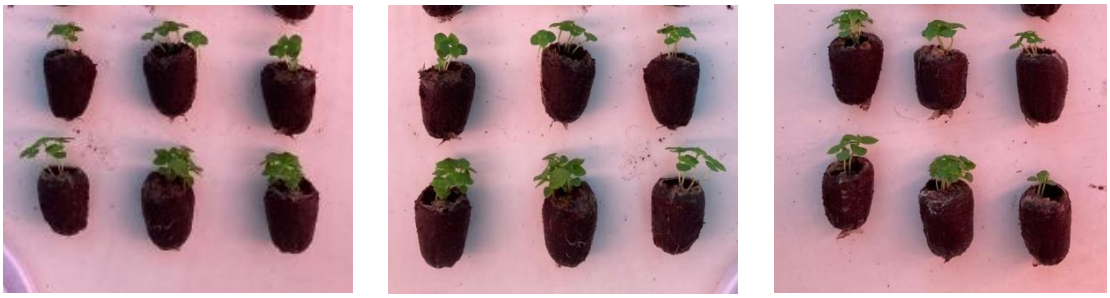

Figure 49 - Pluto basil plants at the start of the first week of the experiment period (Week 0) in Barrel 2 (left), Barrel 4 (middle) and Barrel 6 (right) with DLI targets of 17.5, 15 and 12.5 $mol.m^{-2}.d^{-1}$, respectively.

During the first week, there was no substantial overall growth in terms of plant mass as the median and mean value of both increased by approximately by a gram each. Plants in Barrel 2 presented a relatively larger growth, although the absolute weight growth is insignificantly low (less than 2 grams on average). Figure 50 shows some signs of development for all cases at this stage represented by larger leaf areas, slightly longer stems and a “bushier” appearance. No significant distinguished physiological features between barrel sets yet.

Figure 50 – Pluto basil plants at the start of the second week of the experiment period (Week 1) in Barrel 2 (left), Barrel 4 (middle) and Barrel 6 (right) with DLI targets of 17.5, 15 and 12.5 mol.m^{-2}.d^{-1}, respectively.

During the second week, the growth rate increased a small but noticeable amount relatively to the previous week. On average, Barrel 2 registered a growth of 4g (17%), Barrel 4 of 3.17g (14%) and Barrel 6 of 2.33g (10%). Here the plants started to approach the 30-gram mark, with the heaviest one measuring 30g from Barrel 2. The progress of Barrel 2 is noted to be relatively rapid compared to the others. Barrel 2 was averaging 27.33g while barrels 4 and 6 were averaging an equal 26.17g at this time. This positions Barrel 2 ahead of the others despite starting with the lower plant masses. The trends beginning to be observed for each barrel may not be fully settled as the absolute mass differences are still low and could be associated to other factors.

Regarding their physiological development, overall, there are significant differences from the previous week. All plants appear with larger number of leaves, longer stems and green profile areas significantly larger. The roots also seem to have developed significantly compared to the previous week when most had not protruded beyond the jiffy material. Some variations within the same barrel can be noticed, although with unclear cause. The differences between barrels are still insignificant in their totality.

Figure 51 – Pluto basil plants at the start of the third week of the experiment period (Week 2) in Barrel 2 (left), Barrel 4 (middle) and Barrel 6 (right) with DLI targets of 17.5, 15 and 12.5 mol.m^{-2}.d^{-1}, respectively.

During the third week all plants grew at an unprecedented rate until then reported, especially the ones on Barrel 2. There was a substantial relative increase of the mass for all cases, as well as the first significant increases of mass in absolute terms. Barrel 2 experienced an average growth of 16.33g (60%), Barrel 4, of 7.67g (29%) and Barrel 6 of 10g (38%). Barrel 2 showed much faster growth than the other two barrels, particularly from Barrel 4 (more than double). This set of plants can clearly be seen distancing itself from the rest in Figure 48, with a mean value of 42.5g

comparing to 35g in Barrel 4 and 37g in Barrel 6. Furthermore, Barrel 2 presented quartiles between 42 and 50g, indicating many plants were weighting close to 50g. Barrel 4 had half of its plants weighting below 35g while Barrel 6 had only one below this mark (outlier). An unexpected trend was forming as the results for Barrel 6 appeared higher than for Barrel 4, which had a predefined higher DLI target.

Figure 52 clearly depicts the distinctively higher overall rates of growth of week 3 compared to previous weeks. Plants appear with much higher leaf density, longer stems and more sub-branches developing. The root development was also aligned with this trend as roots become longer, thicker and denser, particularly for Barrel 2. The overall appearance of each barrel's plants is not as clearly distinguishable as the mass results. Nonetheless, plants of Barrel 2 appear to have a higher number of branches and leaves, as well as occupying larger profile areas. Plants in Barrel 6 appear with most features similar to Barrel 4's, both showing some clearly less developed specimens, which might justify the mass distinctions.

Figure 52 – Pluto basil plants at the start of the fourth week of the experiment period (Week 3) in Barrel 2 (left), Barrel 4 (middle) and Barrel 6 (right) with DLI targets of 17.5, 15 and 12.5 $mol.m^{-2}.d^{-1}$, respectively.

During the last week of the experiment, the trends were similar as the previous week, with Barrel 2 continuing is similar growth rate, adding 23.8g (55%) on average per plant, and Barrels 4 and 6 started experiencing faster growth rates, but still inferior in absolute terms, adding average plant masses of 18.7g (55%) and 19.2g (53%), respectively. The final results for Barrel 2 recorded the highest average and mean mass of 67.5g and 66g, respectively, per plant with specimens ranging between 78g and 54g. The first quartile was 65g, meaning only one plant recorded with mass below 65g in this barrel while the others barrels had did not produce any plants with more than 65g. Barrel 4 had an average (same as the median) plant mass of 52.5g (22% lower than Barrel 2) and recorded highest range between quartiles (20g). This was an indication of the presence of two substantially smaller plants (38 and 43g) that can be clearly identified in Figure 53, which were counterbalanced by two other plants above 60g. In Barrel 6 the final average (same as the median) was 55g (19% lower than Barrel 2 and 5% higher than Barrel 4). The plant masses results of this barrel were concentrated above 50 grams with one exception of weighting 40g (also easily identifiable in Figure 53). Considering the initial jiffy mass of about 20g, it can be estimated an average of edible basil mass for Barrel 2 of 47.5g, 32.5g for Barrel 4 and 35g for Barrel 6.

The appearance of all Pluto plants at the end of the experiment can be seen Figure 53, together with their green profile areas. Regarding the green profiles, Barrel 4 produced the smallest plants with an average green area of 218cm^2, followed by Barrel 6 with 254 cm^2 and lastly, Barrel 2 with 271 cm^2. The trends in plant size were similar to the ones observed in fresh mass, although Barrel 6 results for fresh mass were closer to Barrel 4 and for green profile areas are closer to Barrel 2. For the plants green profile area, Barrel 6 and 4 presented an average plant green profile area 6% and 20% smaller (respectively) than the highest average plant area seen for Barrel 2. It is also noted that Barrel 4 was not able to produce plants larger than 300cm^2 as opposed to the other barrels. Moreover, it can be seen a large discrepancy between plants in the same barrel. Some seem clearly underdeveloped compared to others, particularly the ones with green profile areas below 200cm^2. Considering this subjective approach, Barrel 2 produced one underdeveloped unit and barrels 4 and 6 presented 2 units, after 4 weeks of growth in the greenhouse.

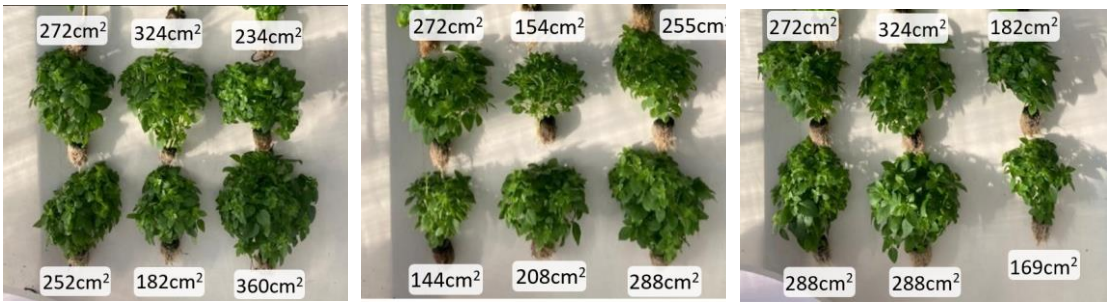

Figure 53 – Pluto basil plants at the end of the experiment period (Week 4) in Barrel 2 (left), Barrel 4 (middle) and Barrel 6 (right) with DLI targets of 17.5, 15 and 12.5 mol.m^{-2}.d^{-1}, respectively.

The plants subjected to the highest DLI target of 17.5 mol.m^{-2}.d^{-1} (Barrel 2) showed the highest fresh mass and green profile area results, however, plants subjected to the lowest intended DLI target of 12.5 mol.m^{-2}.d^{-1} (Barrel 6) presented fresh mass and green profile areas slightly above the ones with DLI target of 15 mol.m^{-2}.d^{-1} (Barrel 4). The possible explanation for this will be addressed at the end of this section, before are the growth results of Gustosa plants.

6.2.5.2 Gustosa Basil Growth

Figure 54 represents the statistics of the growth progress of the available Gustosa basil plants for each week of the experiment for each barrel, determined using the same method as in the previous analysis on Pluto basil. Each set on plants was again photographed and the images for each of the four weeks of the experiment can be seen in Figures 55 to 59.

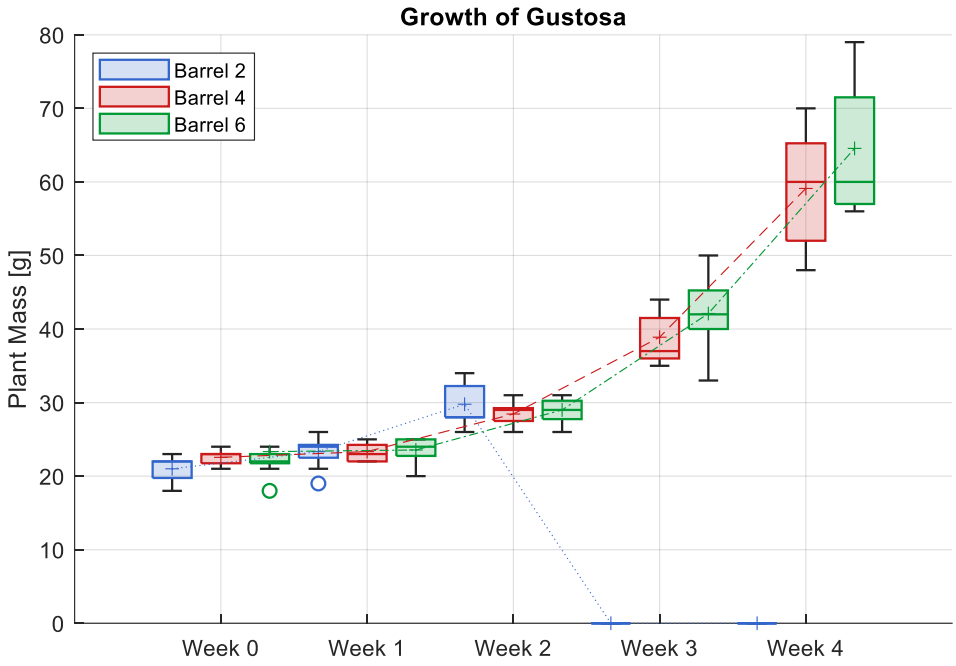

Figure 54 – Fresh mass of Gustosa basil (entire) plants on each barrel for each week of the experiment.

Similarly to the Pluto variety, the Gustosa basil plants also started the experiment will similar masses around the 20g, mostly representing the jiffy's mass, varying overall between 18 and 24g. Again, the plants in Barrel 2 initiated the test with slightly lower average masses than the rest. Figure.55 shows the image of the Gustosa plants on the first day of the experiment.

Figure 55 – Gustosa basil plants at the start of the first week of the experiment period (Week 0) in Barrel 2 (left), Barrel 4 (middle) and Barrel 6 (right) with DLI targets of 17.5, 15 and 12.5 mol.m^{-2}.d^{-1}, respectively.

After the first week growth there was no substantial increase of mass. The averages of Barrel 4 and 6 increased less than 1g, and Barrel 2 increased 2g, resulting on all barrels having equal average plant mass of 23g. The growth is better noted in Figure 56 which denotes the significant increase of leaf size, as well as stem length.

Figure 56 – Gustosa basil plants at the start of the second week of the experiment period (Week 1) in Barrel 2 (left), Barrel 4 (middle) and Barrel 6 (right) with DLI targets of 17.5, 15 and 12.5 mol.m^{-2}.d^{-1}, respectively.

During the second week of growth is when the first signs of fresh mass development started to be noticed. Once again, plants in Barrel 2 are seen to start to surpass the ones in the other barrels, showing four plants above the 30-gram mark, compared to only one in barrels 4 and 6. The average plant mass per barrel is still very similar at this point, Barrel 2 increased to 30g (28%), Barrel 4 to 28g (22%) and Barrel 6 to 30g (23%). Barrels 4 and 6 show almost equal results with the exact same variety ranges recorded for the 9 plants (26-31g). Regarding the physiological development, plants presented similar development between barrels, mostly consisting in leaf area growth and some sub-branch development resulting in significantly larger apparent green profile areas than the previous week. The roots also become thicker, longer and with more density.

Figure 57 – Gustosa basil plants at the start of the third week of the experiment period (Week 2) in Barrel 2 (left), Barrel 4 (middle) and Barrel 6 (right) with DLI targets of 17.5, 15 and 12.5 mol.m^{-2}.d^{-1}, respectively.

During the third week is when the plants registered a substantial increase in the growth rate by adding 10g (37%) average plant weight in Barrel 4 and 13g (45%) in Barrel 6 (and Barrel 2 plants were terminated). This distinctive growth of the third week was also seen for the Pluto variety. The tendencies in Barrel 6 start indicating higher productivity (than Barrel 4) with median of 42g (vs 37g) although the plants have higher range from 33 to 50g (vs 35 to 44g). From Figure 58, it can be noticed the appearance of the first large leaves on top of some plants, appearing fully

developed leaves. Sub-branches and their leaves also grow significantly but still not fully developed. The main branch grows significantly in all plants causing a notable increase in overall plant hight. The roots prolongate further and their density increases greatly for all plants. The plants in Barrel 6 appear with higher number of leaves than Barrel 4, giving them a “bushier” aspect, which aligns with fresh mass results.

Figure 58 – Gustosa basil plants at the start of the fourth week of the experiment period (Week 3) in Barrel 4 (left), and Barrel 6 (right) with DLI targets of 15 and 12.5 $mol.m^{-2}.d^{-1}$, respectively.

During the fourth and final week of the experiment, the plant’s growth rates were the highest recorded, Barrel 4 added 20g (52%) on average per plant, finishing with 59.1g and Barrel 6 added 22g (53%) finishing with 64.6g. The median of the 2 barrels were the same (60g) although Barrel 6 produced plants between 56 and 79g and Barrel 4 between a smaller range of 48 and 70g. The final average fresh mass per plant appeared 9% higher for Barrel 6 compared to Barrel 4 despite the higher DLI targets set for Barrel 4. The Gustosa plants were harvested at this time and prepared for sales by removing the roots and remaining’s of the jiffy material and saving the stems and leaves. The average mass of the roots/jiffy was around 33g (recall the average mass of 20g per jiffy substrate) for plants in both barrels. This represents mostly the root weight, as the jiffy organic material is either absorbed by the plant or lost in the irrigation water flow. This meant the averages of the edible mass per plant were 25.2g for Barrel 4 and 31.2g for Barrel 6. This placed the productivity of Barrel 4 relatively further ahead of Barrel 4 (24%), more than counting with the entire plant due to higher proportion of root mass in Barrel 4.

Regarding the plant’s principal aspects of growth are the main-branch elongation and increased number of fully developed leaves. This results in tall basil plants with mostly large and heavy leaves, which is the intended physiognomy for harvesting. The final green profile areas are marked in Figure 59 and confirm the previous trends of plant growth in fresh mass. Barrel 6 is observed with an average green profile are of $392cm^2$ while Barrel 4 produced slightly smaller plants (11%) with average of $347cm^2$. Across the two barrels it can be seen a variation of plant formats, from slimmer and tall, with one main branch, to wider and “bushier”, with multiple main branches. Some of the largest plants show a mix of both characteristics and are more often seen on Barrel 6, such as the ones reaching 460 and $546cm^2$.

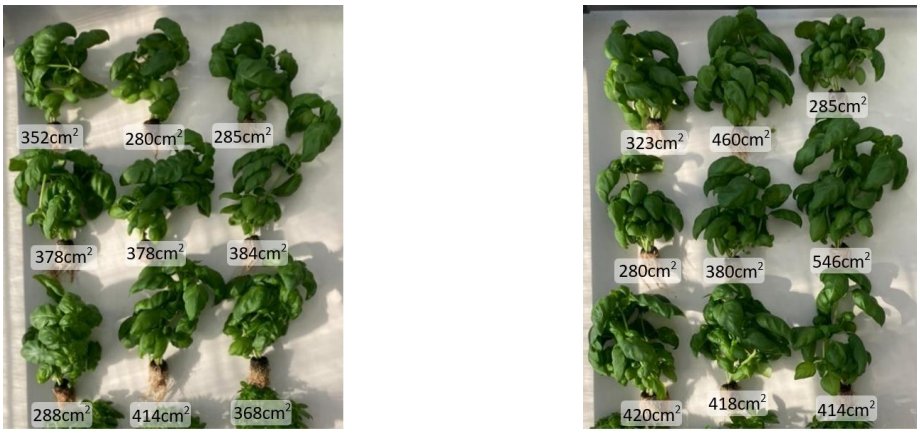

Figure 59 - Gustosa basil plants at the start of the fourth week of the experiment period (Week 3) in Barrel 4 (left), and Barrel 6 (right) with DLI targets of 15 and 12.5 mol.m^{-2}.d^{-1}, respectively.

6.2.6 DLI Regime Performance and Experimental Anomalies

This section will assess the main findings that characterise each DLI regime according to the experimental conditions that each Barrel was subjected. The efficiency of each DLI level will be presented regarding plant yield and LED energy consumption to understand which results are plausible and which indicate occurrence of anomalies. Finally, the performance of each system/DLI target will be concluded based on the reliable experimental outcomes. The previous results are summarised in Table 15.

Table 15 – Summary of the main results of the experiment for each barrel.

Barrel		**2**	**4**	**6**
Intended DLI Regime [mol.m^{-2}.d^{-1}]		17.5	15	12.5
Recorded Average DLI Regime [mol.m^{-2}.d^{-1}]		17.55	15.22	13.37
Final Average Edible Plant Fresh Mass [g]	Pluto	47.5	32.5	35
	Gustosa	---	25.2	31.6
LED Total Energy Consumption per growth cycle [kWh]		13.75	12.43	4.48

The final Pluto average fresh mass (6 weeks after sowing) relative to the recorded average DLI (biomass efficiency) that each barrel was exposed to resulted in yields per DLI target of 2.71 g.DLI^{-1} for Barrel 2, 1.66 g.DLI^{-1} for Barrel 4, and 2.14 g.DLI^{-1} for Barrel 6. These results are aligned with the ones reported in literature for the study [76] under similar conditions which reported an average plant biomass efficiency 2.36, 2.65 and 3.22 g/DLI under DLI regimes of 12.06, 14.22 and 16.38 mol.m^{-2}.d^{-1}, respectively. This work's results show a clear disproportion of plant productivity per light exposure between barrels. Assuming the results of Barrel 2 as reference, Barrel 6, which was subjected to a DLI 24% lower, produced 26% lower yields, indicating an approximately proportional relation between plant fresh mass and DLI exposure.

However, the results of (middle) Barrel 4 presented much lower yield per DLI exposed than the corner barrels, exactly 32% lower than Barrel 2, (with DLI exposure 13% inferior). This can happen due to the lateral light at the corners of the farm being influencing the corner barrels in a way not accounted for by the light sensors installed, assuming that other environmental factors were not sufficiently distinct between barrels based on the experimental procedure measures explained in section 5.

Since the LED light incidence was equivalent between all barrels (due to the same frontal disposition) there was likely an underrepresentation of the actual natural light incidence on Barrel 6 (and potentially Barrel 2 in the other corner) due to undetected lateral light insertion. The cylindrical shape of the barrels allows a significant part of the light reaching the plants to arrive from the side as opposed to the direction the sensors were placed for (normal to the barrel surface). The empty spaces of the edges of the greenhouse allow presence of this type of reflected/diffuse light, especially during the morning and afternoon, resulting in the corner barrel's actual illumination probably higher than the one accounted for by the system. The existent (final) results of Gustosa for Barrels 4 and 6 show the same tendency, with even higher masses of Barrel 6 compared to Barrel 4. Gustosa plants in Barrel 4 showed a final edible mass of 1.67 g/(mol.m^{-2}.d^{-1}) considering the DLI average registered, while Barrel 6 showed a yield per DLI of 2.35 g/(mol.m^{-2}.d^{-1}), 41% higher than the previous. Due to these circumstances, the results of the two corner barrels are more appropriate to compare.

Regarding the LED energy efficiency for plant yield, the experiment showed that a DLI regime of 17.55 mol.m^{-2}.d^{-1} (Barrel 2) had an average plant efficiency of 3.45 g/kWh for final edible mass of Pluto basil, for Barrel 4 (DLI of 15.22 mol.m^{-2}.d^{-1}) presented a more inefficient performance of 2.61 g/kWh, due to the higher LED load stress. Barrel 6 of recorded DLI regime 13.37 mol.m^{-2}.d^{-1} showed the higher energy efficiency per basil fresh mass production of 7.81 g/kWh. When compared with study [76] with lower efficiencies between 0.30 and 1.83 g/kWh, for a similar cultivation area (1.44m^2 and 1.88m^2, for the setup in [76] and for half a barrel, respectively) which is mainly due to a difference in the efficiency of conversion LED energy consumption to DLI experienced by the plants, almost 9 times better for Raiz's setup. This is related to, not only the LED equipment efficiency, but also to the plants disposition to artificial light on each setup. Figure 60 presents the relation between the final Pluto fresh (edible) mass (left axis), as well as total energy consumption (right axis) and the (registered) DLI levels of the three regimes studied based on the experimental results.

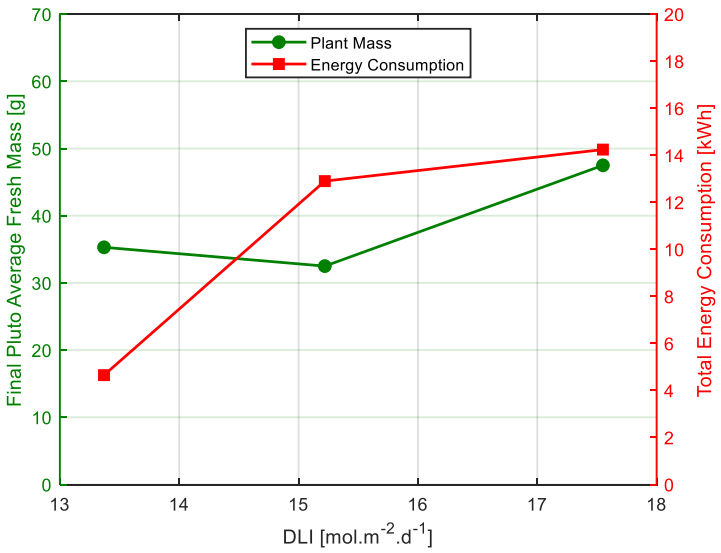

Figure 60 – Final average edible mass of Pluto Basil and total LED energy consumption according to registered DLI levels for the three tested conditions.

Disregarding the information for Barrel 4, (DLI of 15.22 mol.m^{-2}.d^{-1}), the tendency of plant growth according to DLI can be observed. The identification of the peak optimal DLI for plant productivity as in Figure 4 was not possible with the reduced number of DLI regimes tested. There is the possibility of higher DLI regimes than the highest tested in this work to produce higher yields, which is suggested in some studies referred in literature (Table 3). Nonetheless, the plant yield of the other barrels 4 and 6, with certainly lower DLI regimes, was not above production of Barrel 2. The intended DLI regime of 17.5 mol.m^{-2}.d^{-1} (Barrel 2) presented improved yield results of at least 36% (compared with Barrel 6) of final Pluto basil edible mass although requiring 3 times more energy to produce. This relatively higher energy consumption provides important information in the vision of scaling farm operations although it must be analysed according to the time of the year. In absolute terms, this difference represents less than 10kWh and therefore is in the best interest to program the LED system for higher DLI regimes, such as 17.5 mol.m^{-2}.d^{-1}, to boost productivity at the current facility.

7. Conclusions and Future Developments

7.1 Conclusions

The work presented fulfilled the main goal of analysing the impacts of different DLI regimes, delivered by a mix of natural and artificial light, on the productivity of Basil plants in a vertical farm facility and the associated energy consumption of LED equipment to deliver the DLI targeted of each regime. This was accomplished through an experimental campaign evaluating plant yield regarding plant fresh mass and size over a four-week period of development under controlled environment conditions. The secondary goal of development and analysis of performance of a dynamic LED control system, based on natural light exposure, was additionally carried out and the LED accurate adaptation of operation to the required artificial light complements was verified with modified light sensor for PPFD measurements with a maximum error of 13%.

In the experimental campaign, three sets of plants composed of samples of the two basil varieties were investigated under different predefined DLI regimes of 12.5, 15 and 17.5 $mol.m^{-2}.d^{-1}$ based on optimal values suggested in literature, delivered by variable combinations of the amounts of sunlight and LED artificial light during the months of September and October in Lisbon, Portugal.

It was possible to verify the dependency of plant fresh mass and size to the level of DLI exposure as presented in literature and identification of the most adequate DLI regime (between the three analysed) for maximization of plant productivity as well as LED energy consumption in a greenhouse farm facility with a translucent envelope.

The analysed farm facility presented a high daily penetration of natural light during September and October delivering, on average, 2/3^{rds} of the DLI targets, even for the most demanding one of 17.5 $mol.m^{-2}.d^{-1}$. This is not only aligned with sustainable practice by passively exploring the potential of local environmental conditions, but also, emphasises the value of a adjustable artificial lighting solution to explore these benefits, while never undersupplying light to the crops.

The installation of three different developed LED control systems at different growing barrels on the farm allowed the identification of differences in natural light insertion between middle and corner barrels which was noted and compensated by the system. The light incidence was registered 15% lower for the middle barrel compared to the corner ones, which resulted in this barrel's LED system showing higher energy consumption relative to its DLI target.

It was observed from the experimental results that the final plant edible fresh mass correlation to the DLI average exposure is 1.66 to 2.71 g/DLI for Pluto and 1.67 to 2.35 g/DLI for Gustosa, with variations depending on the barrel position. The final average Pluto edible fresh mass was recorded at 47.5g for the DLI regime of 17.5 $mol.m^{-2}.d^{-1}$, 32.5g for the DLI regime of 15 $mol.m^{-2}.d^{-1}$ and 35g for the DLI regime of 12.5 $mol.m^{-2}.d^{-1}$ which presented disproportional growth related to the DLI targets due to barrel positioning. Nevertheless, improved yield appears for the highest DLI regime (17.5 $mol.m^{-2}.d^{-}1$) of at least 36%, compared to the others. The experiment analysing

Gustosa plants was compromised resulting in only two final plant sets with DLI regimes of 12.5 and 15 mol.m^{-2}.d^{-1} and final edible plant fresh mass of 31.2g and 25.2g, respectively.

Regarding the energy consumption of the LEDs for each DLI regime of 12.5, 15 and 17.5 mol.m^{-2}.d^{-1} registered for the entire period of plant development of 28 days were, in total, 13.75, 12.43 and 4.48 kWh, respectively, corresponding to average daily consumptions of 160, 444 and 491 Wh, which represent energy savings of 81%, 49% and 43% respectively, compared to original LED operation (without the developed control system). Regarding the energy efficiency in biomass, each DLI regime of 12.5, 15 and 17.5 mol.m^{-2}.d^{-1} represented an average per plant of 3.45 g/kWh, 2.61 g/kWh and 7.81 g/kWh, respectively. The lowest DLI regime (12.5 mol.m^{-2}.d^{-1}) was the most energy efficient per DLI targeted, met 91% by natural light and 9% by artificial light consuming approximately one-third of the energy of the most demanding DLI regime (17.5 mol.x.d^{-1}). The daily energy consumption of the LEDs had a high dependency on the cloud coverage condition, showing variations between 127 and 848 Wh.

7.2 Future Developments

For the future year-round farm operation, it is recommended to target higher DLI regimes than the ones experimented in the present work, i.e., regimes with DLI targets above 17.5 mol.m^{-2}.d^{-1}, to explore the possibility of higher plant productivity. Further investigation for different times of the year is of interest to understand the full scope of the natural light conditions possible to be experienced and how that may affect the system energy consumption and additional requirements. This analysis may be done independently of plant growth and using available models of climacteric type conditions for the whole year.

Regarding the performance of the LED control system, some updates are required for the accurate capture of the natural light condition present at the farm, including higher number of measuring nodes and diversification of the angle of light capture which should improve the inaccuracies noted of this study setup. The main points of improvement for future developments of this system are:

- Improvement of the sensor positioning to capture more complete natural light condition
- Improvement of barrel positioning inside the farm to enhance optimal natural light exposition for all barrels
- Exploration of different dimming hardware that allows control from 0-100% instead of 10-100%
- Decrease the number of parts of the system, ex: one microcontroller for all systems reduces points of failure and costs
- Expansion of the analysis to the spectral composition of light and suggestion of light complements with targeted wavelengths, using LEDs of adjustable light spectrum
- Analysis of other types of crops with the vision of determining optimal DLI level for the entire farm

References

[1] *World population to reach 8 billion this year, as growth rate slows | UN News* (no date) *United Nations*. Available at: https://news.un.org/en/story/2022/07/1122272 (Accessed: 30 January 2023).

[2] GATES, B. (2021) *How to avoid a climate disaster*. ALFRED A KNOPF. (Accessed: 30 January 2023).

[3] *A five-step plan to feed the world* (2022) *Feeding 9 Billion - National Geographic*. Available at: https://www.nationalgeographic.com/foodfeatures/feeding-9-billion/ (Accessed: 30 January 2023).

[4] Ritchie, H., Rosado, P. and Roser, M. (2022) *Environmental impacts of food production*, *Our World in Data*. Available at: https://ourworldindata.org/environmental-impacts-of-food (Accessed: 3 March 2023).

[5] World Bank Group (2022) *5 key issues in agriculture in 2021*, *World Bank*. Available at: https://www.worldbank.org/en/news/feature/2021/12/16/5-key-issues-in-agriculture-in-2021 (Accessed: 3 March 2023).

[6] (No date) *Overview of greenhouse gases | US EPA*. Available at: https://www.epa.gov/ghgemissions/overview-greenhouse-gases (Accessed: 6 March 2023).

[7] (No date a) *Emissions due to agriculture - Food and Agriculture Organization*. Available at: https://www.fao.org/3/cb3808en/cb3808en.pdf (Accessed: 6 March 2023).

[8] Conchedda, G. and Tubiello, F.N. (2020) *Drainage of organic soils and GHG emissions: Validation With Country Data*, *Earth System Science Data*. Available at: https://essd.copernicus.org/articles/12/3113/2020/#:~:text=Drainage%20of%20organic%20soils%20releases%20large%20quantities%20of,the%20underlying%20organic%20matter%20once%20water%20is%20removed. (Accessed: 6 March 2023).

[9] *Fertilizer and climate change* (no date) *MIT Climate Portal*. Available at: https://climate.mit.edu/explainers/fertilizer-and-climate-change (Accessed: 16 March 2023).

[10] Bridget Huber, N. 1 (2022) *Report: Fertilizer responsible for more than 20 percent of total agricultural emissions*, *Food and Environment Reporting Network*. Available at: https://thefern.org/ag_insider/report-fertilizer-responsible-for-more-than-20-percent-of-total-agricultural-emissions/ (Accessed: 16 March 2023).

[11] *Sizing up how agriculture connects to deforestation* (no date) *NASA*. Available at: https://earthobservatory.nasa.gov/images/148674/sizing-up-how-agriculture-connects-to-deforestation (Accessed: 16 April 2023).

[12] *What is erosion? effects of soil erosion and land degradation* (no date) *WWF*. Available at: https://www.worldwildlife.org/threats/soil-erosion-and-degradation?ref=collapsemusings.com (Accessed: 16 April 2023).

[13] Li, M. *et al.* (2022) *Global food-miles account for nearly 20% of total food-systems emissions*, *Nature News*. Available at: https://www.nature.com/articles/s43016-022-00531-w (Accessed: 16 April 2023).

[14] Center for Food Safety and Applied Nutrition (no date) *Food loss and waste*, *U.S. Food and Drug Administration*. Available at: https://www.fda.gov/food/consumers/food-loss-and-waste (Accessed: 18 April 2023).

[15] *Groundwater: Information on Earth's water* (no date) *Default*. Available at: https://www.ngwa.org/what-is-groundwater/About-groundwater/information-on-earths-water#:~:text=The%20earth%20has%20an%20abundance%20of%20water%2C%20but,the%200.3%20percent%20that%20is%20useable%20is%20unattainable. (Accessed: 5 May 2023).

[16] *Water in agriculture* (no date) *World Bank*. Available at: https://www.worldbank.org/en/topic/water-in-agriculture (Accessed: 5 May 2023).

[17] McNabb, D.E. (1970) *Agriculture and inefficient water use*, *SpringerLink*. Available at: https://link.springer.com/chapter/10.1007/978-3-030-04085-7_7 (Accessed: 5 May 2023).

[18] *Regenerative agriculture 101 – center for regenerative agriculture and resilient systems* (no date) – *Center for Regenerative Agriculture and Resilient Systems – Chico State*. Available at: https://www.csuchico.edu/regenerativeagriculture/ra101-section/index.shtml (Accessed: 5 May 2023).

[19] Constantinoiu, M. (2023) *How Israel used innovation to beat its water crisis*, *ISRAEL21c*. Available at: https://www.israel21c.org/how-israel-used-innovation-to-beat-its-water-crisis/ (Accessed: 5 May 2023).

[20] Dupuis, A. (2023) *Hydroponics vs. traditional farming: 10 major differences*, *Eden Green*. Available at: https://www.edengreen.com/blog-collection/hydroponics-vs-traditional-farming (Accessed: 7 May 2023).

[21] Dupuis, A. (2023a) *Environmental impact of traditional farming: 5 effects*, *Eden Green*. Available at: https://www.edengreen.com/blog-collection/environmental-impact-of-traditional-and-vertical-farming-2021-report (Accessed: 7 May 2023).

[22] (No date) *2023 plantlab whitepaper - water scarcity*. Available at: https://plantlab.com/wp-content/uploads/2023/03/2023-Plantlab-Whitepaper-Water-scarcity.pdf (Accessed: 15 May 2023).

[23] Raman, R. (2023) *GMO pros and cons, backed by evidence*, *Healthline*. Available at: https://www.healthline.com/nutrition/gmo-pros-and-cons#cons (Accessed: 15 May 2023).

[24] Bayer (2023) *How has technology changed farming?*, *Bayer Global*. Available at: https://www.bayer.com/en/agriculture/article/technology-agriculture-how-has-technology-changed-farming (Accessed: 15 May 2023).

[25] masschallenge, A. (2023) *Agriculture innovation: 10 tech trends to watch in 2023*, *MassChallenge*. Available at: https://masschallenge.org/articles/agriculture-innovation/ (Accessed: 15 May 2023).

[26] StartUs Insights (2023) *Uncover the top 10 agriculture trends for 2024*, *StartUs Insights*. Available at: https://www.startus-insights.com/innovators-guide/agriculture-trends-innovation/ (Accessed: 15 May 2023).

[27] Goedde, L. *et al.* (2020) *Agriculture's connected future: How technology can yield new growth*, *McKinsey & Company*. Available at: https://www.mckinsey.com/industries/agriculture/our-insights/agricultures-connected-future-how-technology-can-yield-new-growth (Accessed: 21 May 2023).

[28] Sandison, F., Yeluripati , J. and Stewart, D. (2022) *Does green vertical farming offer a sustainable alternative to conventional methods of production?: A case study from Scotland*. dissertation. (Accessed: 21 May 2023).

[29] Engler, N. and Krarti, M. (2021) *Review of energy efficiency in controlled environment agriculture*. dissertation. (Accessed: 21 May 2023).

[30] Goedde, L. *et al.* (2020) *Agriculture's connected future: How technology can yield new growth*, *McKinsey & Company*. Available at: https://www.mckinsey.com/industries/agriculture/our-insights/agricultures-connected-future-how-technology-can-yield-new-growth (Accessed: 30 May 2023).

[31] *NASA research launches a new generation of indoor farming* (2023) *NASA*. Available at: https://www.nasa.gov/directorates/spacetech/spinoff/NASA_Research_Launches_a_New_Generation_of_Indoor_Farming (Accessed: 30 May 2023).

[32] Author links open overlay panelNicholas Engler, Highlights•Controlled environment agriculture or CEA can help in meeting the increasing global food needs.•This review evaluates the limited studies to enhance the energy performance of CEA facilities.•Research needs to design and operate energy efficient and applications, A.E.A. (CEA) (2021) *Review of energy efficiency in controlled environment agriculture*, *Renewable and Sustainable Energy Reviews*. Available at: https://www.sciencedirect.com/science/article/abs/pii/S1364032121000812?fr=RR-2&ref=pdf_download&rr=80d3c9a6baa1dd50 (Accessed: 30 May 2023).

[33] Burgos, S. and Stapel, M. (2018) COMPARISON BETWEEN DIFFERENT FARMING METHODS IN LETTUCE PRODUCTION. rep. Netherlands: OneFarm. (Accessed: 30 May 2023).

[34] Farhangi, H. (2023) *Optimizing growth conditions in vertical farming: enhancing lettuce and basil cultivation through the application of the Taguchi method*. dissertation. (Accessed: 31 May 2023).

[35] (2016) *Vertical Farming - Nuffield farming scholarships*. Available at: https://www.nuffieldscholar.org/sites/default/files/reports/2016_BR_Luciano-Loman_Vertical-Farming-Can-It-Change-The-Global-Food-Production-Landscape.pdf (Accessed: 3 June 2023).

[36] Saha, P. (2021) *Temperature and plant growth: How does temperature affect plant growth*, *Gardening ABC*. Available at: https://gardening-abc.com/How-Does-Temperature-Affect-Plant-Growth/?utm_content=cmp-true (Accessed: 3 June 2023).

[37] Farhangi, H. (2023) *Optimizing growth conditions in vertical farming: enhancing lettuce and basil cultivation through the application of the Taguchi method*. dissertation. (Accessed: 3 June 2023).

[38] Pennisi , G. (2020) *https://www.sciencedirect.com/science/article/pii/S0304423820303368*. dissertation. (Accessed: 3 June 2023).

[39] Chang, X. (2004) *Effect of light and temperature on volatile compounds and growth parameters in sweet basil (ocimum basilicum L.)*. dissertation. (Accessed: 3 June 2023).

[40] Picot, A. (2023) *How many hours of dark do plants typically need?*, *thegrowingleaf.com*. Available at: https://thegrowingleaf.com/how-many-hours-of-dark-do-plants-typically-need/ (Accessed: 4 June 2023).

[41] Temperature acclimation of photosynthesis: mechanisms involved in the changes in temperature dependence of photosynthetic rate (Hikosaka, 2006) (Accessed: 4 June 2023).

[42] Putievsky, E. (2015) *Temperature and daylength influences on the growth and germination of sweet basil and oregano*. dissertation. (Accessed: 4 June 2023).

[43] Chang, X. (2004) *Effect of light and temperature on volatile compounds and growth parameters in sweet basil (ocimum basilicum L.)*. dissertation. (Accessed: 4 June 2023).

[44] Kellie, J. (2019) *Growth and Development of Basil Species in Response to Temperature*. dissertation. (Accessed: 5 June 2023).

[45] Wright, J. (2019) *Managing air temperatures for Basil Growth and development*, *Greenhouse Grower*. Available at: https://www.greenhousegrower.com/production/crop-inputs/managing-air-temperatures-for-basil-growth-and-development/ (Accessed: 7 June 2023).

[46] Oren, R., Sperry, J. S., & Katul, G. G. (1999). Survey and synthesis of intra- and interspecific variation in stomatal sensitivity to vapor pressure deficit. Plant, Cell & Environment, 22(12), 1515-1526. doi: 10.1046/j.1365-3040.1999.00513.x

[47] Grange, R. I., & Hand, D. W. (1987). *A review of the effects of atmospheric humidity on the growth of horticultural crops. Journal of Horticultural Science, 62(2), 125–134.* doi:10.1080/14620316.1987.11515760 (Accessed: 7 June 2023).

[48] Park, K. (2016) *Development of a Coupled Photosynthetic Model of Sweet Basil Hydroponically Grown in Plant Factories*. dissertation. (Accessed: 7 June 2023).

[49] Chang, X. (2004) *Effect of light and temperature on volatile compounds and growth parameters in sweet basil (ocimum basilicum L.)*. dissertation. (Accessed: 7 June 2023).

[50] Paradiso, R., Proietti, S. (2022) Light-Quality Manipulation to Control Plant Growth and Photomorphogenesis in greenhouse Horticulture: The State of the Art and the Opportunities of Modern LED Systems. J Plant Growth Regul 41, 742–780 Available at: https://doi.org/10.1007/s00344-021-10337-y (Accessed: 25 June 2023).

[51] Research, C. (2009) *The influence of colors on plants*, *CANNA CANADA*. Available at: https://www.canna.ca/articles/influence-colors-plants (Accessed: 25 June 2023).

[52] Kong, Y., Kamath, D. and Zheng, Y. (2019) Blue versus red light can promote elongation growth independent of photoperiod: A study in four brassica microgreens species, hortsci. American Society for Horticultural Science. Available at: https://doi.org/10.21273/HORTSCI14286-19 (Accessed: 23 June 2023).

[53] K.J., M.C. (1970) THE ACTION SPECTRUM, ABSORPTANCE AND QUANTUM YIELD OF PHOTOSYNTHESIS IN CROP PLANTS. rep. Elsevier Publishing Company. (Accessed: November 18, 2022).

[54] R.W., I. and T.S., M. (1991) Light-emitting Diodes as a Radiation Source for Plants. rep. HortScience. (Accessed: November 18, 2022).

[55] Chamovitz, D. (2017) *What a plant knows: A field guide to the Senses*. New York: Scientific American/Farrar, Straus and Giroux. (Accessed: 22 June 2023).

[56] A. and Matsuda, R. (no date) Analysis of the relationship between blue-light photon flux density and the photosynthetic properties of spinach (Spinacia oleracea L.) leaves with regard to the acclimation of photosynthesis to growth irradiance, Taylor & Francis. Available at: https://www.tandfonline.com/doi/abs/10.1111/j.1747-0765.2007.00150.x (Accessed: November 15, 2022).

[57] Samuoliene, G. and Viršilė, A. (no date) The effect of red and blue light component on the growth and ... Available at: https://www.researchgate.net/publication/228448846_The_effect_of_red_and_blue_light_component_on_the_growth_and_development_of_frigo_strawberries (Accessed: November 25, 2022).

[58] Nanya, K., Ishigami, Y. and Hikosaka, S. (no date) doi:10.17660/actahortic.2012.956.29K. Nanya, Y. Ishigami, S. Hikosaka and E. Goto, Effects of blue and red light on stem elongation and flowering of tomato seedlings. Available at: https://www.actahort.org/books/956/956_29.htm (Accessed: November 25, 2022).

[59] Naznin, M.T. et al. (2019) Blue light added with red leds enhance growth characteristics, pigments content, and antioxidant capacity in lettuce, spinach, kale, basil, and Sweet Pepper in a controlled environment, MDPI. Multidisciplinary Digital Publishing Institute. Available at: https://www.mdpi.com/2223-7747/8/4/93 (Accessed: December 6, 2022).

[60] Hogewoning, S.W.,et al. (2012). FINDING THE OPTIMAL GROWTH-LIGHT SPECTRUM FOR GREENHOUSE CROPS. Acta Hortic. Available at: https://doi.org/10.17660/ActaHortic.2012.956.41 (Accessed: December 6, 2022).

[61] Sarlikioti, V., et al. (2011). Exploring the spatial distribution of light interception and photosynthesis of canopies by means of a functional-structural plant model. Ann. Bot.-London 107:875-883. (Accessed: December 6, 2022).

[62] Kelly, K.J. *et al.* (2021) *Interactions between ultraviolet B radiation, warming, and changing nitrogen source may reduce the accumulation of toxic pseudo-nitzschia multiseries biomass in future coastal oceans*, *Frontiers*. Available at: https://www.frontiersin.org/articles/10.3389/fmars.2021.664302/full#:~:text=Growth%20rates%20were%20inhibited%20by%20UVB%2C%20but%20photosynthesis,Additionally%2C%20DA%20synthesis%20continued%20despite%20UVB-induced%20growth%20inhibition (Accessed: 1 June 2023).

[63] Davis, D. (2023) *UV and UVB lights for plants: Everything you need to know*, *Hydrobuilder Learning Center*. Available at: https://hydrobuilder.com/learn/uv-light-for-plants/ (Accessed: 1 June 2023).

[64] Paradiso, R. and Proietti, S. (2021) Light-quality manipulation to control plant growth and photomorphogenesis in Greenhouse Horticulture: The state of the art and the opportunities of modern LED systems - Journal of Plant Growth Regulation, SpringerLink. Springer US. Available at: https://link.springer.com/article/10.1007/s00344-021-10337-y (Accessed: 1 June 2023).

[65] Larsen, D.H. et al. (2020) Response of basil growth and morphology to light intensity and spectrum in a vertical farm, Frontiers. Frontiers. Available at: https://www.frontiersin.org/articles/10.3389/fpls.2020.597906/full (Accessed: December 20, 2022).

[66] Mawphlang, O.I.L. and Kharshiing, E.V. (2017) Photoreceptor mediated plant growth responses: Implications for photoreceptor engineering toward improved performance in crops, Frontiers. Frontiers. Available at: https://www.frontiersin.org/articles/10.3389/fpls.2017.01181/full (Accessed: December 21, 2022).

[67] Support, E.W. (2022) What are short-day and long-day plants?, OSU Extension Service. Oregon State University Extension Service. Available at: https://extension.oregonstate.edu/news/what-are-short-day-long-dayplants (Accessed: January 3, 2023).

[68] Maglia, D. (2022) *The daily light integral of plants*, *Photone - Grow Light Meter*. Available at: https://growlightmeter.com/how-much-light-does-my-plant-need/ (Accessed: 1 May 2023).

[69] Zhang X, He D, Niu G, Yan Z, Song J. (2018) Effects of environment lighting on the growth, photosynthesis, and quality of hydroponic lettuce in a plant factory. Int J Agr Biol Eng (Accessed: January 3, 2022).

[70] Avgoustaki, D.D. (2019) Optimization of photoperiod and quality assessment of basil plants grown in a smallscale indoor cultivation system for reduction of energy demand, MDPI. Multidisciplinary Digital Publishing Institute. Available at: https://www.mdpi.com/1996-1073/12/20/3980 (Accessed: January 3, 2022).

[71] Dorais M. (2003) The use of supplemental lighting for vegetable crop production: light intensity, crop response, nutrition, crop management, cultural practices. Proceeding of the Canadian Greenhouse Conference; Ontario, Canada (Accessed: January 6, 2023).

[72] Lee HI, Kim YH. (2013) Utilization efficiencies of electric energy and photosynthetically active radiation of lettuce grown under red LED, blue LED and fluorescent lamps with different photoperiods. J. Biosyst. Eng. 38: 279–286. (Accessed: January 6, 2023).

[73] Delfine S. et al. (2005) isoprenoids content and photosynthetic limitations ... - researchgate. Available at: https://www.researchgate.net/publication/222186532_Isoprenoids_content_and_photosynthetic_limitations_in_rosemary_and_spearmint_plants_under_water_stress (Accessed: January 5, 2022).

[74] Beaman, A. (2009) *Sweet Basil Requires an Irradiance of 500 mmolm–2 s–1 for Greatest Edible Biomass Production*. dissertation. (Accessed: 19 June 2023).

[75] Park, K. (2016) *Development of a Coupled Photosynthetic Model of Sweet Basil Hydroponically Grown in Plant Factories*. dissertation. (Accessed: 17 June 2023).

[76] Hunter, A. and Dean, A. (2023) Application timing and duration of LED and HPS supplements differentially influence yield, nutrient bioaccumulation, and light use efficiency of greenhouse basil across seasons. dissertation. frontier. Available at: https://doi.org/10.3389/fpls.2023.1174823 (Accessed: November 26, 2023).

[77] Pereira, J. and Foo, M. (2021) A framework of artificial light management for optimal plant development for smart greenhouse application. Available at: https://doi.org/10.1371/journal. pone.0261281 (Accessed: January 6, 2023).

[78] Velasco MH, Mattsson A. (2019) Light quality and intensity of Light-Emitting Diodes (LEDs) during precultivation of Picea abies (L.) Karst. and Pinus sylvestris L. seedlings—impact on growth performance, seedling quality and energy consumption. Scand J For Res.; 34: 1–49. (Accessed: January 6, 2023).

[79] Kang, J.H. et al. (2014) Light intensity and photoperiod influence the growth and development of hydroponically grown leaf lettuce in a closed-type plant factory system - horticulture, environment, and biotechnology, SpringerLink. Springer Netherlands. Available at: https://link.springer.com/article/10.1007/s13580-013- 0109-8 (Accessed: January 7, 2023).

[80] Hiroki R, Shimizu H, Ito A, Nakashima H, Miyasaka J, Ohdoi K. (2013) Identifying the optimum light cycle for lettuce growth in plant factory. International Symposium on New Technologies for Environment Control, EnergySaving and Crop Production in Greenhouses and Plant; Jeju, South Korea. (Accessed: January 8, 2023).

[81] *How much electricity does a vertical farm use with iFarm Technologies?* (no date) *Company*. Available at: https://ifarm.fi/blog/2020/12/how-much-electricity-does-a-vertical-farm-consume (Accessed: 30 August 2023).

[82] *Energy and led costs and differences of vertical farms* (no date) *Hortibiz Daily*. Available at: https://www.hortibiz.com/newsitem/news/energy-and-led-costs-and-differences-of-vertical-farms/#:~:text=With%20these%20lamps%20operating%2012%20to%2018%20hours,for%2050%20to%2065%25%20of%20the%20electricity%20bill. (Accessed: 1 September 2023).

[83] Eva, D. et al. (2014) Photosynthesis under artificial light: The shift in primary and secondary metabolism, Philosophical Transactions of the Royal Society B: Biological Sciences. Available at: https://royalsocietypublishing.org/doi/10.1098/rstb.2013.0243 (Accessed: 1 September 2023).

[84] Engler, N. (2022) *Optimal designs for net zero energy controlled environment agriculture facilities*. dissertation. (Accessed: 1 September 2023).

[85] Pimentel, J. (2023) *Optimization of vertical farms energy efficiency via multiperiodic graph-theoretical approach*. dissertation. (Accessed: 2 September 2023).

[86] Liu S, Teng P. HIGH-TECH plant factories: challenges and way forward. Rep. S. Rajaratnam School of International Studies; 2017. p. 11–7. Retrieved April 6, 2020, from, www.jstor.org/stable/resrep17149.6.

[87] (No date) *Product document - AMS*. Available at: https://ams.com/documents/20143/36005/AS7341_DS000504_3-00.pdf/5eca1f59-46e2-6fc5-daf5-d71ad90c9b2b (Accessed: 4 September 2023).

[88] *Raspberry Pi Zero 2 W*. Available at: https://datasheets.raspberrypi.com/rpizero2/raspberry-pi-zero-2-w-product-brief.pdf (Accessed: 5 September 2023).

[89] Raspberry Pi (no date) *Raspberry pi os*, *Raspberry Pi*. Available at: https://www.raspberrypi.com/software/ (Accessed: 5 September 2023).

[90] Nelson, C. (no date) *Working with I2C devices*, *Adafruit Learning System*. Available at: https://learn.adafruit.com/working-with-i2c-devices/address-conflicts (Accessed: 20 October 2023).

[91] Rembor, K. (no date) *Adafruit LTC4311 I2C Extender / Active Terminator*, *Adafruit Learning System*. Available at: https://learn.adafruit.com/adafruit-ltc4311-i2c-extender-active-terminator (Accessed: 22 October 2023).

[92] Morel, A. (1997) *Relation between total quanta and total energy for aquatic photosynthesis1* . dissertation. (Accessed: 22 October 2023).

[93] Bäumker, E. (2021) *A Novel Approach to Obtain PAR with a Multi-Channel Spectral Microsensor, Suitable for Sensor Node Integration*. dissertation. Available at: https://doi.org/10.3390/s21103390. (Accessed: 22 April 2023).

[94] GmbH, L.I. (no date) *Photone - Grow light meter*, *Photone - Grow Light Meter*. Available at: https://growlightmeter.com/ (Accessed: 31 April 2023).

[95] Measuring light for indoor plants: Using i1Studio as a par PPFD meter (2020). Available at: https://metebalci.com/blog/measuring-light-for-indoor-plants/ (Accessed: January 13, 2023).

[96] *Histórico de Condições Meteorológicas em 2022 EM Lisboa Portugal* (no date) *Condições meteorológicas passadas em Lisboa em 2022 (Portugal) - Weather Spark*. Available at: https://pt.weatherspark.com/h/y/32022/2022/Condi%C3%A7%C3%B5es-meteorol%C3%B3gicas-hist%C3%B3ricas-durante-2022-em-Lisboa-Portugal#Figures-Temperature (Accessed: 28 September 2023).

Appendix

1. Initial Installations/Upgrades of Raspberry Pi

```
sudo apt update
sudo apt upgrade
pip install board
pip install adafruit-circuitpython-as7341
pip install google-cloud-bigquery
sudo pip install adafruit-circuitpython-tca9548a
pip install ephem # Sunsets and sunrise times f(lat,long)
pip install pytz #Convert to local time
```

2. Light Sensor Python Code

```
import time
import csv
import board
from adafruit_as7341 import AS7341
import adafruit_tca9548a
import numpy as np
from google.cloud import bigquery
import os
import subprocess
import ephem
import pytz
from datetime import date, datetime, timedelta
from google.api_core.exceptions import RetryError
from google.auth.exceptions import DefaultCredentialsError
from requests.exceptions import ConnectionError
import threading
import queue

# Initialize the BigQuery client
table_id = 'environment-data.farm_one.LIGHT_B4'
os.environ['GOOGLE_APPLICATION_CREDENTIALS'] = '/home/pi/Cloud'
client = bigquery.Client()

def initialize_bigquery_client():
    while True:
        try:
            client = bigquery.Client()
            return client
        except DefaultCredentialsError:
            print("DefaultCredentialsError: Unable to authenticate. Retrying in 60 seconds...")
            time.sleep(600)
        except Exception as e:
            print(f"An unexpected error occurred while initializing BigQuery client: {e}. Retrying in 60 seconds...")
```

```
            time.sleep(600)


def send_to_bigquery_with_retry(data, client):
    while True:
        try:
            table = client.get_table(table_id)
            errors = client.insert_rows(table, data)
            if errors:
                print("Error inserting rows into BigQuery:", errors)
            return
        except RetryError as e:
            print("RetryError: ", e)
        except DefaultCredentialsError:
            print("DefaultCredentialsError: Re-authenticating BigQuery client...")
            client = initialize_bigquery_client()
        except Exception as e:
            print("An unexpected error occurred:", e)


# Initialize the AS7341 sensor
i2c = board.I2C()
pca = adafruit_tca9548a.TCA9548A(i2c)
sensor1 = AS7341(pca[5]) #top sensor
sensor2 = AS7341(pca[0]) #middle sensor
sensor3 = AS7341(pca[1]) #lower sensor


# Set the location for which you want to calculate sunrise and sunset
latitude = '38.7338'  # Latitude of Beato, Lisbon
longitude = '-9.1054'  # Longitude of Beato, Lisbon
observer = ephem.Observer()
observer.lat = latitude
observer.lon = longitude


# Define the channel names
channel_names = ['415nm', '445nm', '480nm', '515nm', '555nm', '590nm', '630nm', '680nm', 'clear', 'nir']


# Define the conversion matrix [b] from sensor counts to PPFD
b = np.array([[-0.259798617914247], [0.519372750955010], [-0.325667605915621], [-0.146907362168532],
              [0.190374541414311], [0.203441661392086], [-0.150684777829383], [0.0114345340199522],
              [-0.00157026385139988]])


# Define sensor times and nighttime threshold
X = 3 # Time between sensor readings [s]
Y = 12 # Timespan to calculate averages [s]
Z = 20 # Trigger light intensity for night [micromol m-2 s-1]
P = 3 # Avg sensor PPFD at night when it should be 0


# Initialize loops, sumsand led states
counter = 0
channels_sum = np.zeros((10, 1))
PPFD_sum = 0
```

```
# Create a queue to share data between threads
data_queue = queue.Queue(10000)

# Function to read sensors
def read_sensors():
    global counter, channels_sum, PPFD_sum

    lag_sum = 0
    Time_acc = 0
    led_start_time = None
    led_process = None
    last_led_process_date = None

    while True:
        try:
            timestamp = time.time()

            #Take mesurements for the three sensors and calculate the average
            start_sensor = time.time()
            channels_s1 = np.array([sensor1.__getattribute__('channel_' + name.lower()) for name in channel_names]).reshape((10, 1))
            channels_s2 = np.array([sensor2.__getattribute__('channel_' + name.lower()) for name in channel_names]).reshape((10, 1))
            channels_s3 = np.array([sensor3.__getattribute__('channel_' + name.lower()) for name in channel_names]).reshape((10, 1))
            end_sensor = time.time()
            lag = end_sensor - start_sensor
            channels_savg = (channels_s1+channels_s2+channels_s3)/3

            #Preventing shadowed readings (assuming shadows cause >=70% drop to the highest nonshadow one). Assumes at least one isn't shadowed.
            highest_clear = max(channels_s1[8][0], channels_s2[8][0], channels_s3[8][0])
            threshold = 0.3 * highest_clear
            if channels_s1[8][0] < threshold:
                channels_savg = (channels_s2 + channels_s3)/2
                print('SHADOW!')
            if channels_s2[8][0] < threshold:
                channels_savg = (channels_s1+channels_s3)/2
                print('SHADOW!')
            if channels_s3[8][0] < threshold:
                channels_savg =(channels_s2+channels_s1)/2
                print('SHADOW!')

            channels_sum += np.round(channels_savg,0)
            lag_sum += lag

            counter += 1 # Increment the counter

            # Check if Y/X measurements have been taken !!make sure Y/X is a whole number!!
            if counter == Y/X:

                # Set today and get sunrise and sunset
                today = date.today()
                observer.date = today.strftime('%Y/%m/%d')
                sunrise_utc = observer.previous_rising(ephem.Sun()).datetime()
```

```
sunset_utc = observer.next_setting(ephem.Sun()).datetime()
local_timezone = pytz.timezone('Europe/Lisbon')  # Adjust to the desired timezone
sunrise_local = sunrise_utc.astimezone(local_timezone)
sunset_local = sunset_utc.astimezone(local_timezone)

# Calculate the average light measured each reading during Y [count s-1]
channels_Yavg = channels_sum / (Y/X)
channels_PAR = channels_Yavg[:9] #Just the PAR channels (without the NIR)
lag_avg = lag_sum/(Y/X)



# Multiply the average by the conversion matrix and by the amount of seconds it took (Y) (micromol m-2 [Y]s-1)
if led_process is None:
    PPFD_Y_b = max((-4.321), np.round(((np.dot(b.T, channels_PAR))-P) *(Y/X)*(X+lag_avg), 0)) #Accumulated PPFD in Y seconds
else:
    PPFD_Y_b = channels_Yavg[8][0]*(Y/X)*(X+lag_avg) * (750/47000)

#Depending on the the previous, PPFD_Y_b is going to come as either a array or scalar respectivly
if isinstance(PPFD_Y_b, (list, np.ndarray)):
    PPFD_Y = float(PPFD_Y_b[0])
else:
    PPFD_Y = float(PPFD_Y_b)

PPFD = np.round(PPFD_Y/((Y/X)*(X+lag_avg)), 0) #Average PPFD during Y seconds
PPFD_sum += PPFD_Y
Time_cycle = (Y/X)*(X+lag_avg)
Time_acc += Time_cycle
print('PPFD =', PPFD)
print('PPFD Accumulated:', PPFD_sum, 'micromol m-2', Time_acc, 's-1')
time_s = datetime.now().strftime('%Y-%m-%d %H:%M:%S')
data_queue.put((time_s, PPFD, PPFD_sum, Time_acc, channels_s1, channels_s2, channels_s3, lag_avg, channels_Yavg))
print('Time of acc:', time_s)
lag_sum = 0

current_month = time.strftime('%b').lower()
current_year = time.strftime('%Y')
csv_file_name = f'logs_{current_month}_{current_year}.csv'

# Write to the CSV file
with open(csv_file_name, 'a', newline='') as csvfile:
    writer = csv.writer(csvfile)
    writer.writerow([time.strftime('%Y-%m-%d %H:%M:%S'), "PPFD =", PPFD])
    csvfile.flush()
    writer.writerow(["PPFD Accumulated =", PPFD_sum])
    csvfile.flush()

# Check if the result is below the nighttime threshold and if it's past sunset time
if PPFD < Z and (sunset_local - timedelta(hours=1)) <= datetime.now().astimezone(local_timezone) <= (sunset_local + timedelta(hours=2)):
# Start the LED Control subprocess if it's not already running
    if not led_process:
        DLI_sun = PPFD_sum
```

```
                    # Start the LED Control subprocess
                    led_process = subprocess.Popen(['python', 'LED_control.py'])
                    led_start_time = datetime.now()

                # Reset the counter and measurements sum
                counter = 0
                channels_sum = np.zeros((10, 1))

            # Check if the LED process has finished
            if led_process and led_process.poll() is not None:
                # Reset the running sum after LED Control.py finishes
                PPFD_sum = 0
                Time_acc = 0
                led_process = None

        except Exception as e:
            print("An error occurred in the sensor loop:", e)

        # Wait for X seconds before taking the next measurement
        time.sleep(X)



# Function to send data to BigQuery
def send_data_to_bigquery():
    while True:
        try:
            if counter == Y/X:
                time_s, PPFD, PPFD_sum, Time_acc, channels_s1, channels_s2, channels_s3, lag_avg, channels_Yavg = data_queue.get()

                # Insert into BigQuery table
                table_id = 'environment-data.farm_one.LIGHT_B4'  # Replace with your BigQuery table ID
                table = client.get_table(table_id)
                row = [(time_s, PPFD, PPFD_sum, Time_acc, channels_s1[8][0], channels_s2[8][0], channels_s3[8][0]) + tuple(channels_Yavg.flatten().tolist())]
                print(row)
                errors = client.insert_rows(table, row)

        except Exception as e:
            print("An error occurred while sending data to BigQuery:", e)



# Create threads for sensor reading and data sending
sensor_thread = threading.Thread(target=read_sensors)
bigquery_thread = threading.Thread(target=send_data_to_bigquery)

# Start the threads
sensor_thread.start()
bigquery_thread.start()

# Wait for the threads to finish (this will never happen in this setup)
sensor_thread.join()
bigquery_thread.join()
```

3. LED Control Python Code

```
 import csv
import RPi.GPIO as GPIO
import ephem
import pytz
from datetime import date, datetime, timedelta
import time
from google.cloud import pubsub_v1, bigquery
import os


os.environ['GOOGLE_APPLICATION_CREDENTIALS'] = '/home/pi/Cloud'
# Create a publisher client
publisher = pubsub_v1.PublisherClient()
project_id = 'datalogger'
topic_name = 'projects/environment-data/topics/datalogger'
client = bigquery.Client()


# Open readings file and take the DLI measured at the end of the day (check units)
with open('measurements.csv', 'r') as csv_file:
    csv_reader = csv.reader(csv_file)
    rows = list(csv_reader)
    DLI_m = rows[-1][-1]
    DLI_m = float(DLI_m)
    DLI_m = round(DLI_m/1000000, 4) #micromol m-2 s-1 => mol m-2 d-1
    print('DLI measured was:',DLI_m)


# Set the location for which you want to calculate sunrise and sunset
latitude = '38.7338'  # Latitude of Beato, Lisbon
longitude = '-9.1054'  # Longitude of Beato, Lisbon
# Create a PyEphem observer object
observer = ephem.Observer()
observer.lat = latitude
observer.lon = longitude
# Set the date to today
today = date.today()
observer.date = today.strftime('%Y/%m/%d')


# Calculate sunrise and sunset times (in UTC) and then local times
sunrise_utc = observer.previous_rising(ephem.Sun()).datetime()
sunset_utc = observer.next_setting(ephem.Sun()).datetime()
local_timezone = pytz.timezone('Europe/Lisbon')  # Adjust to the desired timezone
sunrise_local = sunrise_utc.astimezone(local_timezone)
sunset_local = sunset_utc.astimezone(local_timezone)


#Calculate the period of LED op. [P_LED] that allows a dark period [P_dark] to the plants
```

```
LED_start = datetime.now(pytz.timezone('Europe/Lisbon')) - timedelta(hours=1)
if sunrise_local < LED_start:
    # If sunrise is on the same day, add one day to sunrise_time
    sunrise_local += timedelta(days=1)
P_dark = 6 #hrs
P_day = (LED_start - sunrise_local)
P_day_sec = P_day.total_seconds()
P_LED = round(((24*3600 - P_day_sec) - P_dark*3600)/3600, 3) #hrs

#Calculate the Light brightness
PPFD_LED = 750; #LED_PPFD of 3 blades (at night) measured in the stem base [micromol m-2 s-1] (525 for the barrel wall and 892 10cm from the wall)
DLI_t = 17.5;

if int(DLI_m) < DLI_t:
 B_LED = round((((DLI_t-DLI_m)*1000000)/(PPFD_LED*P_LED))/3600,2) #Brightness of LED
 B_LED_r = min(1,B_LED)
else:
 B_LED_r = 0
 B_LED = 0
print('Turn LEDs for', P_LED, 'hours')
print('at', B_LED, 'brightness')

#Sending to GCP
topic_path = publisher.topic_path('datalogger', 'projects/environment-data/topics/datalogger')
publisher.publish('projects/environment-data/topics/datalogger', str(DLI_m).encode())
# Insert into BigQuery table
table_id = 'environment-data.farm_one.LED_B2'  # Replace with your BigQuery table ID
table = client.get_table(table_id)
row = [(datetime.now().strftime('%Y-%m-%d %H:%M:%S'), DLI_m, DLI_t, B_LED, P_LED, P_dark)]
print(row)
errors = client.insert_rows(table, row)
if not errors:
    print("Data inserted successfully into BigQuery.")
else:
    print("Errors occurred while inserting data into BigQuery:")
    for error in errors:
        print(error)

# PMW dimming of LEDs
GPIO.setmode(GPIO.BCM)
led_pin = 18 #Check the correct pin in pi
frequency = 500 #PMW freq
GPIO.setup(led_pin, GPIO.OUT)
pwm = GPIO.PWM(led_pin, frequency)
dim_level = B_LED_r*100 #Dimming level (%)
pwm.start(dim_level)
time.sleep(P_LED*3600) #Substitute with LED period (s)
```

```
pwm.stop()

GPIO.cleanup()
```